Extreme Temporal and Spatial Variation of Precipitation and Temperature (1953-2017)

Abdi-Basid Ibrahim Adan – abdi-basid@outlook.com

Abstract

This study evaluates satellite precipitation products (CHIRPS, PERSIANN-CDR, TAMSAT, ARC2, and ERA5) against in-situ rainfall data from Djibouti-Airport station (1983–2017) using multiple statistical metrics: Correlation Coefficient, RMSE, Percentage Bias, Nash-Sutcliffe Efficiency (NSE), and Relative Standard Deviation. ERA5 demonstrated the best overall performance with the highest correlation (0.75) and NSE (0.56), while TAMSAT and ARC2 showed poorer accuracy ($R^2 \approx 0.09$). Seasonal analysis revealed ERA5 performed exceptionally during JF (R^2=0.81, COR=0.90), while PERSIANN-CDR excelled during MAM and OND.

Principal Component Analysis (PCA) of 14 rainfall stations identified two distinct precipitation regimes: eastern coastal stations (influenced by the Red Sea/Gulf of Aden) and western/interior stations (altitude-dependent). The first two principal components explained 70.3% of total variance, with PC1 capturing interannual variability (92.1%) and PC2 capturing annual cycle variability (40.75%). Four imputation methods (PPCA, AMELIA II, MICE, missMDA) were applied to reconstruct missing data from 1946–2017.

Trend analysis indicated significant decreasing rainfall trends in MAM (Airport: -3.15 mm/season, p=0.009; CHIRPS: -0.71 mm/season, p=0.010), with mixed seasonal patterns across products. These findings establish ERA5 as the most reliable satellite product for Djibouti's rainfall estimation and confirm the country's spatially heterogeneous precipitation regime shaped by both maritime influence and orographic factors.

Keywords ERA5, CHIRPS, Nash-Sutcliffe, PCA, Djibouti.

1. Introduction

Unprecedented desertification during the past decade has led to the emergence of drought, the reduction of groundwater, the shrinking of arable reduction of biodiversity (coral cover, mangroves and endemic species), displacement of rural populations, increased poverty. Global climate change has regional and local impacts. The climate of the Republic of Djibouti ranks among the extremes in the world. The annual average temperature of Djibouti over the study period from 1953 to 2017 is 30.17 ° C. The annual evaporation threshold is 734.4 ° C, well above the average annual precipitation of 147.4mm. The latter is less than 50% of the threshold (371.7 ° C> 147.4mm). With an annual average temperature of 30.17 ° C (> 18 ° C), Djibouti enjoys a desert climate, dry and warm. The climatic classification based on precipitation and temperatures of Köppen describes Djibouti of the same kind, giving it the notation BWh (André, 2001). In addition, the average temperature varies between 22.90 ° C in February and 39.25 ° C in July. The mean annual precipitation is 147.4 mm over the study period. The climatic year of the country is divided into two great seasons interspersed with two periods of transitions. The cooler season, spreads between January to February with a respective annual average precipitation of 16.47mm and 14.19mm. The months of March, April and May, the spring season (or transition to summer) is determined by the most important rainfall of the year. On the coast, it is very humid because of the evaporation of the sea. The water vapor saturates the atmosphere which is not ventilated. The rains are distributed differently over the whole country according to the altitude. The hot season starts from June, July August and ends in September. This is the time when the westerly winds blow, especially the khamsin, violent, dry and hot wind. It usually blows in the day and subsides at dusk. It is then followed by a light easterly wind: the sea breeze. The khamsin is a westerly wind coming from the interior of the mountains, from the mountains of Ethiopia. It can raise the temperature up to 47 ° C. The arrival of khamsin in June is preceded by a wind from the west, a wind also dry but less hot: the sabo (Figure1). The months of October to December are the months of transitions (autumn) to the cool season. During this season, the wind blows from the Northeast to the Southeast. It comes from the Indian Ocean or southern Arabia: It is the trade wind, a cool and wet wind. In addition, the rainfall regime of Djibouti is multimodal. The volume of rainfall varies between years, we talk about interannual heterogeneity.

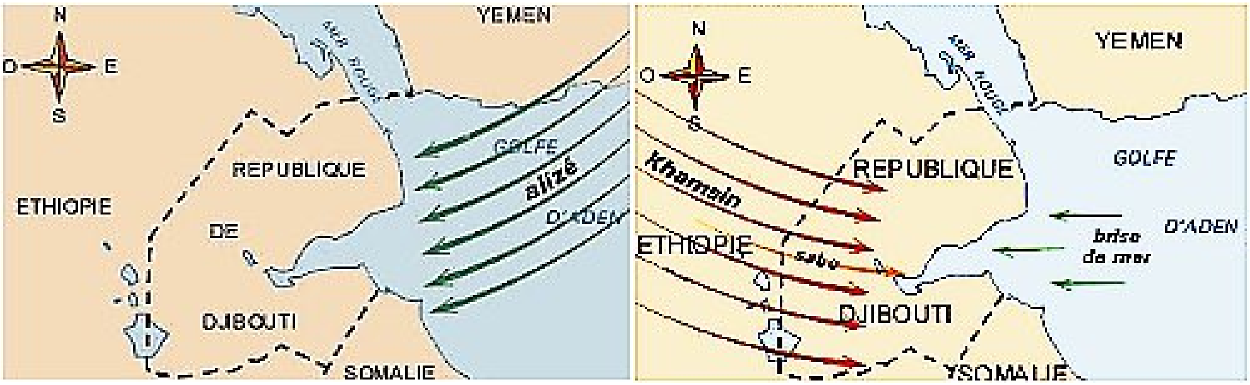

Source : *© 2001- 2002 Benoît Billiet*

Figure 1 Wind direction season cool season and hot season

2. Study area regions

Djibouti a country in the Horn of Africa, located in East Africa. It is the smallest province in this region. "Djibouti District" is the capital of the Republic of Djibouti and one of the six regional administrative divisions of the country. Covering an area of 630 km2, the city of Djibouti is populated in 2013 with about 570 000 inhabitants, or more than two thirds of the total population of the country. The study covers climate change in Djibouti. The data come from the Djibouti airfield station located southwest of the capital of the Republic of Djibouti (11.33 and l: 43.50 lat). A second framework studies the spatial aspect of climate change in the five regions of the Republic of Djibouti, including Tadjourah, Dikhil (11.10 and Long: 42.37), Ali-Sabieh (11.15 and Long: 42.70).), Arta (11.50 and Long: 42.83). and Obock (Lat: 11.97 and Long: 43.28).

Figure 2 Map of the study area

3. Data sources and Analysis tools

Data from climate change studies come from the Djibouti aerodrome station (11.33 lat and 43.50 long). Monthly precipitation and temperature, from 1953 to 2017, more than 64 years of data. The daily aspect, however, is incomplete from 1974 to 1980, which obliges us to restrict ourselves to the calculation of indices under RClimdex from 1980 to 2017 for precipitation.

However, the temperature is observed from 1953 to 2009. The oldest station dates from 1901, it does not provide any more recent data since 1980. The spatial study generalizes the 6 districts of the Republic of Djibouti, for the recent years. CHIRPS data will also be studied in order to correct and better understand the concept of spatial climate change. In combination these data, we obtain, the following series:

- 1980-2017: Airport station for daily precipitation
- 1953-1974: French colonial data published
- 1966-2009: Airport station for daily temperature

Multiple tools have been considered for the precipitation and temperature analysis among which Anclim, Geoclim, FclimDex RClimDex, Rclimtool, Climatool, Climapact2, RHtest ... etc. However, two are retained RclimDex 1.0 and Climpact2.

4. Methodologies

4.1. Quality Control

Raw data collected was inspected prior to analysis. Verification of the aberrant data presence. Maximum and minimum temperatures (°C) and precipitation (mm) zero and negative precipitation are not considered in the database. The proper technique is the removal of the line. Aberrant values distort the analysis. At no time are they ignored. O can easily identify them with the box of Mustache, at the minimum and minimum... etc. The number of missing values is quantified to adapt the effective technique to it. Values are imputed by the -99.9 value before importing data under the RClimDex program. After a general run of the base and its adaptation for the execution of the indices of temperature and precipitation. The preliminary study on data quality detects the extreme values by realizing the statistics of maximum and minimum. Especially as RClimDex allows us to identify other anomaly as the application of one month, a year or a day before the setting for the calculation of indices. Existence of missing data disrupts the analysis of the observation series for calculating indices under the RclimDex program (Zhang and Yang, 2004). A month containing more than 3 missing days is not considered in the year. An incomplete year is also private in index calculations. Statistical indicators such as the median make it possible to complete the missing values when the proportion of these values is small.

4.2. Homogenization

After the diagnosis of extreme, erroneous and missing values, it is appropriate at this stage to study the homogenization of the series of temperature and precipitation. The tendency of each of its climatological variables in a double vision of diagnosis with parametric and non-parametric methods. We use local regression (also known as LOESS: "Locally weighted Scatterplot Smoother), is a non-parametric regression method based on the k nearest neighbor method. It combines the simplicity of linear least squares regression with the flexibility of nonlinear regression, by performing a simple regression on local subsets of data. One of the main advantages of this method is that it makes it unnecessary to define a single global function that would describe the regression model, since the method consists of calculating as many local functions as there are data segments (William All, 1988). The weighting function generally used to perform a local regression is a weighted cubic function defined by the equation below:

$$w(x) = (1 - |x|^3)^3 [\ |x| < 1\ ] \quad (1)$$

A decrease in precipitation is observed for the last six decades in the southwest of the capital of Djibouti (figure 3). In the same decade, there is an increase in average temperature maximal. We notice the lack of rain leaves room for a rise in temperature (figure4).

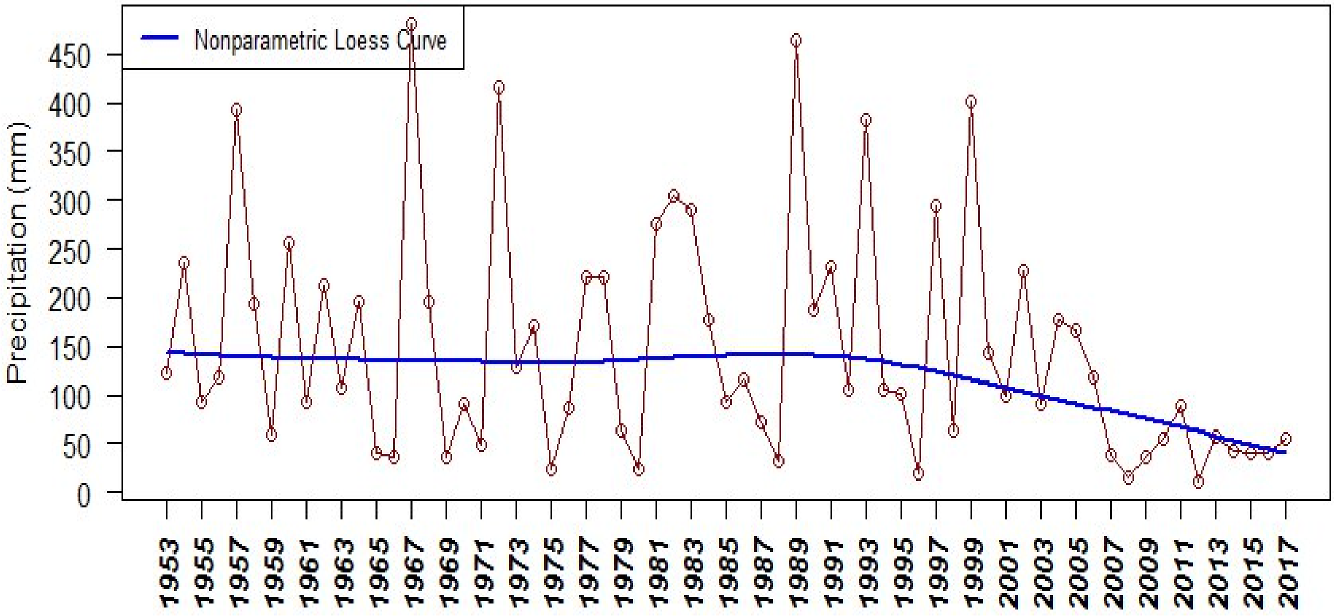

Figure 3 LOESS regression for annual precipitation

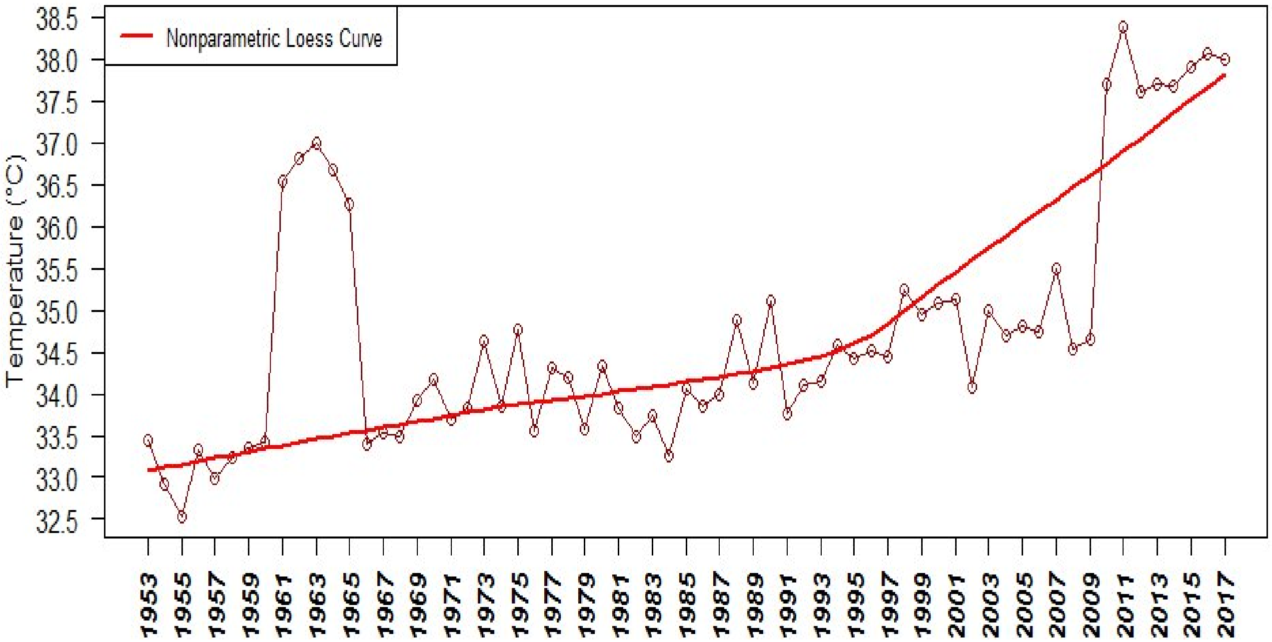

Figure 4 LOESS regression for annual average temperature maximal

The nonparametric Mann-Kendall test is used to detect the annual and seasonal trend of a climatology variable. The null hypothesis is that the data follows a monotonous trend. The Mann-Kendall statistical test is calculated according to equation (2):

$$S = \sum_{k=1}^{n-1} \sum_{j=k+1}^{n} sgn(X_j - X_k) \quad (2)$$

With

$$sgn(x) = \begin{cases} 1 \ \ if \quad x > 0 \\ 0 \ \ if \quad x = 0 \\ -1 \ \ if \ \ x < 0 \end{cases}$$

The mean of S is E(s) =0 and variance $\sigma^2$is

$$\sigma^2 = \frac{\left\{n\,(n-1)\,(2n+5) - \sum_{j=1}^{p}\left(t_j - 1\right)(2t_j - 1)(2t_j + 1\right\}}{18}$$

Where p is the number of tied groups in the data set and t_j is the number of the data points in tied group. The statistics S is approximatively normal distributed provided that the following Z-transformation is employed:

$$Z = \begin{cases} \frac{S-1}{\sigma} & if\ S > 0 \\ 0 & if\ S = 0 \\ \frac{S+1}{\sigma} & if\ S > 0 \end{cases}$$

The statistics S is closely related to Kendall τ as given by:

$$\tau = \frac{S}{D}$$

Where

$$D = \left[\frac{1}{2}n\,(n-1) - \frac{1}{2}\sum_{j=1}^{p} t_j(t_j - 1)\right]^{1/2} \left[\frac{1}{2}n(n-1)\right]^{1/2}$$

Make sure that the series does not correlate with the appropriate time before applying the Mann-Kendall test to the time series in levels. In the case of an autocorrelation revelation, the Mann-Kendall test will be used together with the block priming to take into account the correlation of the series (GSCC, 2014). Examination of the autocorrelation and partial autocorrelation plots suggests that the series does not appear significant. Indeed, most of the vertical spikes in the ACF and partial ACF plots produced fall into the horizontal band defined by the blue dashed lines beyond which autocorrelations and partial autocorrelations would be considered significant. As a result, the Mann-Kendall test is applicable for the precipitation series (Figure 5). The autocorrelation and partial autocorrelation diagrams of the annual temperature time series reveal the presence of significant temporal dependence, so the Mann-Kendall test will be done in conjunction with the block bootstrap method (Figure 6).

The upward or downward trends in the Mann Kendall test are grouped into three classes of significance:

1. Not significant: [**p.value > 0.05**]
2. Significatif: [**0.01 < p.value < 0.05**]
3. Very significant: [**p.value < 0.01**]

The critical probabilities of the Cox-Stuart trend tests Mann-Kendall Trend Sens.slope, Fisher and the Bartels Ratio are all very significant for Temperature's trend annual (Table 2). However, the precipitation trend annual is significant (Table 1). therefore, we have a significant decrease in rainfall during the last 64 years southwest of Djibouti. In contrast, the temperature experienced a positive and significant monotonic trend.

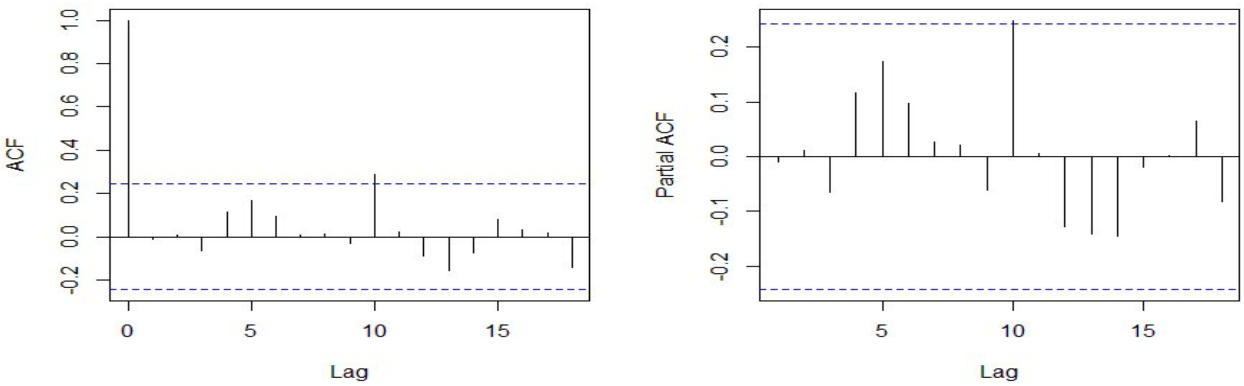

	ıd Stuart	-Kendall trend	lope	stic	s Ratio
	.22	-2.4854	54	8	558
	65	65			5
e	)2642	0.01294	94	9	254

Table 1 Results of trend test of annual rainfall

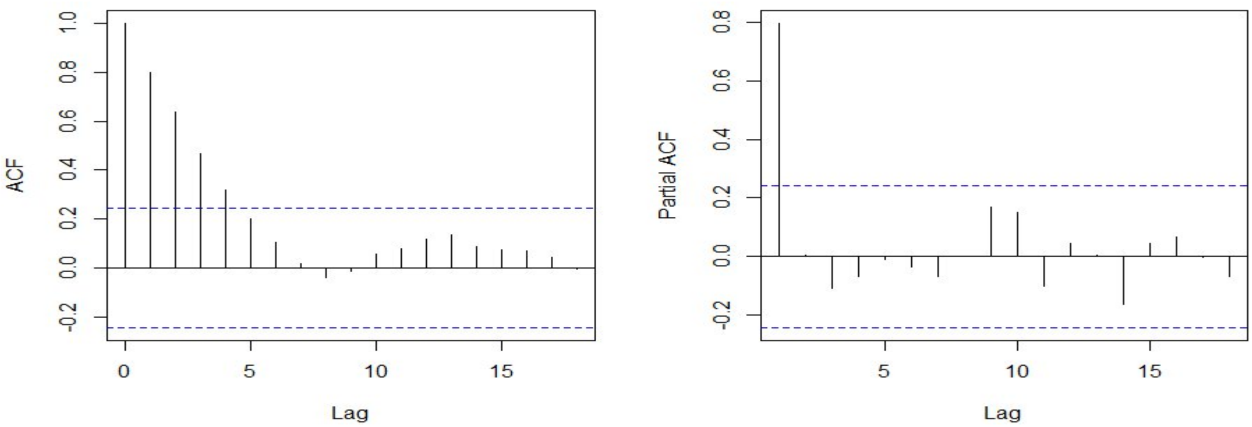

	ıd Stuart	-Kendall trend	lope	stic	s Ratio
	6496	6.171	1	9	6661
	65	65			5
e	**0.01**	**< 0.01**	**)1**	**)1**	**).01**

Table 2 Results of Trend Test of annual average maximal temperature

The interannual variation of precipitation over the period 1953 to 2017 is stationary around the mean value of precipitation total annual 147.4 mm except from 2006 where a change in rupture with the past evolution of precipitation is observed. The downward trend in precipitation is quite significant. The decades 60s, 70s, 80s and 90s were marked by an increase in precipitation in the southwest of the capital of Djibouti. The precipitation of the last decade was 73 times less than the 2000s. This partly justifies the overall downward trend (Table 3).

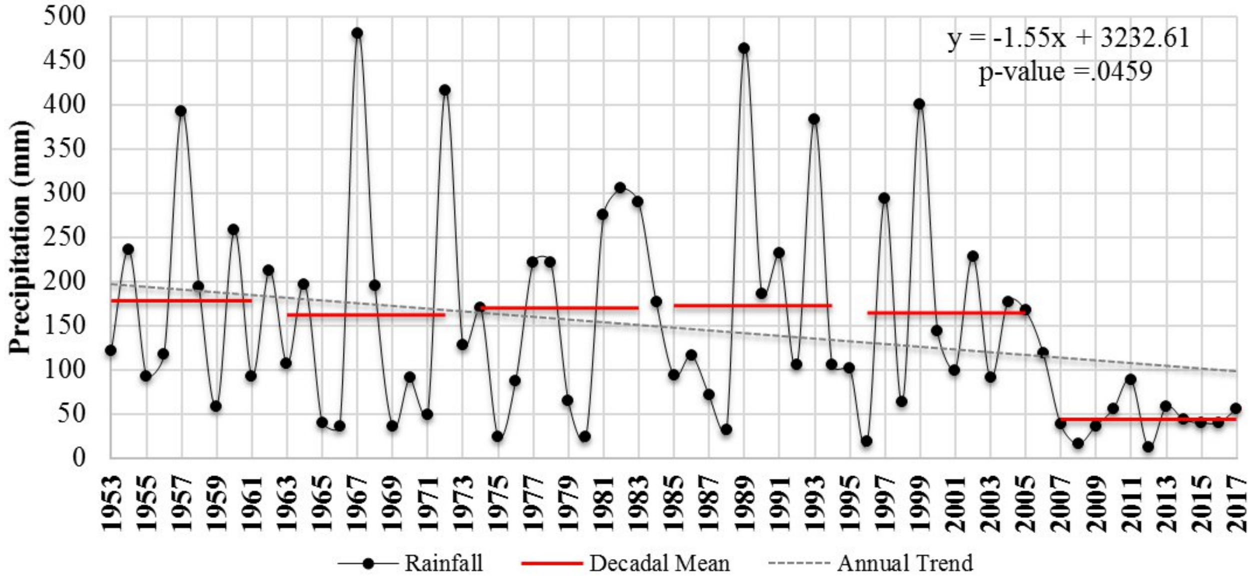

Decade	1960s	1970s	1980s	1990s	2000s	010s
Mean (mm)	77.32	61.33	69.23	71.77	63.76	3.84
Rate(mm/decade)	-0.09	0.048	0.015	-0.046	-0.73	

Table 3 Total precipitation annual in South West of Djibouti from 1953-2017

The box-plot representation shows the dataset in three quartiles Q1 (25%), Q2 (50%) and Q (75%). From lowest to highest in this box, we observe the minimum, the maximum, the median, the first quartile and the third quartile of the dataset. Useful for comparing the distribution between the monthly and annual rainfall in south-west Djibouti. The above-mentioned bridges indicate the extreme values observed in each month and year during the precipitation who is important in March and October. April and September come in second place. In both graphs, the distribution is more homogeneous in the monthly than annual cases (Figure 3 (a); (b). This will help diagnose the presence of seasonality during the observation period from 1953 to 2017.

(a) (b)

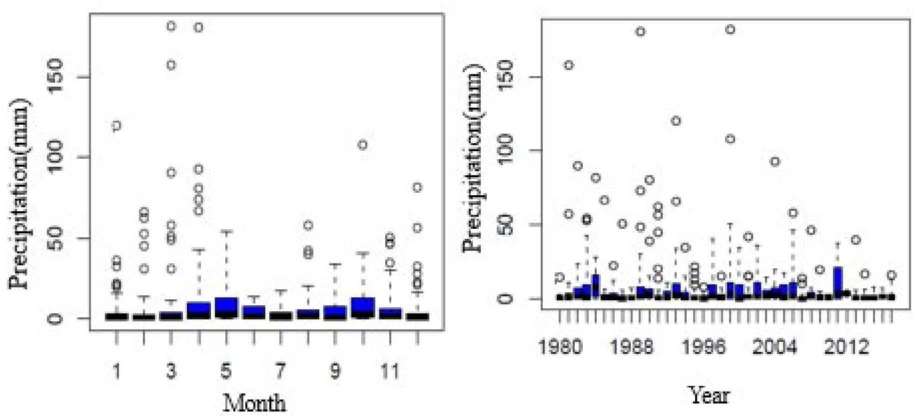

(c) (d)

Figure 3 Boxplot of non-zero monthly and yearly precipitation from1953-2017

The histogram distribution of the annual rainfall of the southwest of the capital of Djibouti is first of multimodal and heterogeneous intra-annulled. The precipitation class 0 to 100 is predominant compared to a class 400 to 500 mm. This distribution shows the low precipitation in this region over the period from 1953 to 2017 (Figure 4 (a)). The average of the maximum temperature is heterogeneously distributed over the observation period from 1953 to 2017. The average temperature class from 33°C to 35°C represents the modal class of temperature at the west. Nevertheless, the modal range 38 ° C to 38.5°C exceeds those of 35°C to 36°C (Figure 4 (b)).

(a) (b)

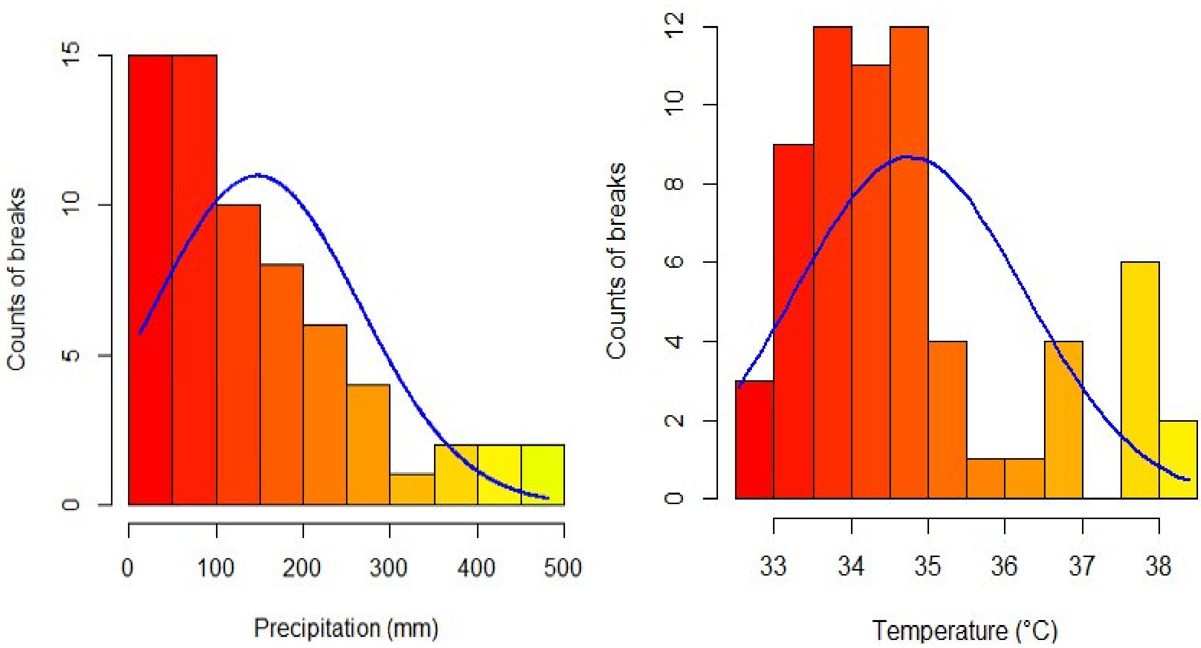

Figure 4 Density of Annual total precipitation and average temperature maximal from1953-2017 in Djibouti-City

Since 1953, the average of the maximum temperature has recorded a strong increase with a very significantly positive trend. A rupture change seems to start from 2008. In accordance with the variability of the precipitation, the interdecadal variability shows a rise in maximum average temperature. The last decade was the hottest southwest of the capital of Djibouti, more than 6.2 times than the decade of 2000s (Table 4).

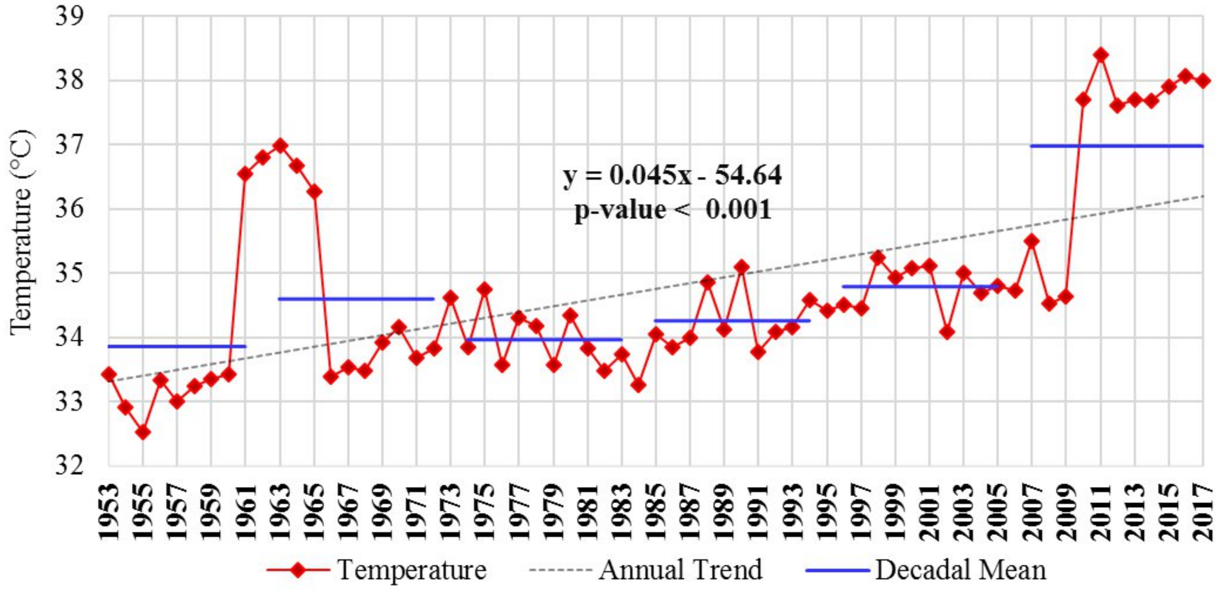

Decade	1960s	1970s	1980s	1990s	2000s	010s
Mean (mm)	33.86	34.60	33.96	34.26	34.79	6.97
Rate(°C/decade)	0.022	-0.018	0.0088	0.015	0.062	

Table 4 Mean Maximal Temperature (°C) in Djibouti from 1953-2017

After studying the trend of changes in precipitation and temperature. Changes of evolution have been diagnosed of those series. The change date (break point) detection test such as Pettitt (1979), Fisher's test, Buishand's test (1982), standard normal homogeneity test (1986) and the sequential test of Mann Kendall will be studied.

The identification of breakage changes using a non-parametric cost function (Haynes, Fearnhead, 2017) and the parametric change of the average (Figure 3) show 9 breakpoint of precipitation (mm) : 1964(180.06mm), 1966(35.50mm), 1968(173.84mm), 1980(24.2mm), 1983(289.4mm) 1988(31.30), 1993(383.2) 1996(18.90mm) and 2006(114.78mm)

One of which is the most significant according to Standard Normal Homogeneity rupture change tests (1986), Pettitt (1979), Buishand U (1982). But the Buishand range (1982) indicate 2002 and still not significant (Table 5). The year of change of precipitation over the period of 1953-2017 in south west of Djibouti-City to had binds in 2006. One applies on the daily series, the rupture adjusts to August 28, 2005, four months before 2006.

(a)

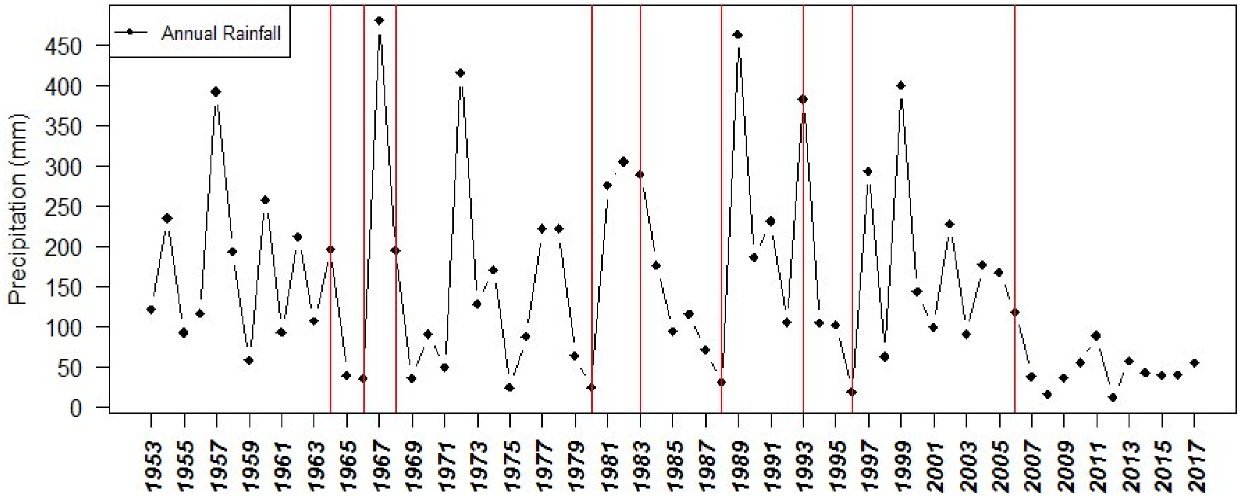

(b)

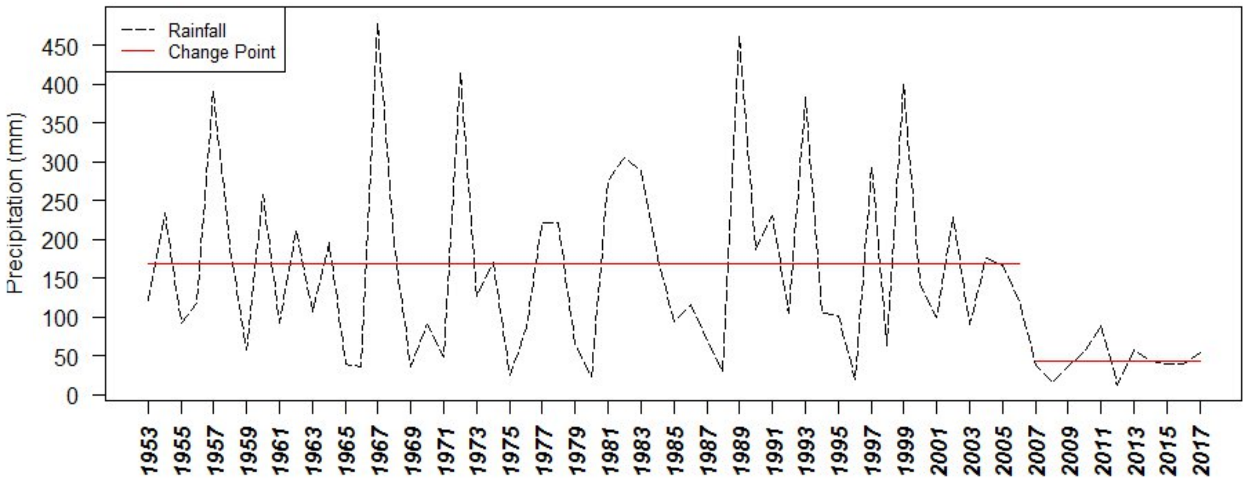

Figure 4 (a) Identifying Changes using a Nonparametric Cost Function and (b) mean change for annual precipitation (mm) over 1953-2017

Test	tandard Normal Homogeneity (SNHT)	ettitt PT)	ıishand U (BU)	ıishand range (BR)
t	10.161	454	0.45908	1.26
n	65	65	65	65
P.value	0.024	02371	0.0462	0.2828
hange Point	2006	2006	2006	2002

Table 5 Breakpoint parameter test in annual precipitation from 1953 to 2017

The identification of break date changes using a non-parametric cost function (Haynes, Fearnhead, 2017) and the parametric change of the average (Figure 4) show 4 breakpoint of mean of maximum temperature annual (°C) : 1960(33.43 °C), 1965 (36.28 °C), 1987 (33.99 °C), 2009 (34.64 °C). According to Standard Normal Homogeneity rupture change tests (1986), 2009 is break date in variation of temperature in Djibouti. Pettitt (1979) test break point on 1993, Buishand U (1982). But the Buishand range (1982) indicate 1997 (Table 6). The year of change of precipitation over the period of 1953-2017 in south west of Djibouti-City to had binds in 2009 with mean variation of temperature. One applies on the daily series; the rupture adjusts to 19 May 1987. Temperature change rupture is observed in 2009 and comes back in two different tests.

(a)

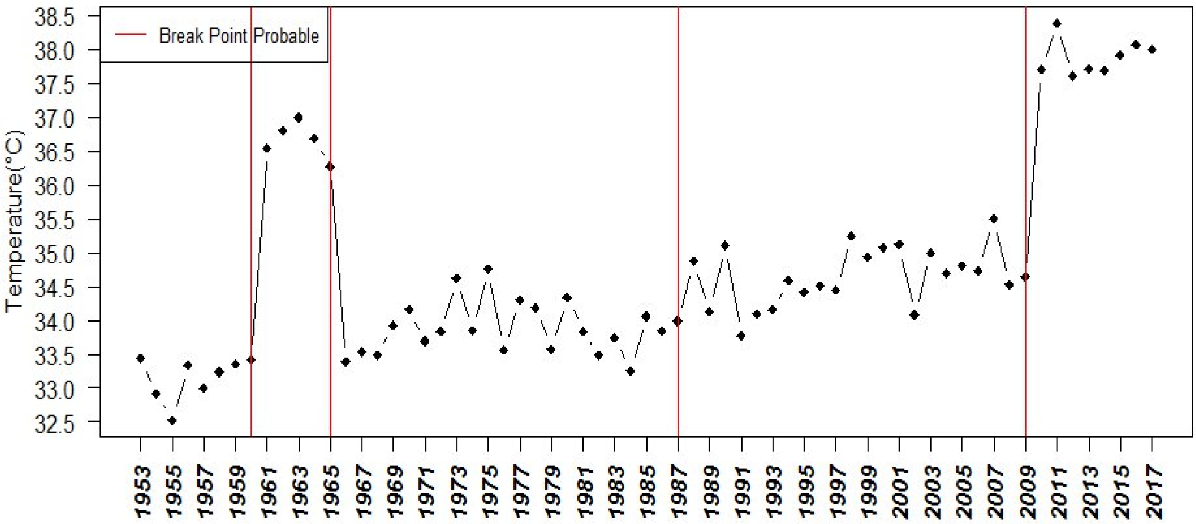

(b)

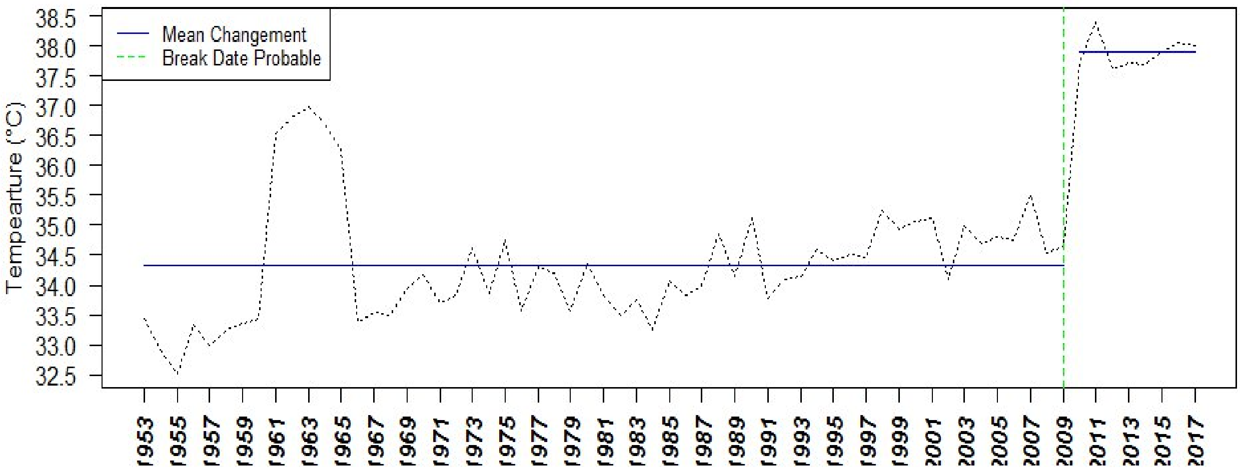

Figure 4 Identifying changes using a nonparametric cost function and mean change for annual mean temperature maximal (°C) over 1953-2017

est	ırd Normal Homogeneity t (SNHT)	ınd U U)	ınd range BR)
t	39.93	908	.177
n	65	5	65
alue	< 0.001	1 ı62	)0015
;e Point	2009	)7	.997

Table 6 Breakpoint parameter test in annual mean maximal temperature from 1953 to 2017

4.3. Climate Change indices

A set of 11 precipitation indices were defined in order to study rainfall variability and extreme events in Djibouti (Table 7). Developed by the expert team on climate change Detection Monitoring Indices (ETCCDMI). Among these are the total annual precipitation indices (PTOT), the simple daily intensity index (SDII) calculated as average rainfall of rainy days, the maximum number consecutive dry days (RR

<1 mm, CDD) and the maximum number of consecutive rainy days (RR≥1 mm, CWD). Other indices are used to determine extreme precipitation events: the maximum annual rainfall recorded during one day (Rx1d) and for five days (Rx5d), the number heavy rainfall (RR≥10 mm, R10 mm) and very heavy rainfall (RR≥20 mm, R20 mm) plus two indices based on the 95th and 99th percentiles (R95p and R99p) that define a very wet day and extreme precipitation event, respectively. These percentile values were calculated from daily rainfall data over the period 1981-2016. All these indices have been calculated annually from January 1st as of December 31st. The calculation of the extreme temperature proposed by the ETCCDMI was applied to our using the Rclimdex package (Zhang and Yang, 2004). Some of them are relative to the hot period. These give warm period duration information (WSDI) the hottest day of the year (TXx), the hottest night of the year (TNx), the frequency of hot days (TX90P) and the hot night frequency (TN90P) with the calculated 90th percentile value from maximum and minimum daily temperature data over the period 1954-2010. The others are relative to cold period. These are the durations of cold periods (CSDI), the coolest day (TXn) and coolest night (TNn) of the year, the cold day frequency (TX10P) and the cool night frequency (TN10P). In addition, a final index is based on the daytime value temperature range (DTR). All temperature indices have been calculated each year from January 1st to December 31st. Their definition and unity are also presented in Table 7.

ID	IDICATOR NAME	DEFINITIONS	ITS
X1day	-day precipitation amount	Monthly maximum 1-day precipitation	m
x5day	-day precipitation amount	Monthly maximum consecutive 5-day precipitation	m
SDII	le daily intensity index	total precipitation divided by the number of wet days (defined as PRCP>=1.0mm) in the year	m/ay
R10	er of heavy precipitation days	Annual count of days when PRCP>=10mm	ys
R20	umber of very heavy precipitation days	Annual count of days when PRCP>=20mm	ys
Rnn	er of days above nn mm	nual count of days when PRCP>= nn mm, nn is user defined threshold	ys
CDD	onsecutive dry days	Maximum number of consecutive days with RR<1mm	ys
CWD	onsecutive wet days	Maximum number of consecutive days with RR>=1mm	ys
R95p	Very wet days	Annual total PRCP when RR>95th percentile	m
R99p	Extremely wet days	Annual total PRCP when RR>99th percentile	m
CPTOT	nnual total wet-day precipitation	Annual total PRCP in wet days (RR>=1mm)	m
SU25	Summer days	Annual count when TX (daily maximum)>25ºC	ys
TR20	Tropical nights	Annual count when TN (daily minimum)>20ºC	ys
GSL	owing season Length	al (1st Jan to 31st Dec in NH, 1st July to 30th June in SH) count en first span of at least 6 days with TG>5ºC and first span after July 1 (January 1 in SH) of 6 days with TG<5ºC	ys
TXx	Max Tmax	Monthly maximum value of daily maximum temp	C
TNx	Max Tmin	Monthly maximum value of daily minimum temp	C

TXn	Min Tmax	Monthly minimum value of daily maximum temp	C
TNn	Min Tmin	Monthly minimum value of daily minimum temp	C
[N10p	Cool nights	Percentage of days when TN<10th percentile	ıys
[X10p	Cool days	Percentage of days when TX<10th percentile	ıys
[N90p	Warm nights	Percentage of days when TN>90th percentile	ıys
[X90p	Warm days	Percentage of days when TX>90th percentile	ıys
WSDI	ı spell duration indicator	al count of days with at least 6 consecutive days when TX>90th percentile	ıys
CSDI	spell duration indicator	al count of days with at least 6 consecutive days when TN<10th percentile	ıys
DTR	rnal temperature range	Monthly mean difference between TX and TN	C

Table 7 Indices of ETCCDI for precipitation and temperature climate change assessment

5. Results and discussion

5.1. Total precipitation change

From 1953 to 2017, the average annual rainfall of southwest Djibouti is 147.4mm with an average annual temperature of 30.17 ° C. On the monthly distribution in this period of study, the average temperature is between 25.24 ° C (January) to 36.77 ° C (July) over the period 1953-2017. The minimum and maximum temperature is low in the period of January to March. The months of April and May announce the arrival of the hot season during the period June to September (summer) which 39.82°C average Temperature maximum. The fresh season temperature drop back to approximately January and February with 29.35 °C (Figure 8). In the same period, the precipitation is of multimodal regime. The months of March, April and May (MAM), spring correspond to the long rainfall season with 33.80% of total annual precipitation. The short rainfall groups together the months of October November and December (OND), autumn which constitutes 31.20% of the precipitation annual total (Figure 9).

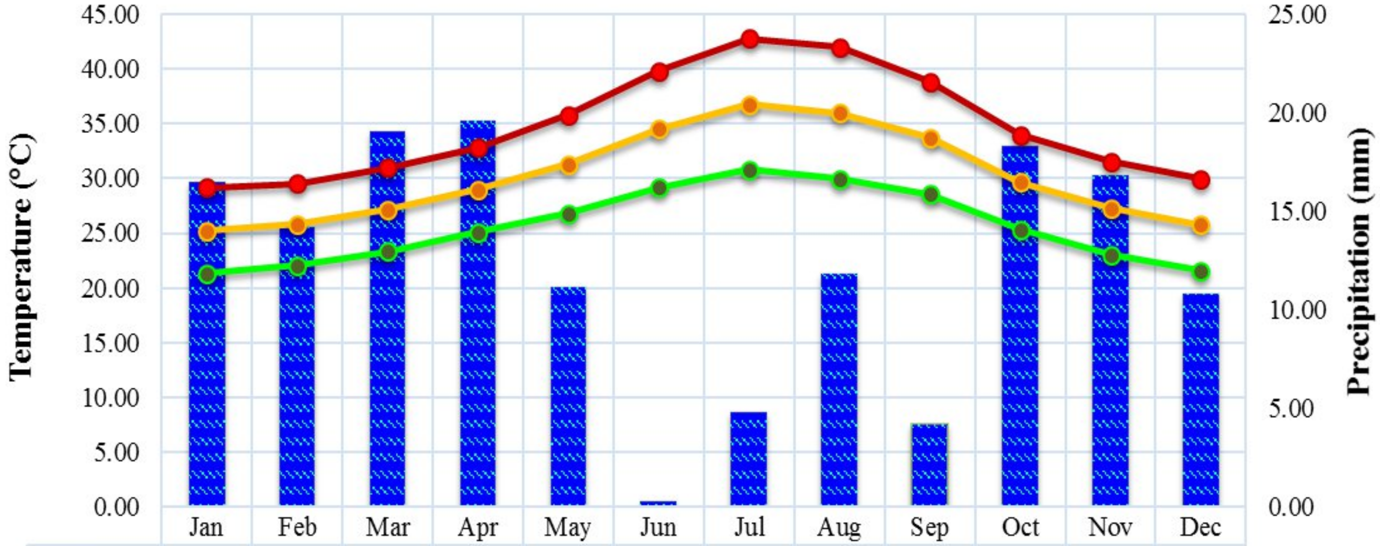

	Jan	Feb	Mar	Apr	May	Jun	Jul	Aug	Sep	Oct	Nov	Dec
PRCP	16.47	14.19	19.04	19.62	11.17	0.28	4.80	11.81	4.23	18.34	16.84	10.82
Tmax	29.16	29.54	30.98	32.81	35.81	39.82	42.75	41.98	38.83	33.96	31.56	29.93
Tmin	21.32	22.05	23.30	25.10	26.78	29.18	30.80	29.92	28.56	25.34	23.04	21.58
Tave	25.24	25.79	27.14	28.96	31.30	34.50	36.77	35.95	33.70	29.65	27.30	25.76

Figure 8 Average monthly air temperature (°C) and precipitation (mm) for Djibouti for the study period (**1953-2017**)

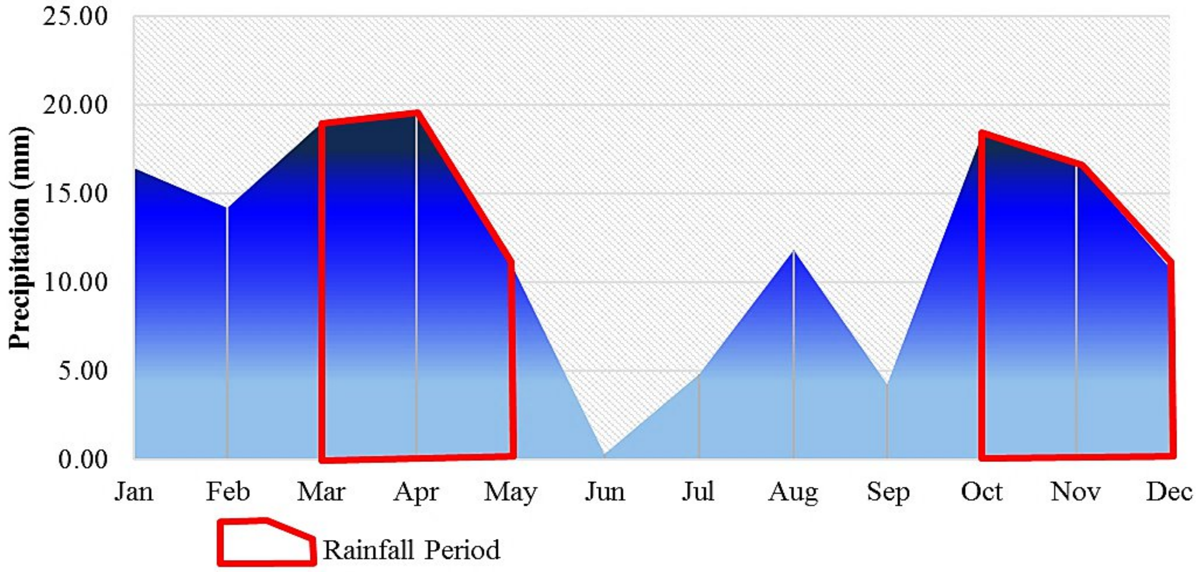

Figure 9 Average precipitation (mm) for Djibouti for the study period (**1953-2017)**

The trends significant in the Mann Kendall test are grouped into three classes such as: Not significant: [p.value > 0.05], Significatif: [0.01 < p.value < 0.05] and Very significant: [p.value < 0.01]. We detect the presence of a significant trend on the season JF (fresh season). The critical probability associated with the Mann Kendal trend test is significant at the risk threshold of 5% (Table 1). In this season the downward trend of precipitation is therefore significant. For the MAM (spring), JJAS (summer), OND (autumn) seasons, their critical probability associated with the Mann Kendall test is not significant at the risk threshold. The hypothesis of non-significant is therefore retained. Seasonal trends show a decrease in precipitation over the precipitation period but are not significant (Figure 10 (b), (c), (d)). However, the last result is consistent with many other countries of region like Asmara (Fessehaye, 2018), Ethiopia (Conway and al,2004), Kenya (Rao and al. 2001).

	Season JF	Season MAM	Season JJAS	;eason OND
z	-2.	-1.56	-0.38	-1.56
n	65	65	65	65
s	-354	-276	-68	-276
arS	31150.7	31198	31187	31198
au	-0.17	-0.13	0.033	-0.13
alue	**0.04549**	0.1195	0.7044	0.1195

Table 1 Mann-Kendall trend seasonal test for precipitation in Djibouti over 1953-2017

(a)

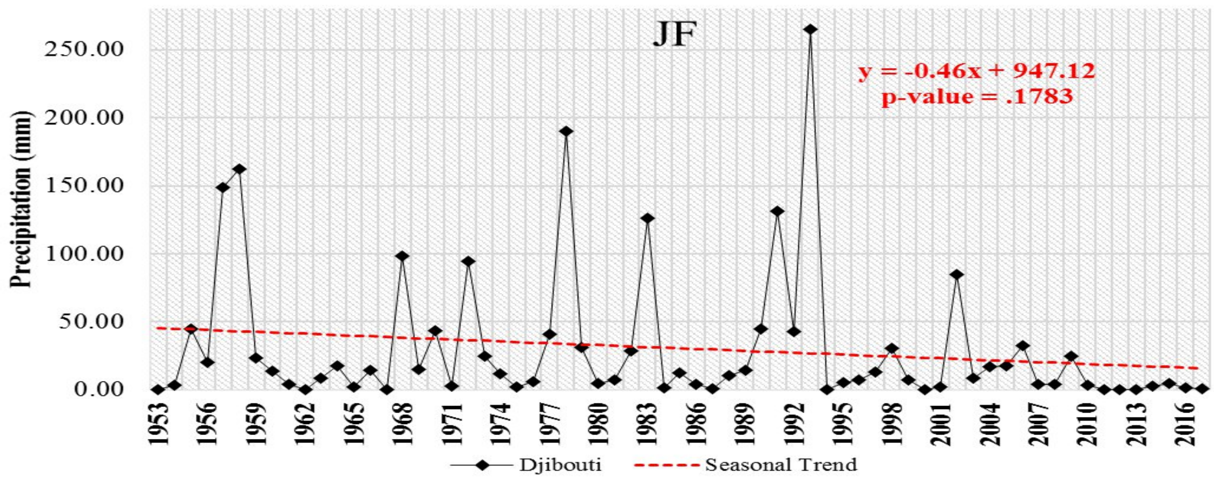

(b)

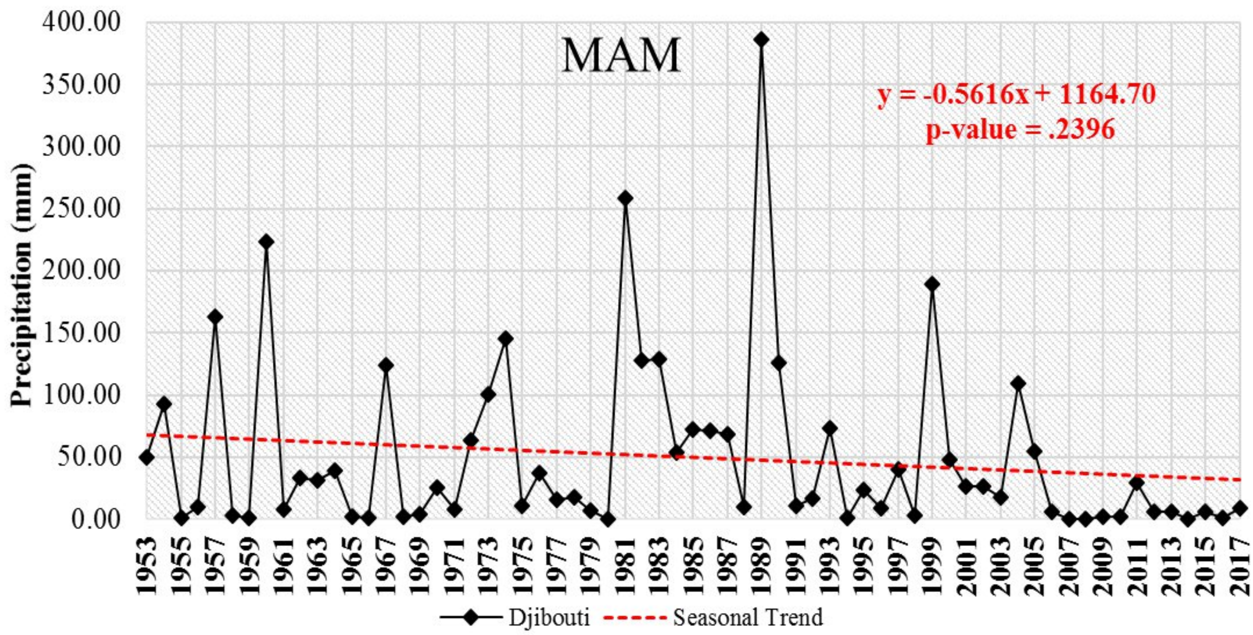

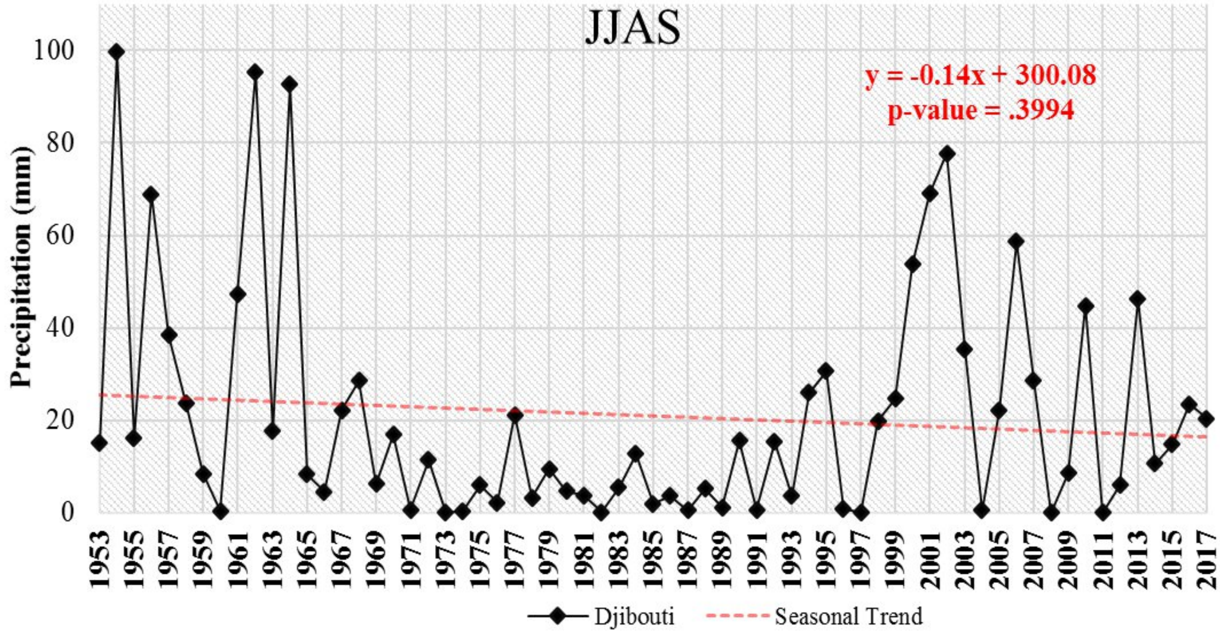

(c)

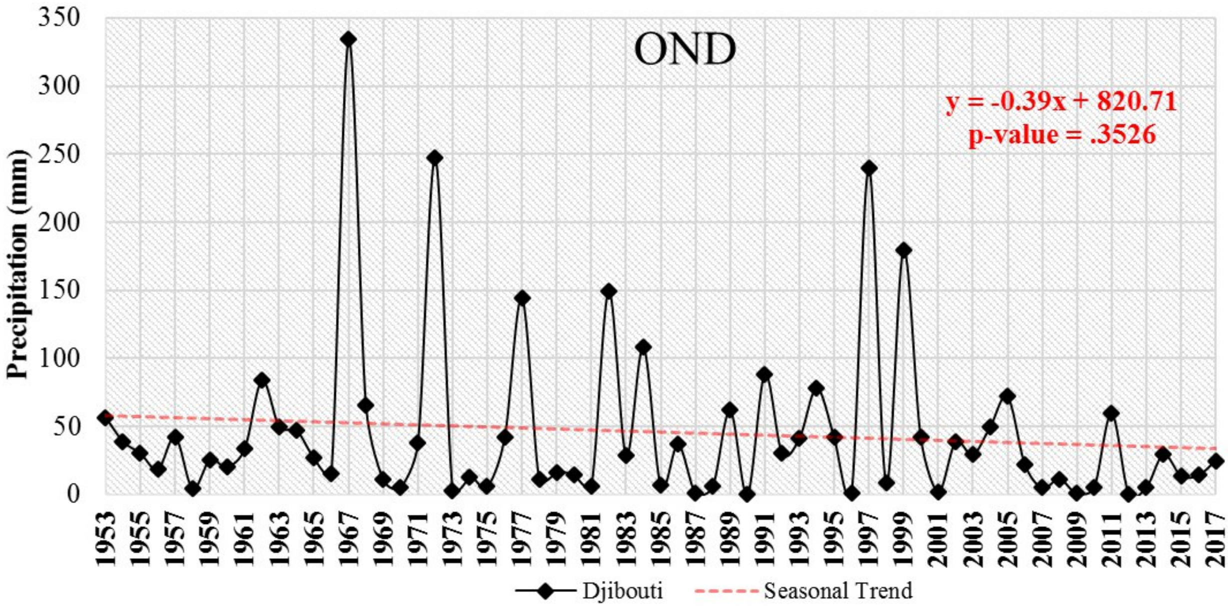

(d)

Figure 10 Seasonal precipitation (mm) of south west Djibouti over the period 1953-2017

		Djibouti-City (1980-2017)			Asmara (1914- 2015)		Ocean (1971–2005)
Index	**Units**	**Trend**	**p-value**	**Annual average**	**Trend**	**Annual average**	
PRCPTOT	mm	**4.518**	**0.008**	134.21	-0.579	509	**81.84**
SDII	mm/day	-0.16	0.101	9.76	**0.019**	9.96	**1.05**
CDD	day	**1.816**	**0.02**	143.97	**0.424**	105	0.66
CWD	day	**0.034**	0.072	2.45	**-0.017**	6	0.10
RX1DAY	mm	**1.763**	**0.009**	47.77	0.060	51	1.12
RX5DAY	mm	**2.675**	**0.003**	64.08	-0.048	94	5.96
R10	day	**0.092**	**0.028**	3.24	**-0.035**	17	2.09
R20	day	**0.063**	**0.042**	.74	0.001	7	1.26
R25	day	**0.044**	**0.046**	.21	NA	NA	NA

	nm	**2.878**	**021**	).59	0.146	118	22.66
	nm	1.104	141	5.83	0.182	35	−12.61
TOT	.	1.1813	.00	..89	NA	NA	NA
TOT	mm	0.334	175	.31	NA	NA	NA

Notes: A trend significant at the 5% level is marked with bold font. Indian Ocena are from Omondi et al. (2013)

Table2. Summary of trends (units of decade) and annual average of the precipitation indices for the analyzed station of airport of Djibouti

Among 13 indices of precipitations, 11 were calculated on daily precipitation of Djibouti from 1980 to 2017 using the RclimDex's software developed at the climate research branch of Meteorological Service of Canada in conjunction with the ETCCDM (Zhang and Yang, 2004). R99PTOT and R95PTOT indices were obtain by using ClimPACT software. It is based on the RClimDex and developed by the WMO CCl/CLIVAR/JCOMM Expert Team on Climate Change Detection and Indices (Alexander, Yang and Perkins, 2013). The Trends were calculated using linear regression and significance levels were determined using anon parametric Mann-Kendall test to determine whether the slope differed significantly from zero. Over all, Nine index of precipitation is significant. The total annual and seasonal precipitation of both Results show that rainfall indices have declined the small (MAM) and the long rainfall (OND) did not indicated a statistically significantly variation, where an average the long and short rainfall periods account for 33.17.% and 33.88% respectively of the total annual rainfall. However, the calculations for the precipitation of decreasing significant statistically indices are computed, as is the case of the total annual of wet day precipitation (PRCPTOT) with a significant statistically ($p<0.05$) decrease of 45.18 mm/decade over the last three decades for Djibouti. for the very wet day R95p, we note a significant decrease of 28.78 mm /decade. The meteorological drought indicators for dry climates (Wanders and all, 2010): the index of the consecutive dry days (CDD) being significant statistically ($p<0.05$) increase of 18.16 day/decade over three decades for Djibouti (figure 7). Also, the index of consecutive days of rain (CWD) decrease but not yet significant ($p>0.05$). The same index (CDD) for Eritrea is very significant statistically increase 4.24day/decade over the last one century (Fessehaye and all, 2018). Djibouti have more increase consecutive dry day than Asmara (Eritrea). The number of very heavy precipitation day greater than 20 mm (R20) significantly decreases by 0.63 days/ decade. A significant statistically decrease of 0.92day / decade is also observed in (R10), which describes the annual count of the days with very high precipitation greater than 10 mm. The same index (R10) at Eritrea is significant statistically decrease of 0.35 day/decade. Once again, we notice more decrease Djibouti than Asmara. The index (R25) is also significantly decreasing by 0.46day / decade. The simple daily intensity index (SDII) is also decreasing but not significant. The maximum one day and 5 days precipitation amount (RX1day) and (RX5day) are very significant statistically ($p<0.01$) decrease 17.63mm and 26.75mm per decade respectively (Table 1).

(a)

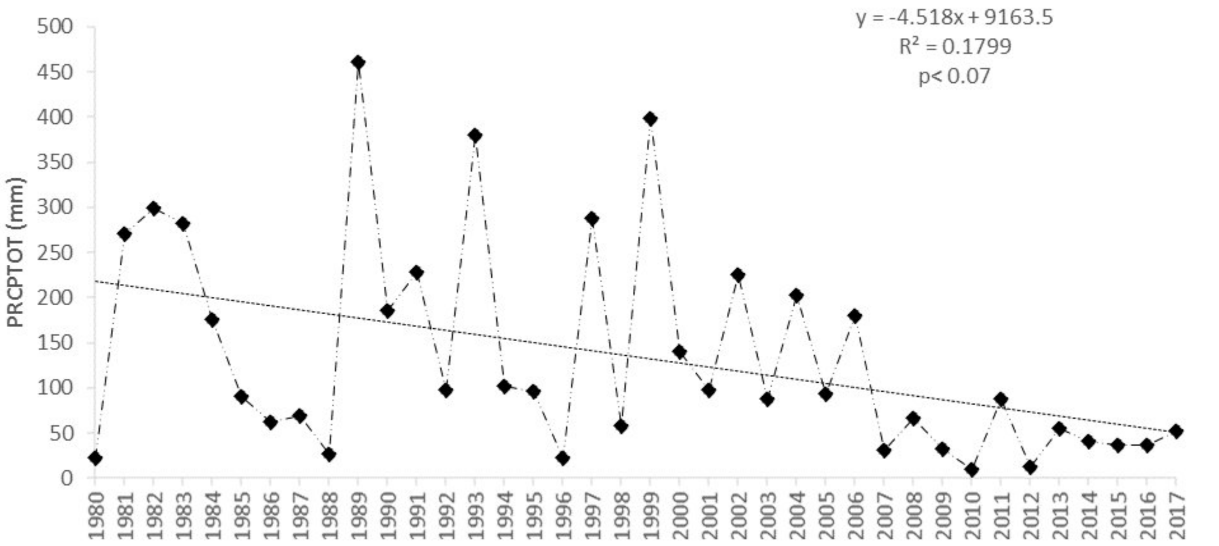
y = -4.518x + 9163.5
R² = 0.1799
p< 0.07
PRCPTOT (mm)

(b)

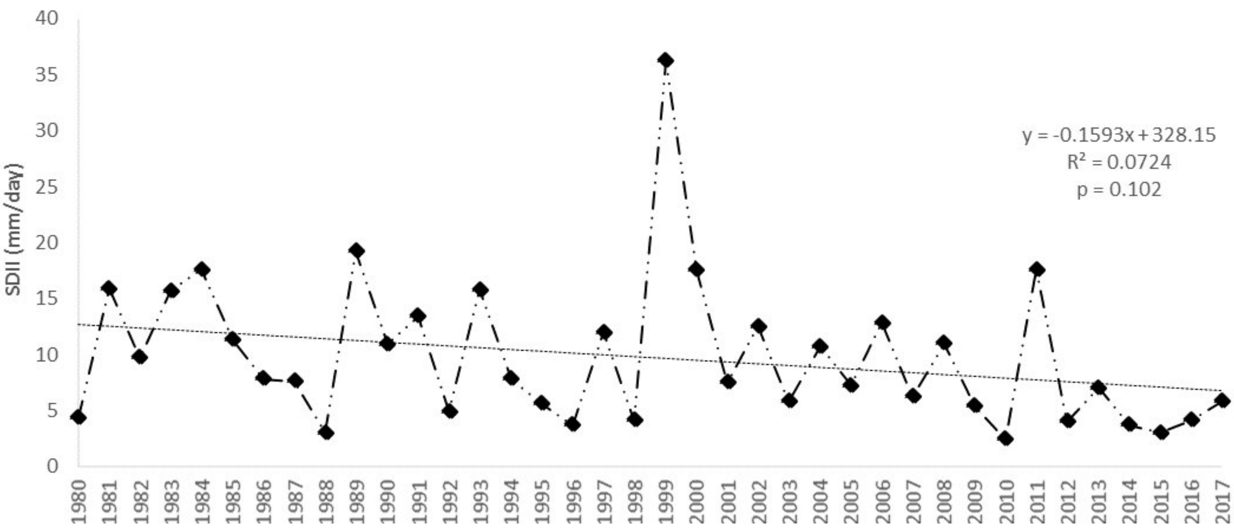
y = -0.1593x + 328.15
R² = 0.0724
p = 0.102
SDII (mm/day)

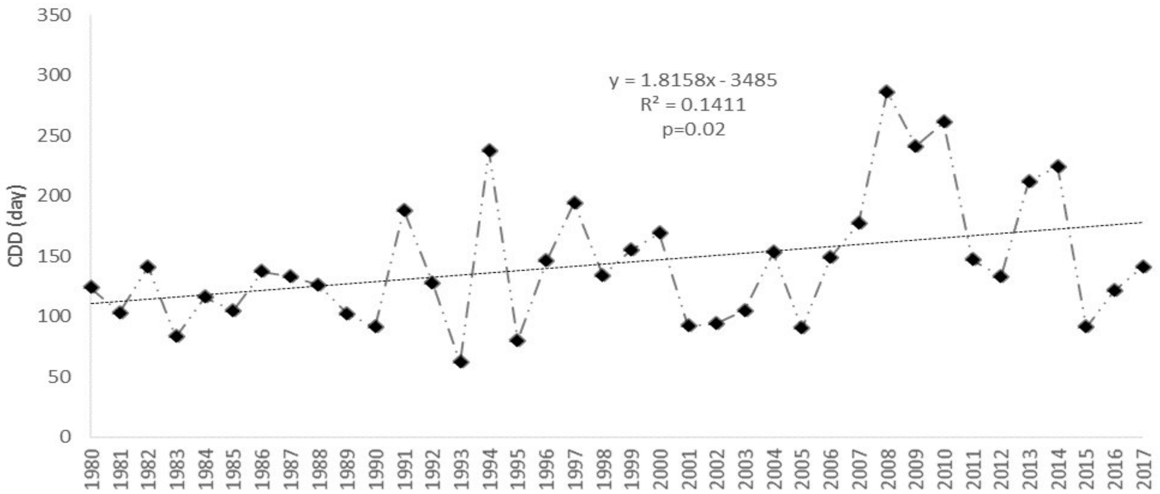
y = 1.8158x - 3485
R² = 0.1411
p=0.02
CDD (day)

(c)

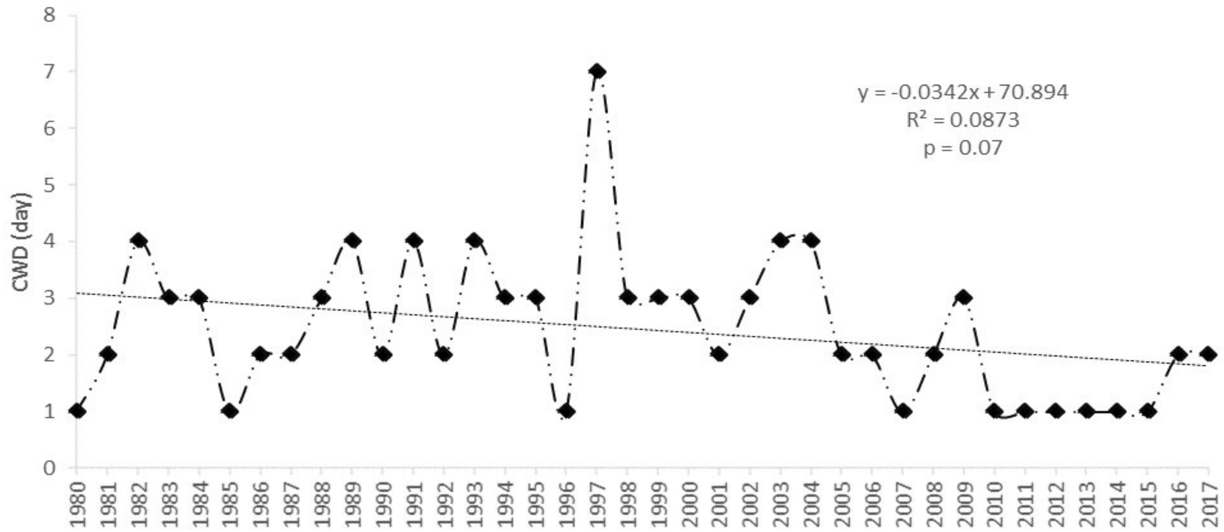
y = -0.0342x + 70.894
R² = 0.0873
p = 0.07
CWD (day)

(d)

(e)

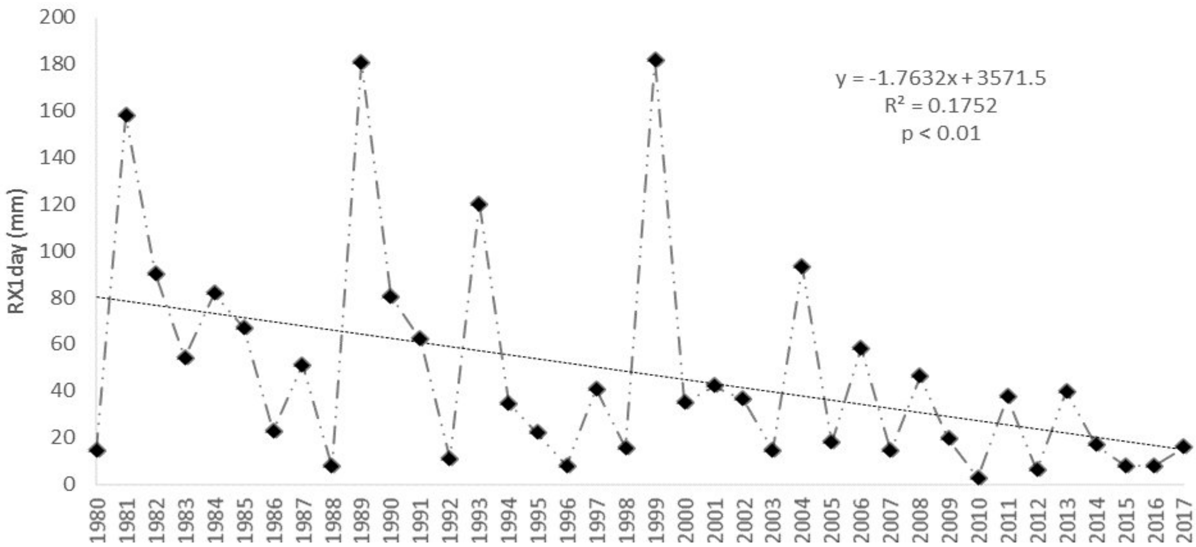
y = -1.7632x + 3571.5
R² = 0.1752
p < 0.01
RX1day (mm)

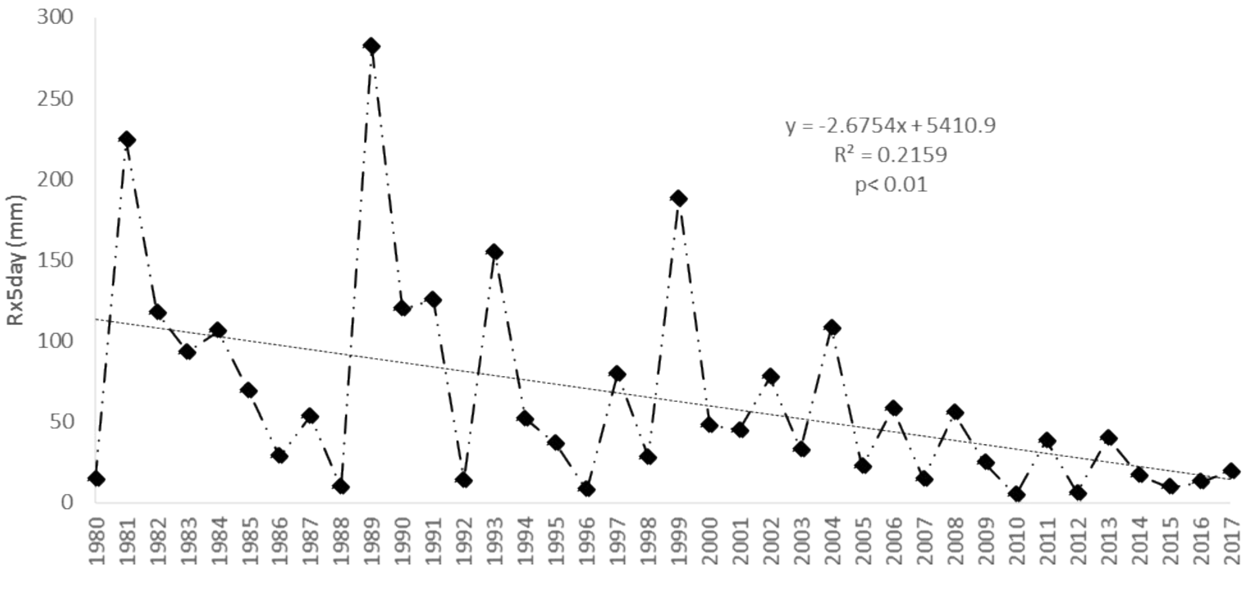
y = -2.6754x + 5410.9
R² = 0.2159
p< 0.01
Rx5day (mm)

(f)

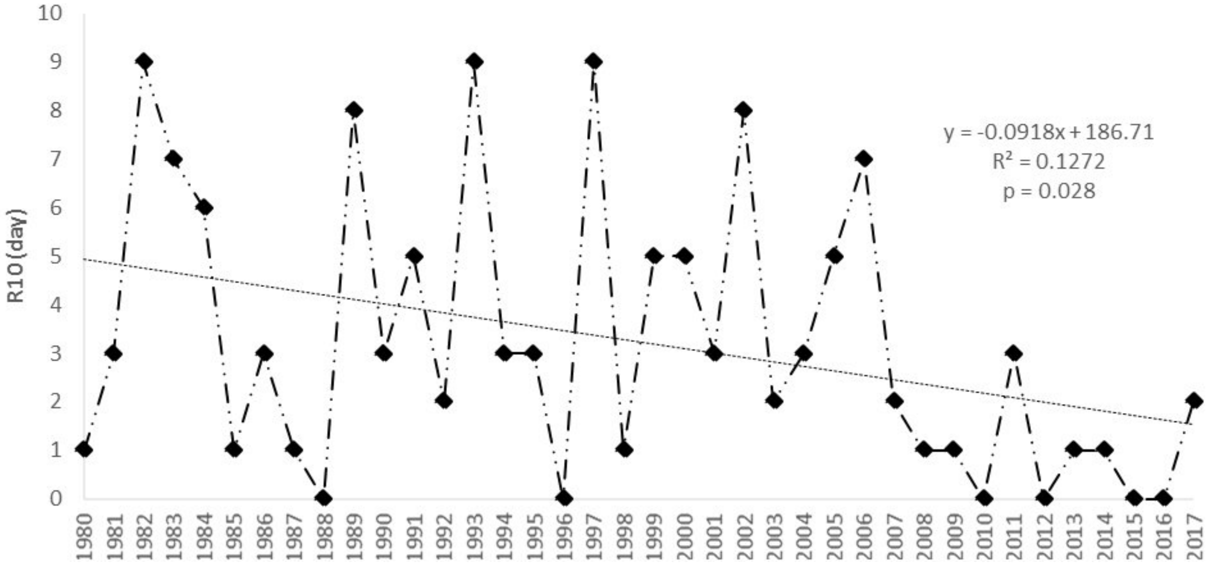
R10 (day)
y = -0.0918x + 186.71
R² = 0.1272
p = 0.028

(g)

(h)

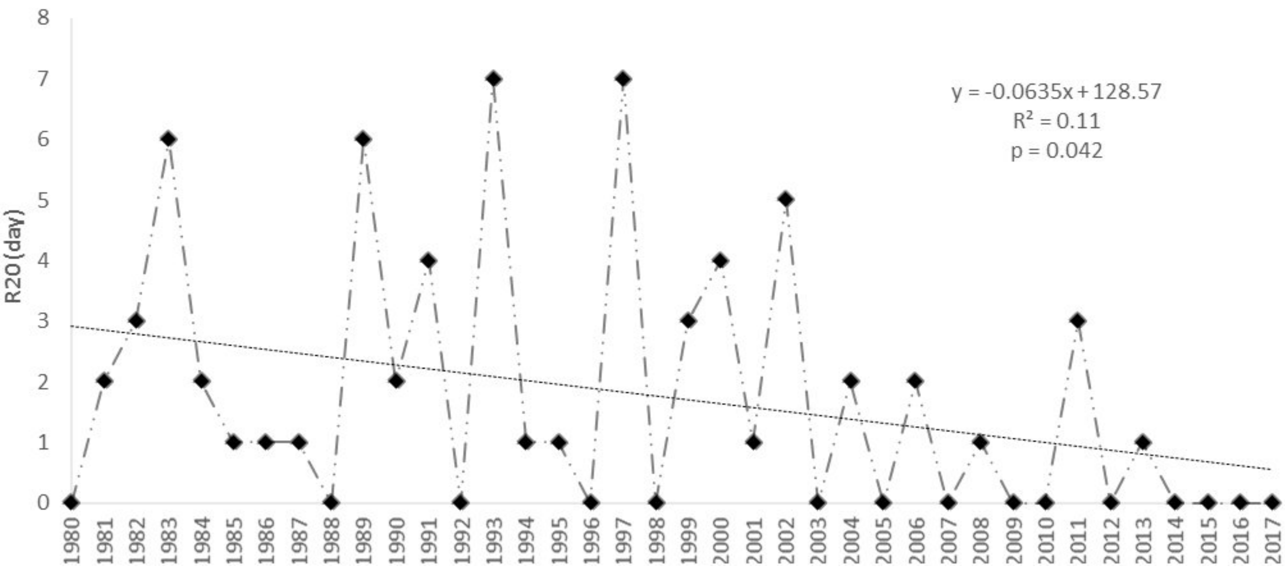
R20 (day)
y = -0.0635x + 128.57
R² = 0.11
p = 0.042

(i)

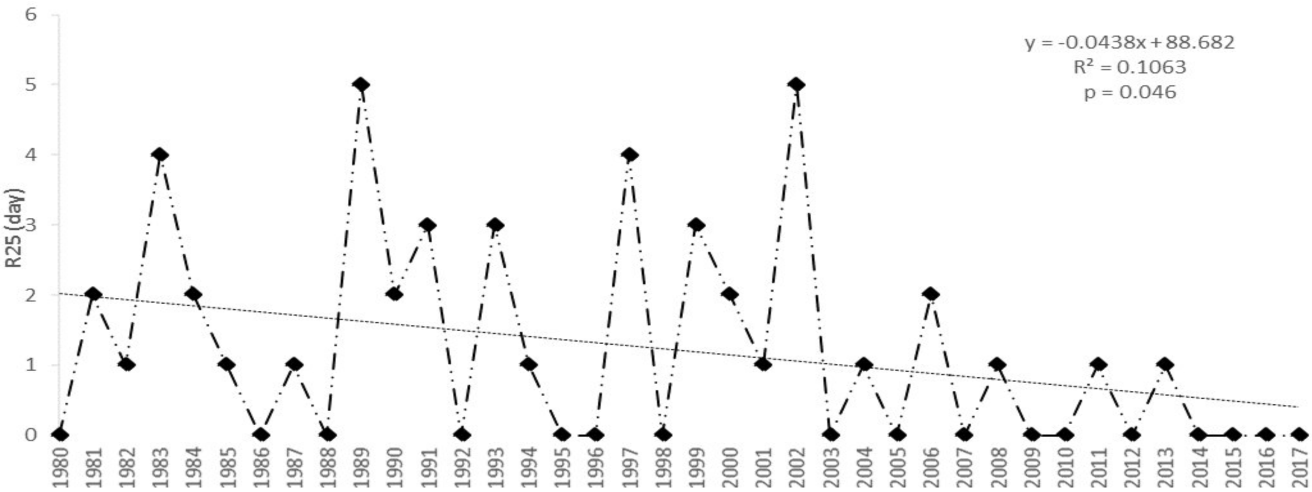
R25 (day)
y = -0.0438x + 88.682
R² = 0.1063
p = 0.046

(j)

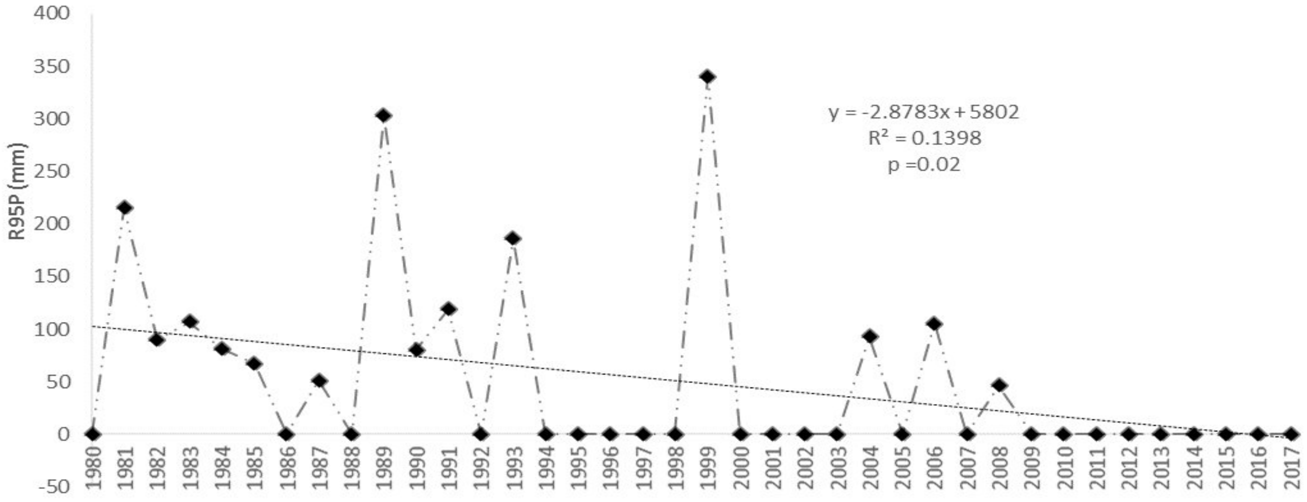
y = -2.8783x + 5802
R² = 0.1398
p =0.02
R95P (mm)

(k)

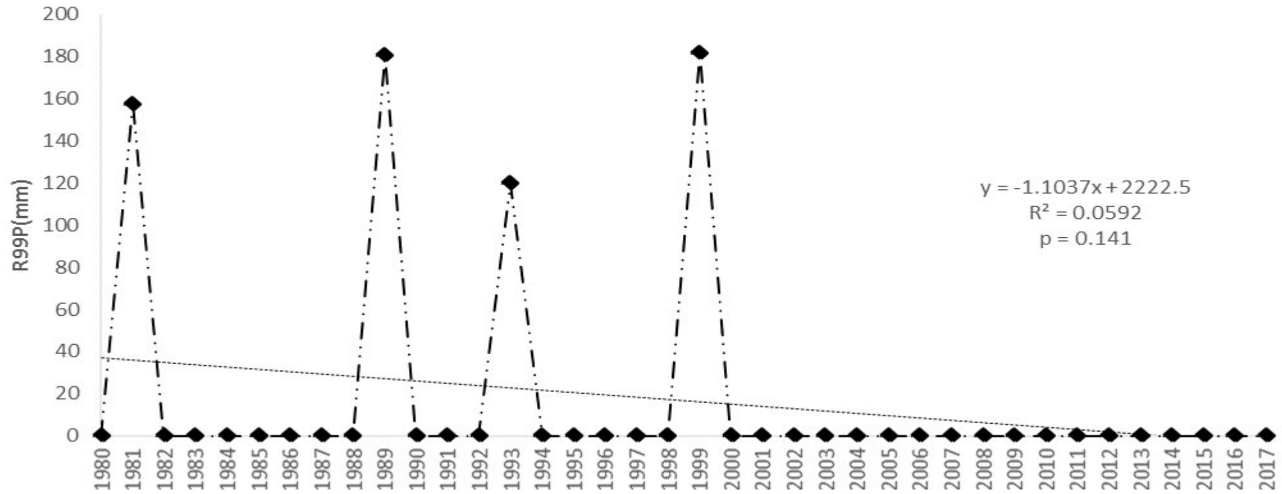
y = -1.1037x + 2222.5
R² = 0.0592
p = 0.141
R99P(mm)

(l)

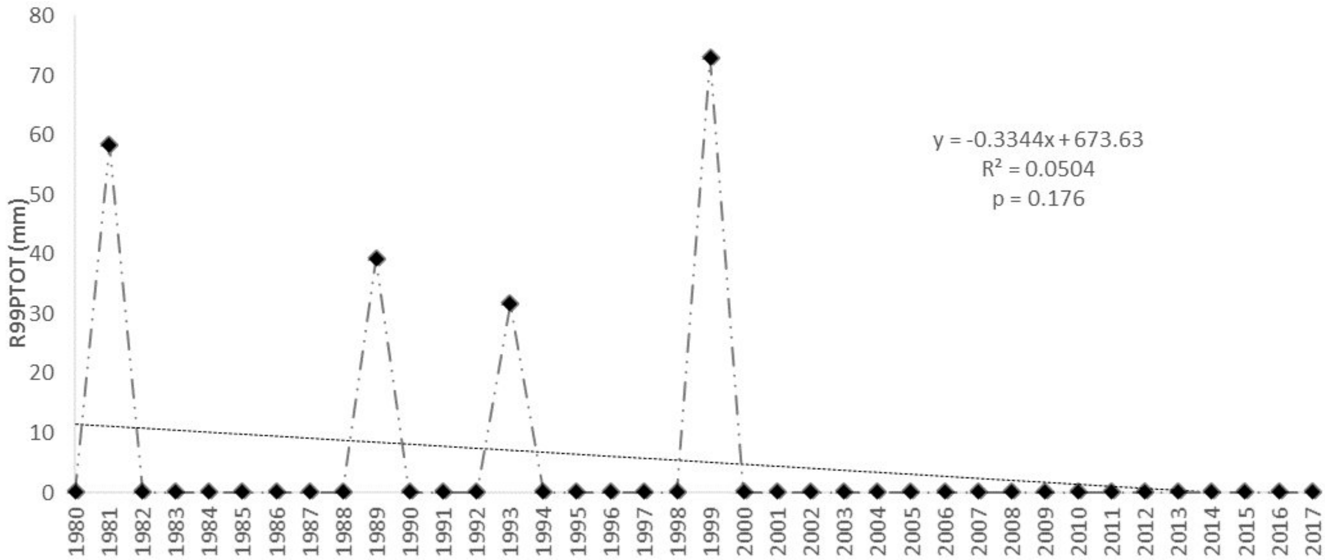
y = -0.3344x + 673.63
R² = 0.0504
p = 0.176
R99PTOT (mm)

(m)

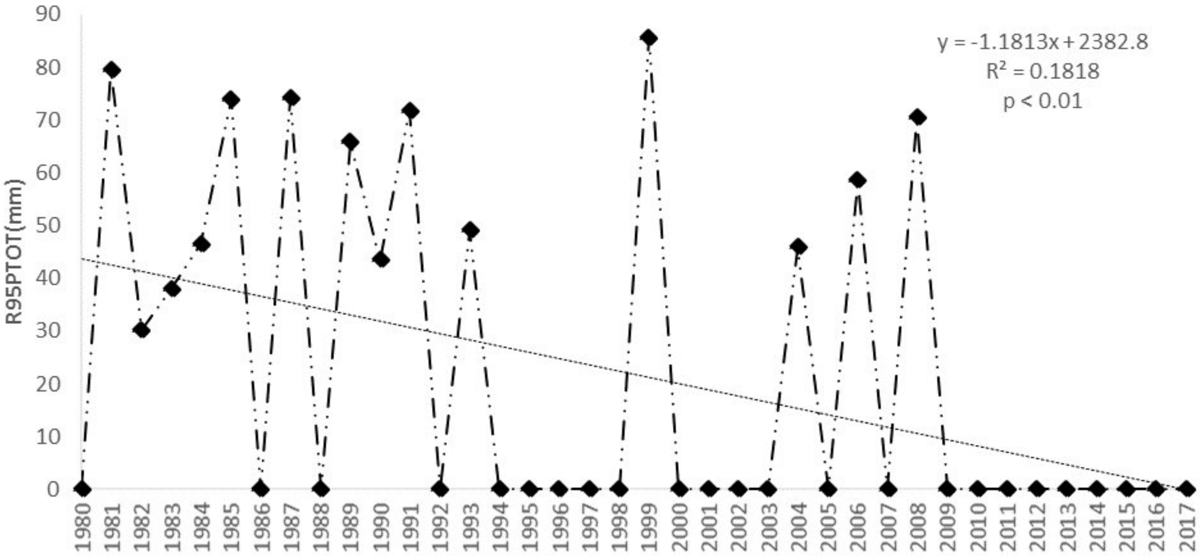

(n)

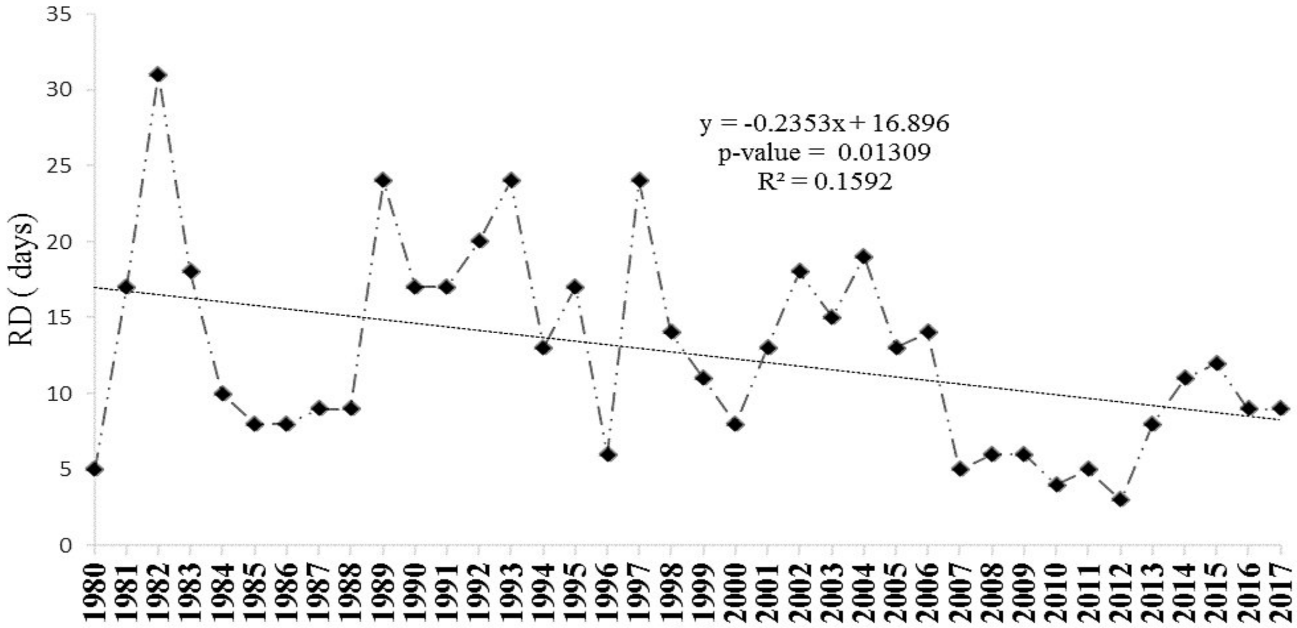

Figure7. Precipitation indices trend

5.2. Air Temperature Change Study

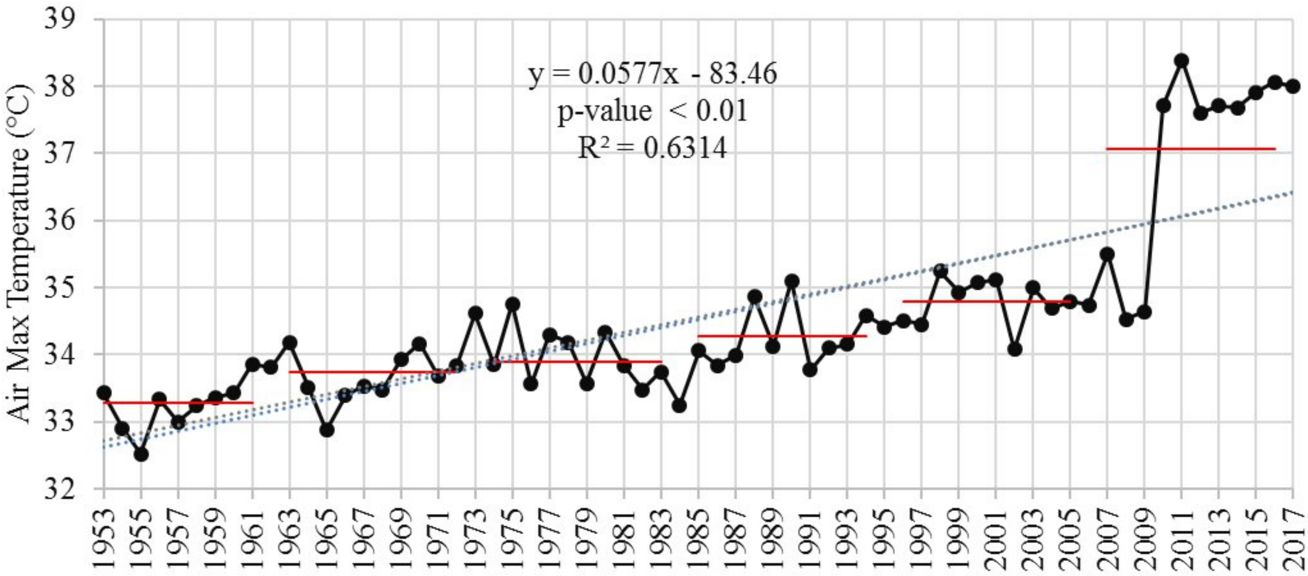

Figure 1. Air max temperature average variation for Djibouti over the period (1953-2017)

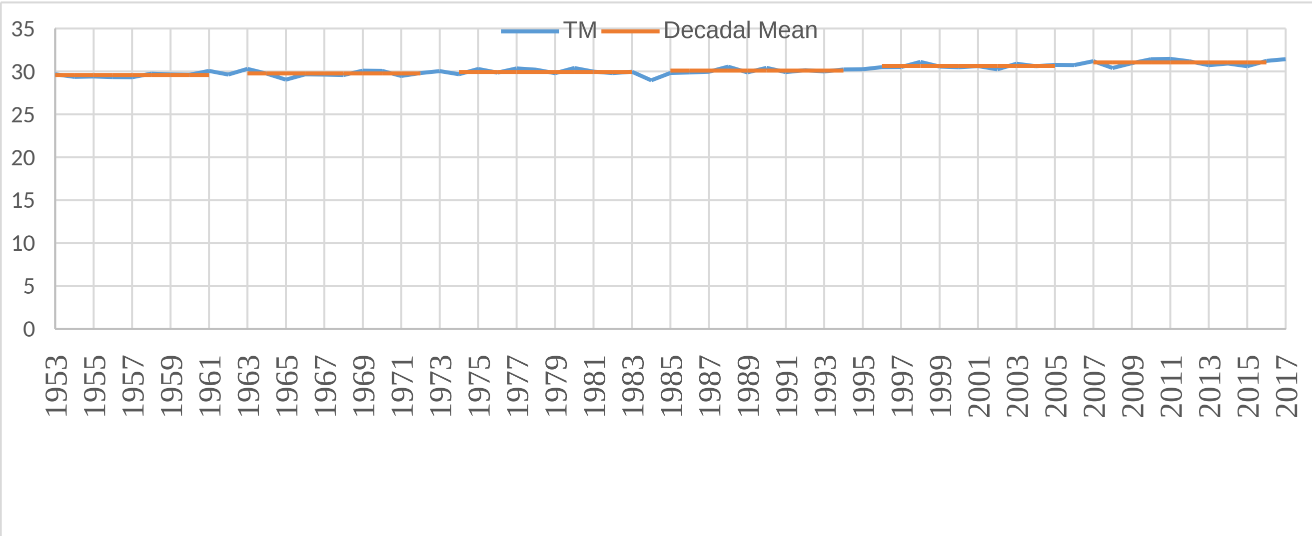

Figure 2. Air mean temperature average variation for Djibouti over the period (1953-2017)

Figure 3. Air min temperature average variation for Djibouti over the period (1953-2017)

Figure Max, mean and min Temperature Average Variation in Djibouti over the period (1953-2017)

(a)

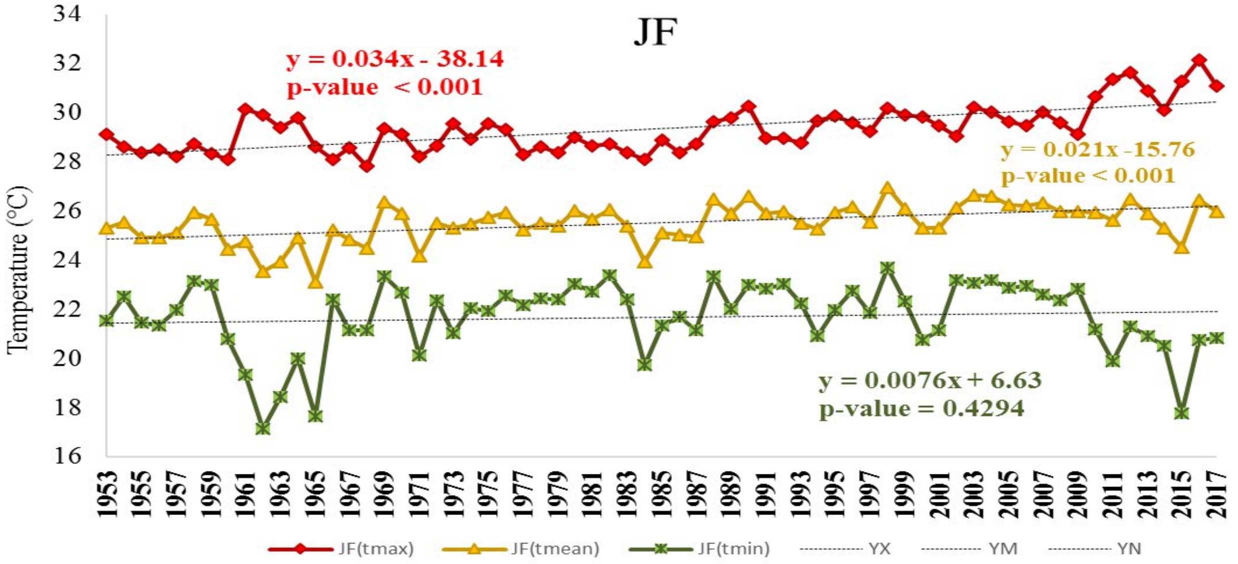
JF
y = 0.034x - 38.14
p-value < 0.001
y = 0.021x -15.76
p-value < 0.001
y = 0.0076x + 6.63
p-value = 0.4294
Temperature (°C)
JF(tmax)
JF(tmean)
JF(tmin)
YX
YM
YN

(b)

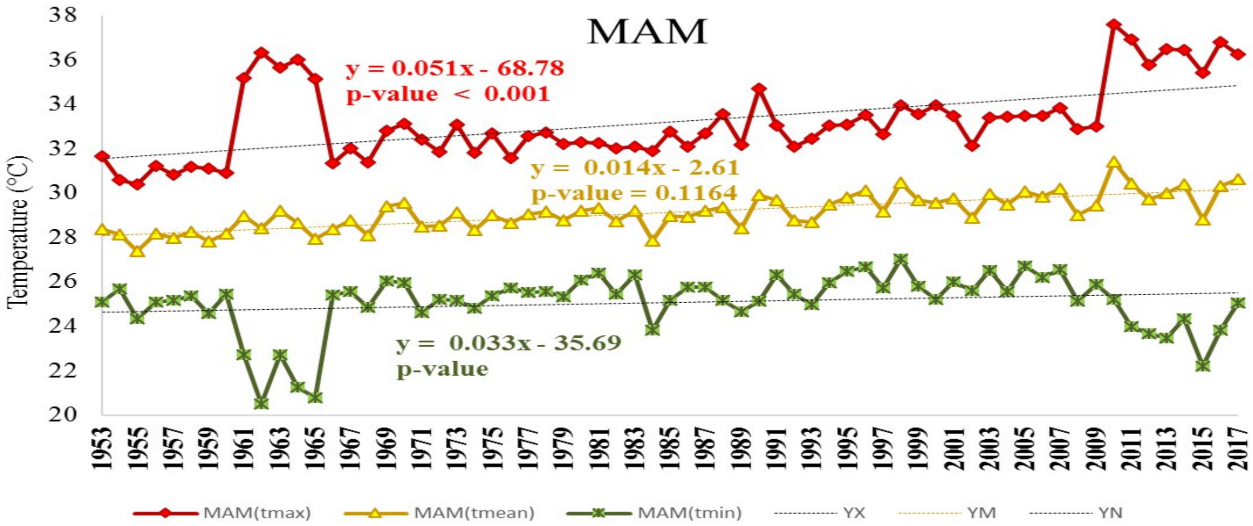
MAM
y = 0.051x - 68.78
p-value < 0.001
y = 0.014x - 2.61
p-value = 0.1164
y = 0.033x - 35.69
p-value
Temperature (°C)
MAM(tmax)
MAM(tmean)
MAM(tmin)
YX
YM
YN

(c)

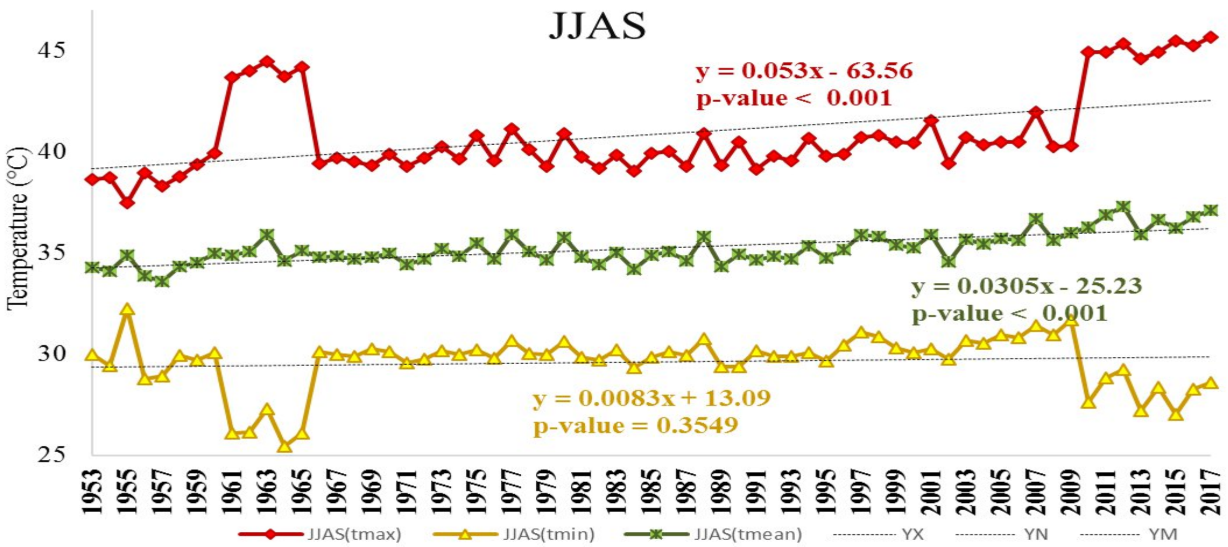

(d)

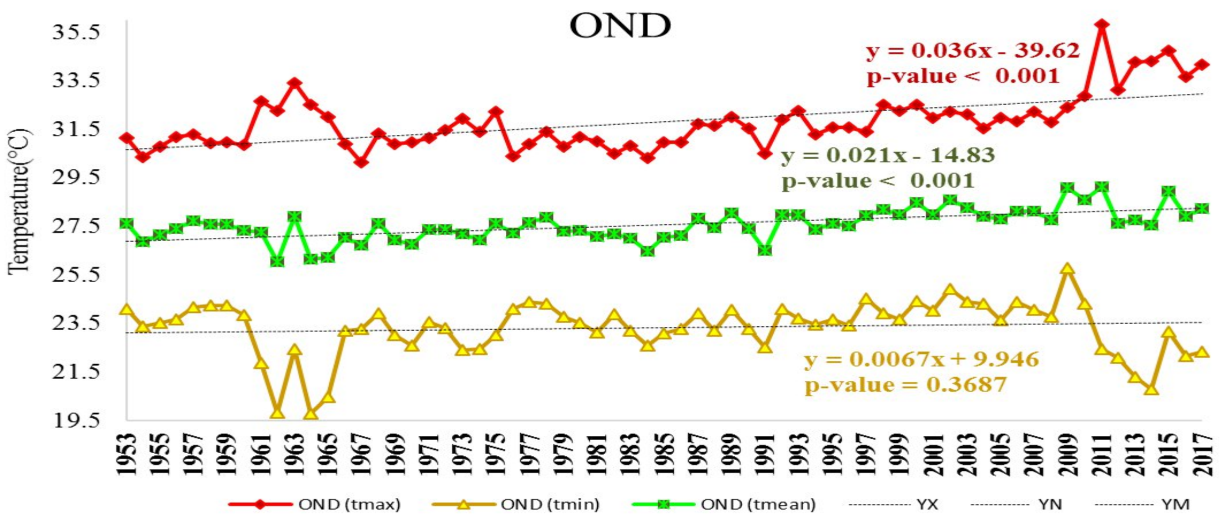

Figure 4. Seasonal Air temperature variation for Djibouti over the period (1953-2017)

	Season JF	Season MAM	Season JJAS	Season OND
z	11.77	5.58	4.98	5.17
n	65	65	65	65
s	2080	986	881	914
varS	31200	31200	31196	31200
tau	1	0.474	0.423	0.44
p.value	< 0.001	< 0.001	< 0.001	< 0.001

Table1. Mann-Kendall trend seasonal test for Maximal Temperature in Djibouti over 1953-201

	Season JF	Season MAM	Season JJAS	Season OND
z	0.41328	1.6984	1.31	0.93
n	65	65	65	65
s	7.4	301	23.40	165
varS	31.20	31199	31200	31199
tau	0.036	0.144	0.112	0.0793

p.value	0.6794	0.08942	0.1871	0.3532

Table1. Mann-Kendall trend seasonal test for Minimal Temperature in Djibouti over 1953-2017

	Season JF	**Season MAM**	**Season JJAS**	**Season OND**
z	4.27	6.99	6.04	5.21
n	65	65	65	65
s	756	1236	1068	921
varS	31200	31200	31200	31199
tau	0.36	0.594	0.513	0.44
p.value	< 0.001	< 0.001	< 0.001	< 0.001

Table1. Mann-Kendall trend seasonal test for Mean Temperature in Djibouti over 1953-2017

		jibouti-City (1953-2010)			**a (1943-2015)**	**thiopia**	**enya**	**obal**
Index	**nits**	**end**	**alue**	**l average**	**Trend**	**Trend**	**rend**	**end**
	ay	002	596	55.05	**0.596**	0.11	**.35**	**.21**
Mean	C	**021**	**000**	4.18	**0.013**	NA	NA	
Mean	C	**013**	**000**	6.08	**0.019**	NA	**-1.6**	**.62**
	C	**058**	**012**	7.40	**-0.022**	NA	NA	A
	C	**027**	**.00**	4.49	**0.038**	NA	NA	A
	ays	**206**	**026**	48.89	NA	NA	NA	A
P	ays	.078	105	.56	NA	**−1.23**	**1.10**	**.26**
P	ays	**178**	**000**	.76	NA	**2.14**	**.44**	**.58**
P	ays	**.226**	**000**	.55	NA	**−1.0**	**-1.6**	**.62**
P	ays	**167**	**000**	.55	NA	0.65	**.07**	**.89**
	C	**021**	**.05**	6.40	**0.032**	NA	NA	A
	C	**023**	**.00**	5.40	0.009	NA	NA	A
	ays	**224**	**000**	4.53	NA	NA	NA	A
	ays	.033	555	4.98	NA	NA	NA	A
	C	**009**	**024**	3.09	-0.006	0.61	NA	.08

Notes: A trend significant at the 5% level is marked with bold font. Regional and Global trends are from Omandi et al (2013)

Table2. Summary of trends (units of decade) and annual average of the precipitation indices for the analyzed station of airport of Djibouti

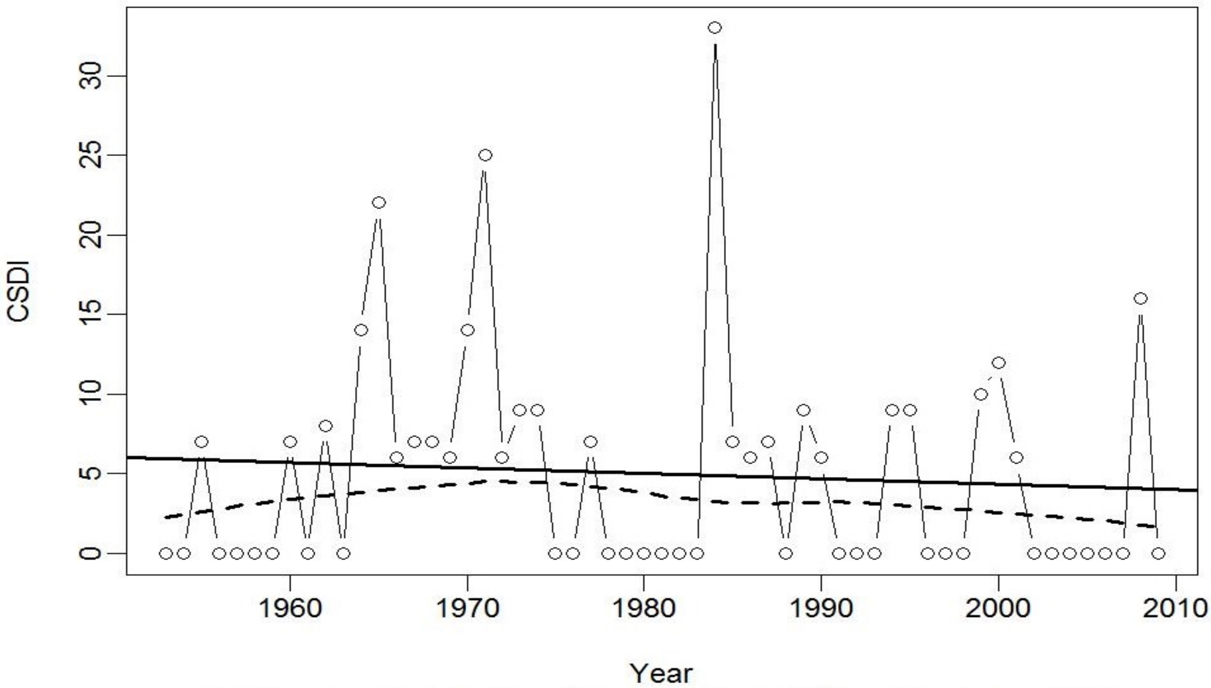

R2= 0.6 p-value= 0.555 Slope estimate= -0.033 Slope error= 0.056

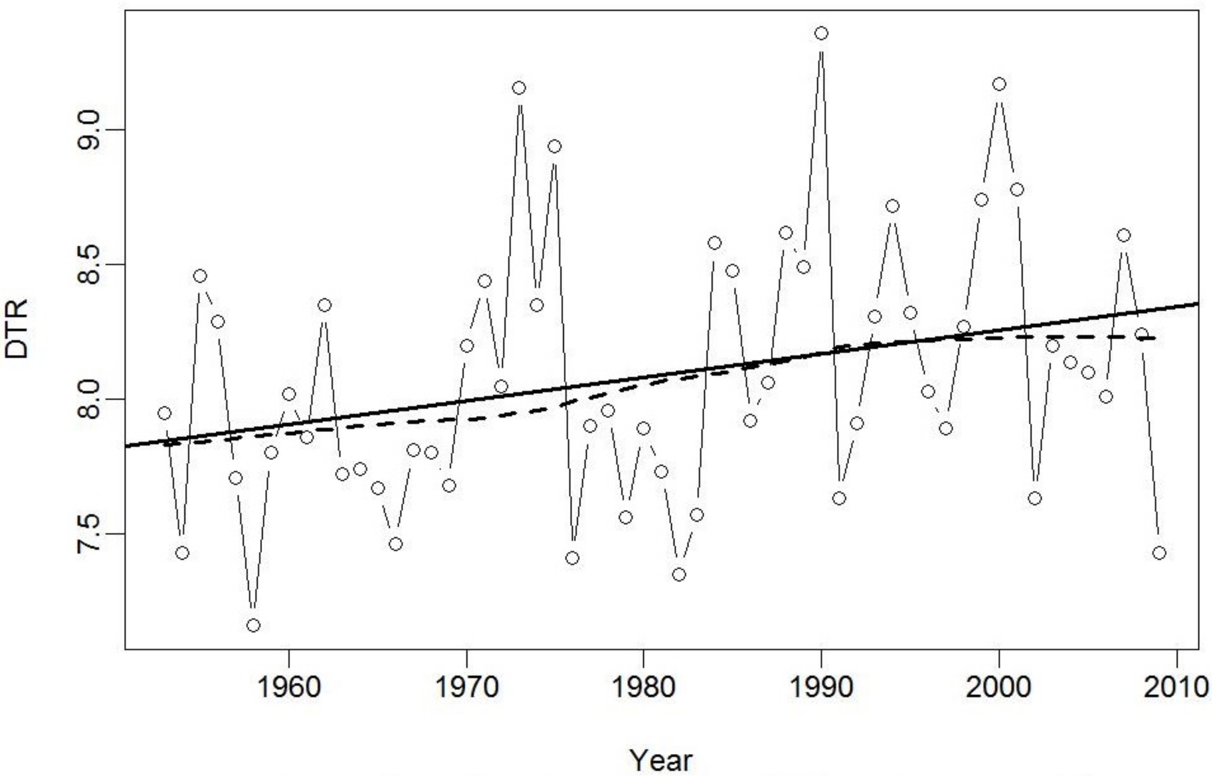

R2= 8.9 p-value= 0.024 Slope estimate= 0.009 Slope error= 0.004

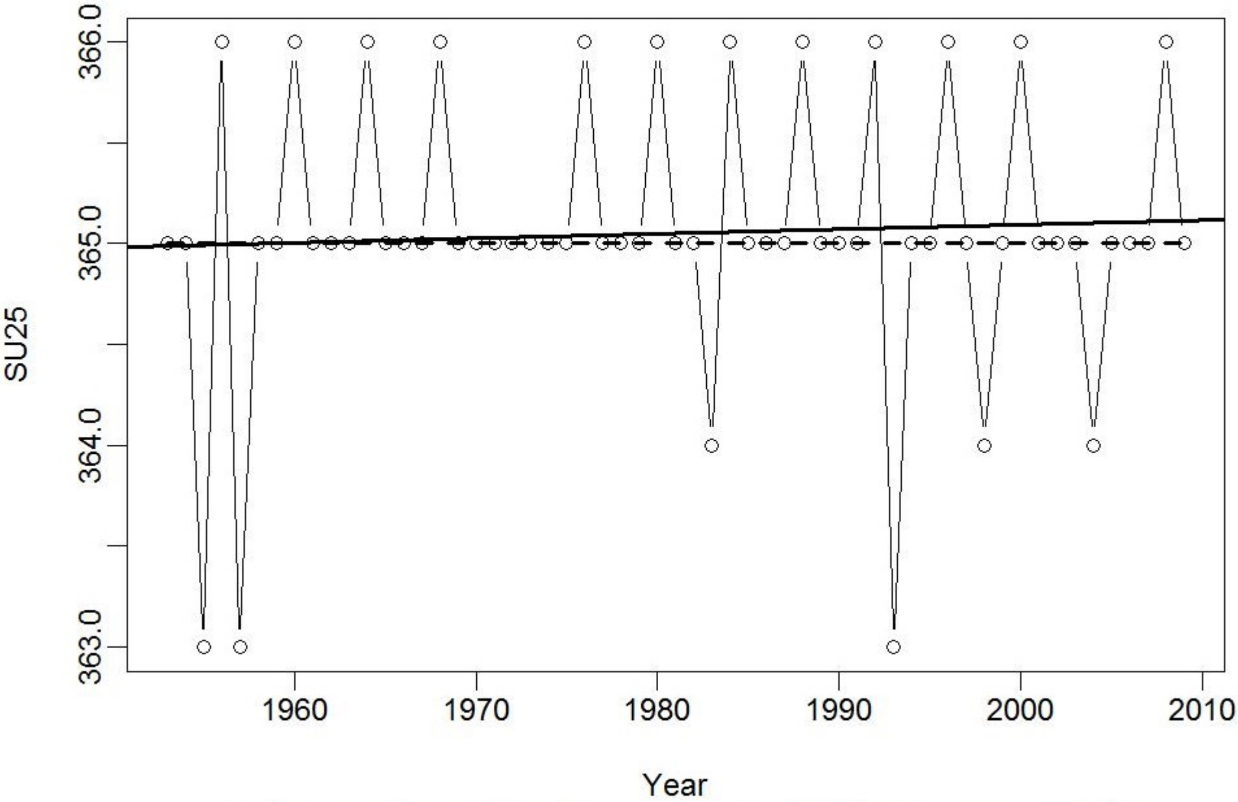

R2= 0.3 p-value= 0.696 Slope estimate= 0.002 Slope error= 0.006

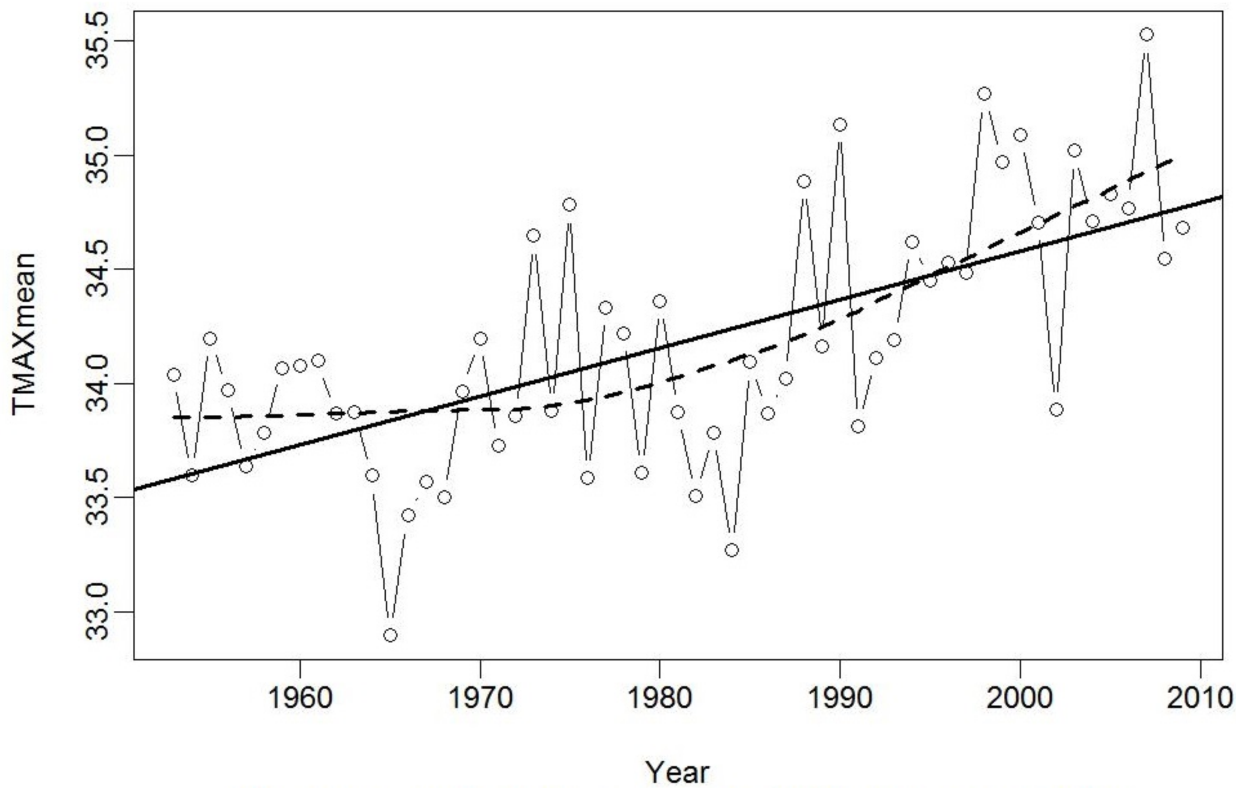

R2= 41.1 p-value= 0 Slope estimate= 0.021 Slope error= 0.003

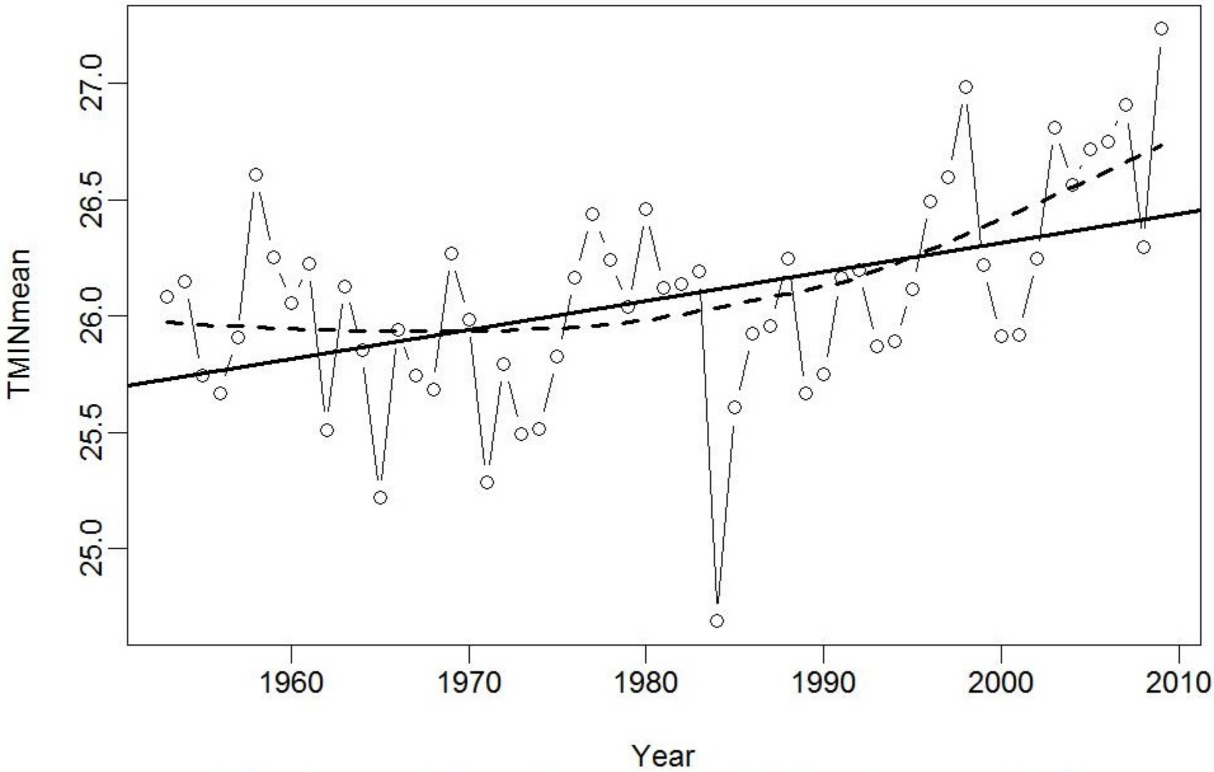

R2= 20.9 p-value= 0 Slope estimate= 0.013 Slope error= 0.003

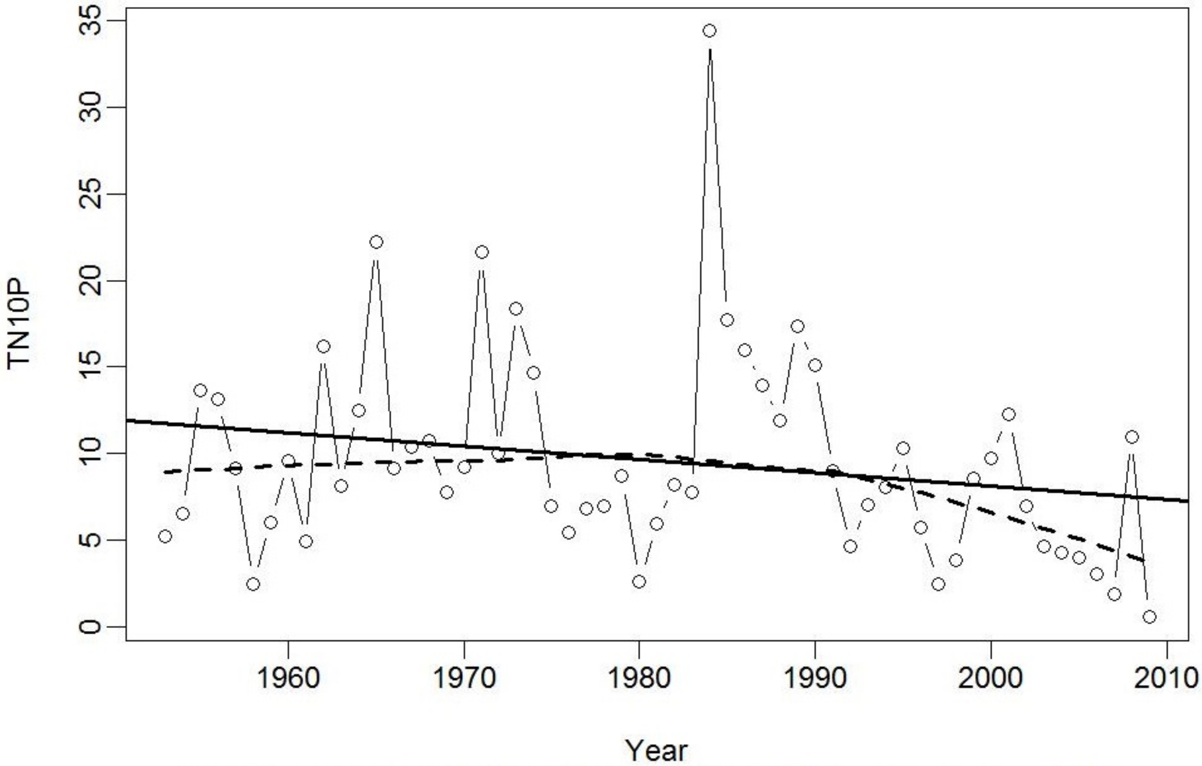

R2= 4.7 p-value= 0.105 Slope estimate= -0.078 Slope error= 0.047

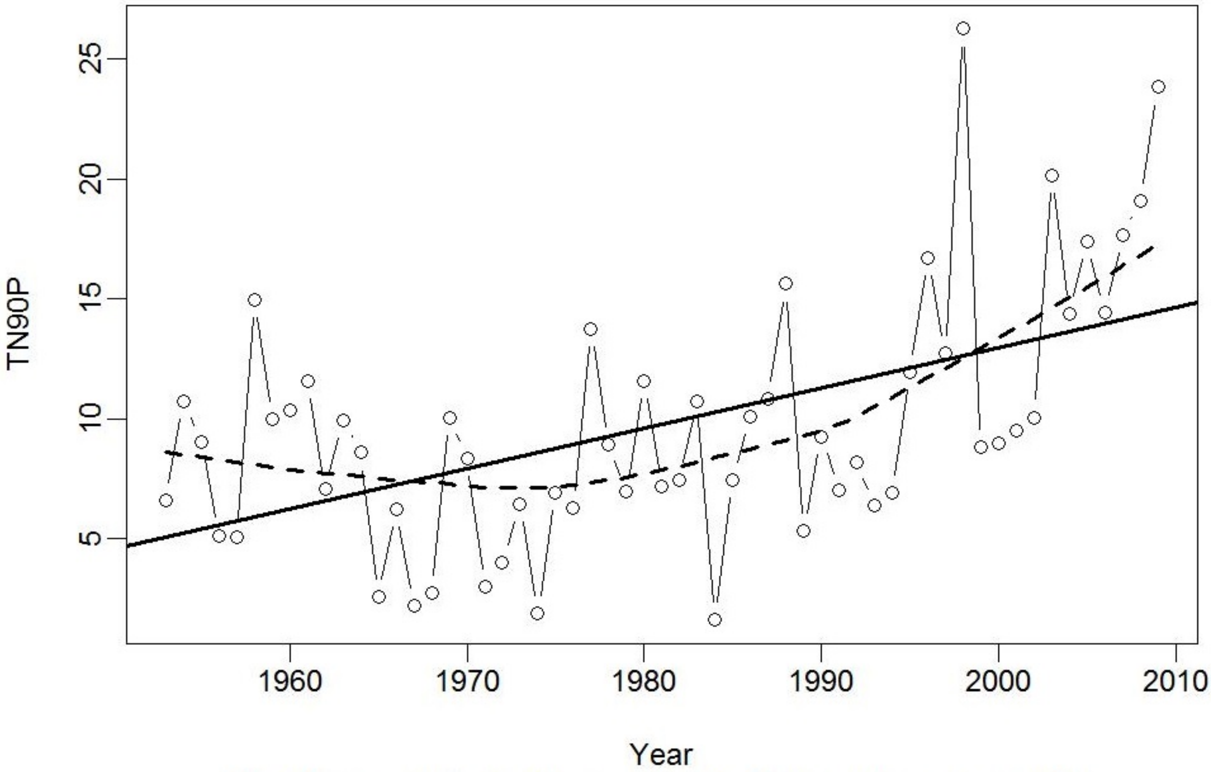

R2= 28.2 p-value= 0 Slope estimate= 0.167 Slope error= 0.036

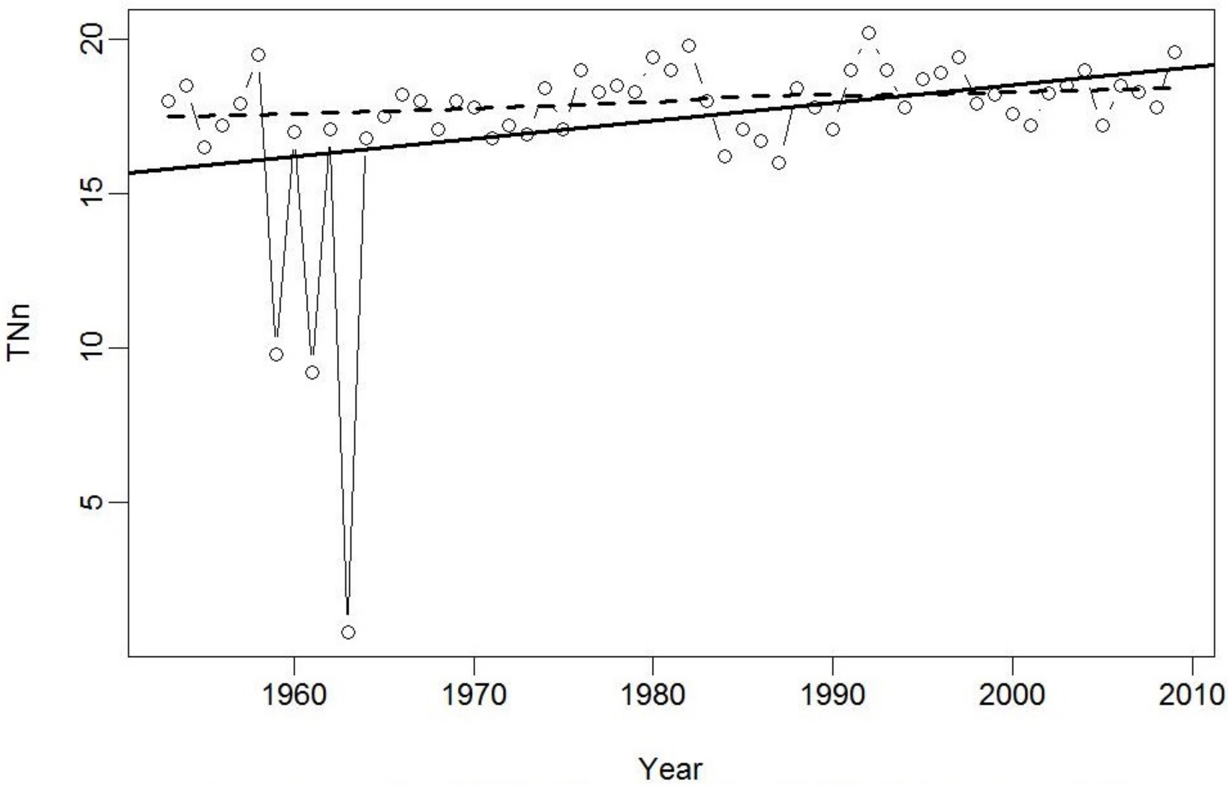

R2= 11 p-value= 0.012 Slope estimate= 0.058 Slope error= 0.022

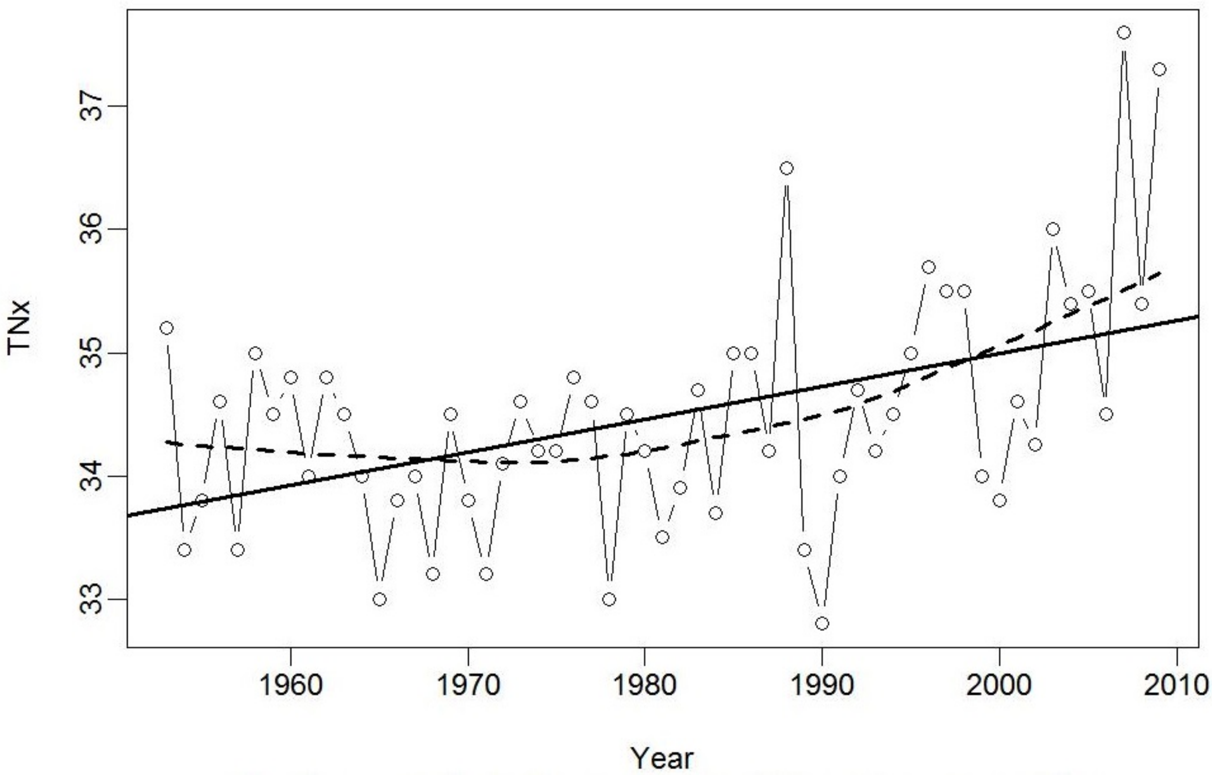

R2= 21.3 p-value= 0 Slope estimate= 0.027 Slope error= 0.007

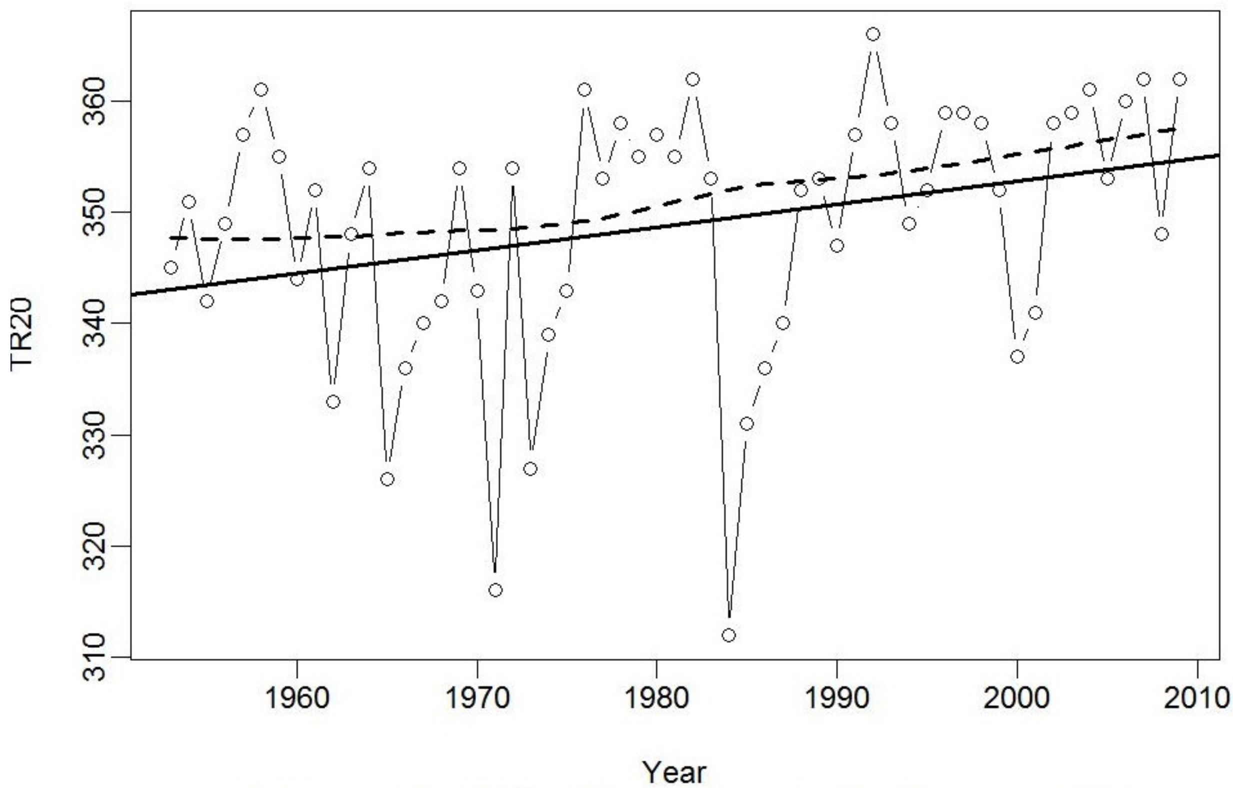

R2= 8.7 p-value= 0.026 Slope estimate= 0.206 Slope error= 0.09

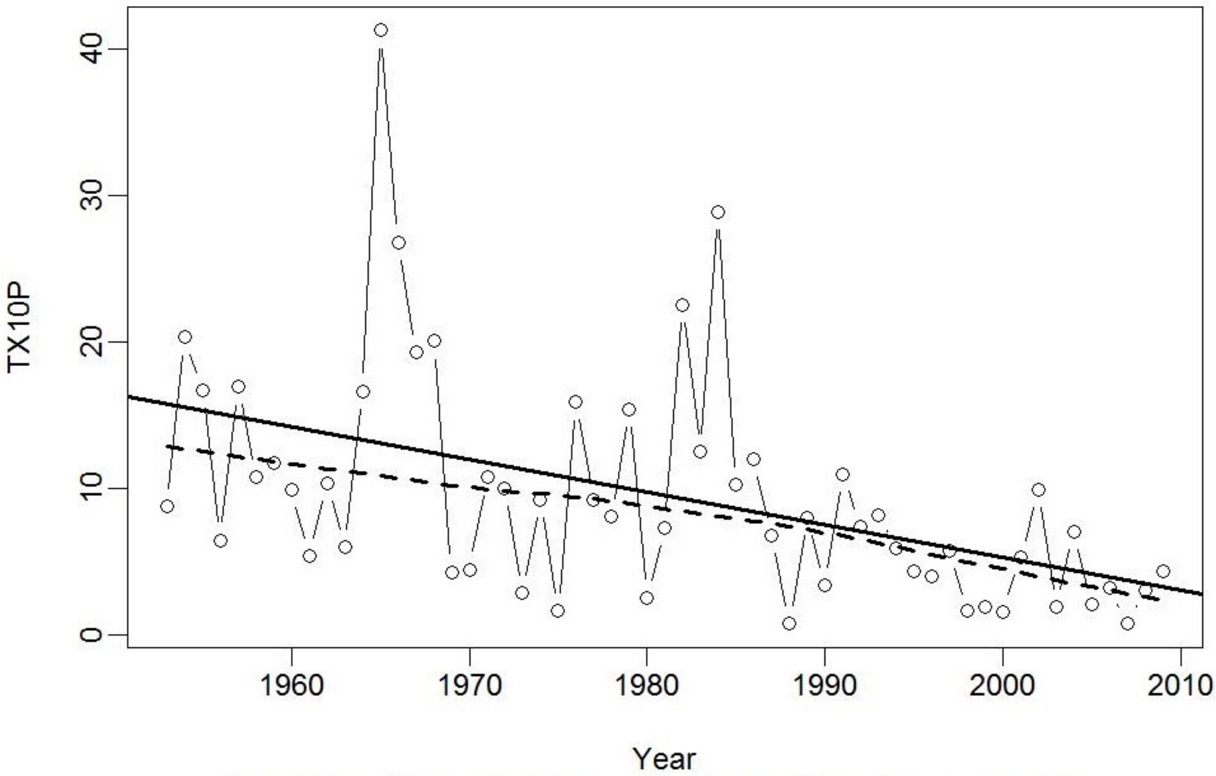

R2= 22.6 p-value= 0 Slope estimate= -0.223 Slope error= 0.056

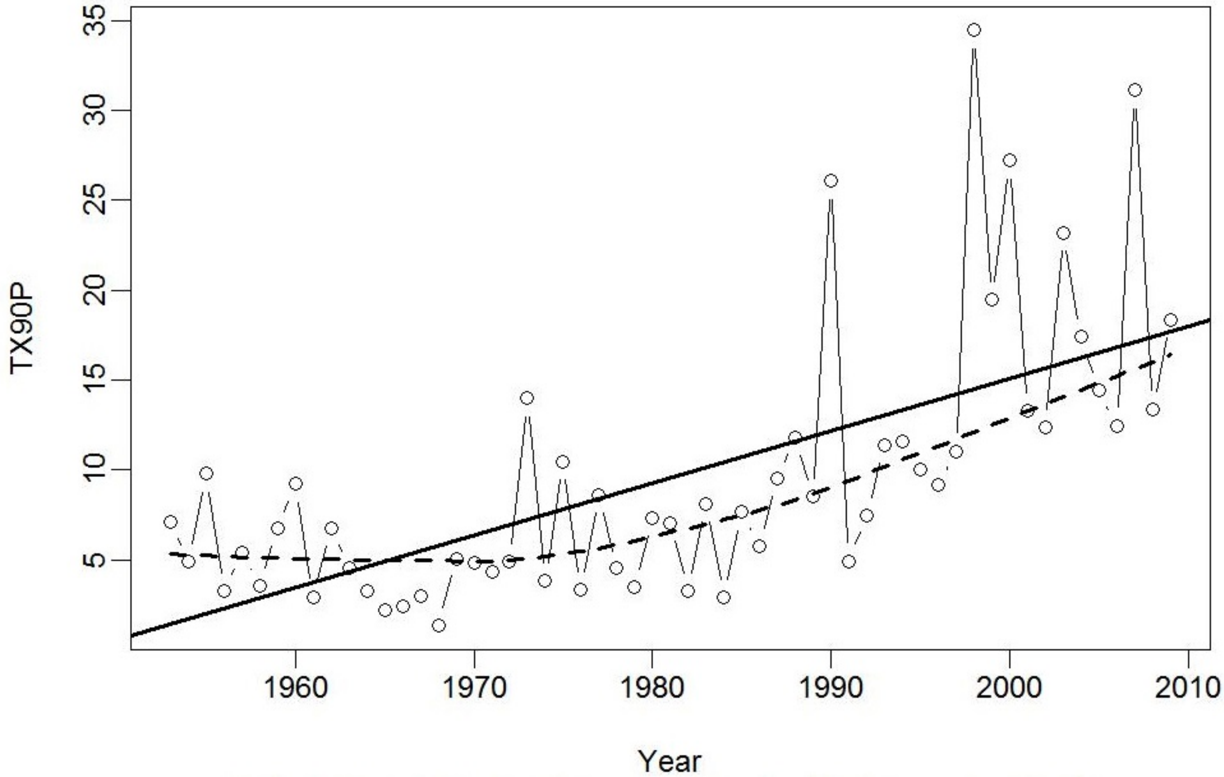

R2= 42.9 p-value= 0 Slope estimate= 0.29 Slope error= 0.045

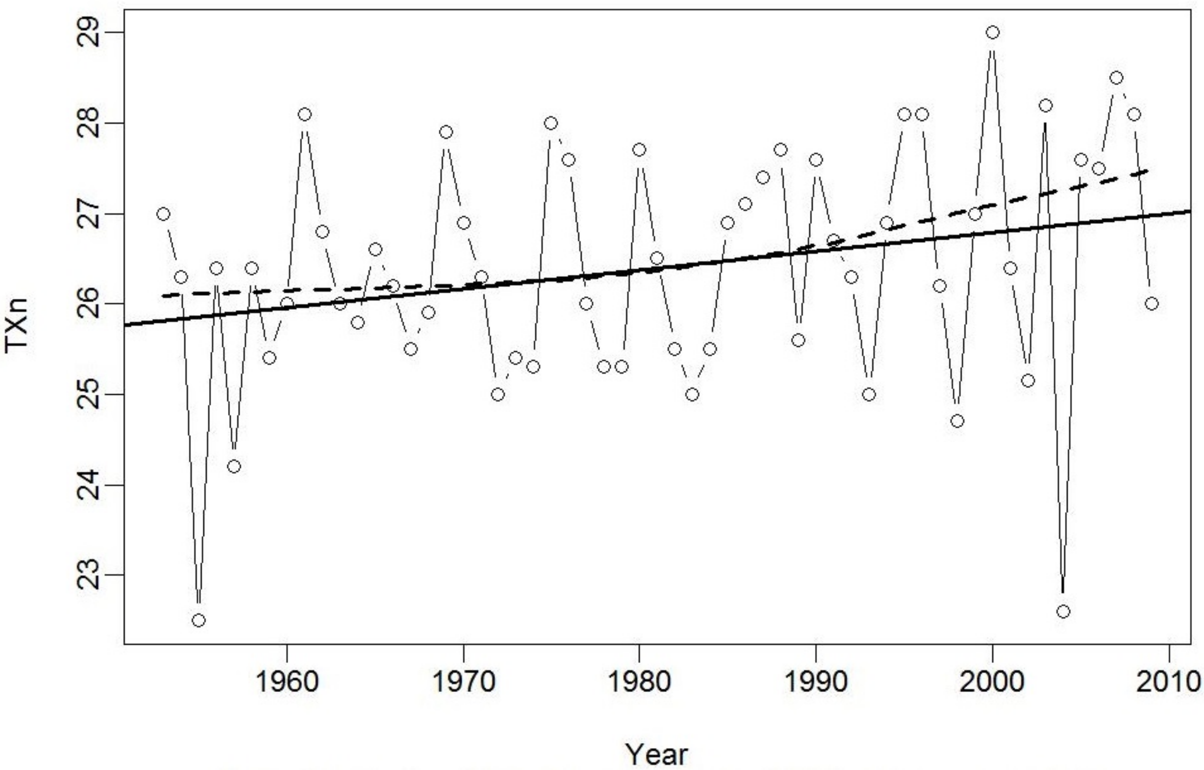

R2= 6.8 p-value= 0.05 Slope estimate= 0.021 Slope error= 0.01

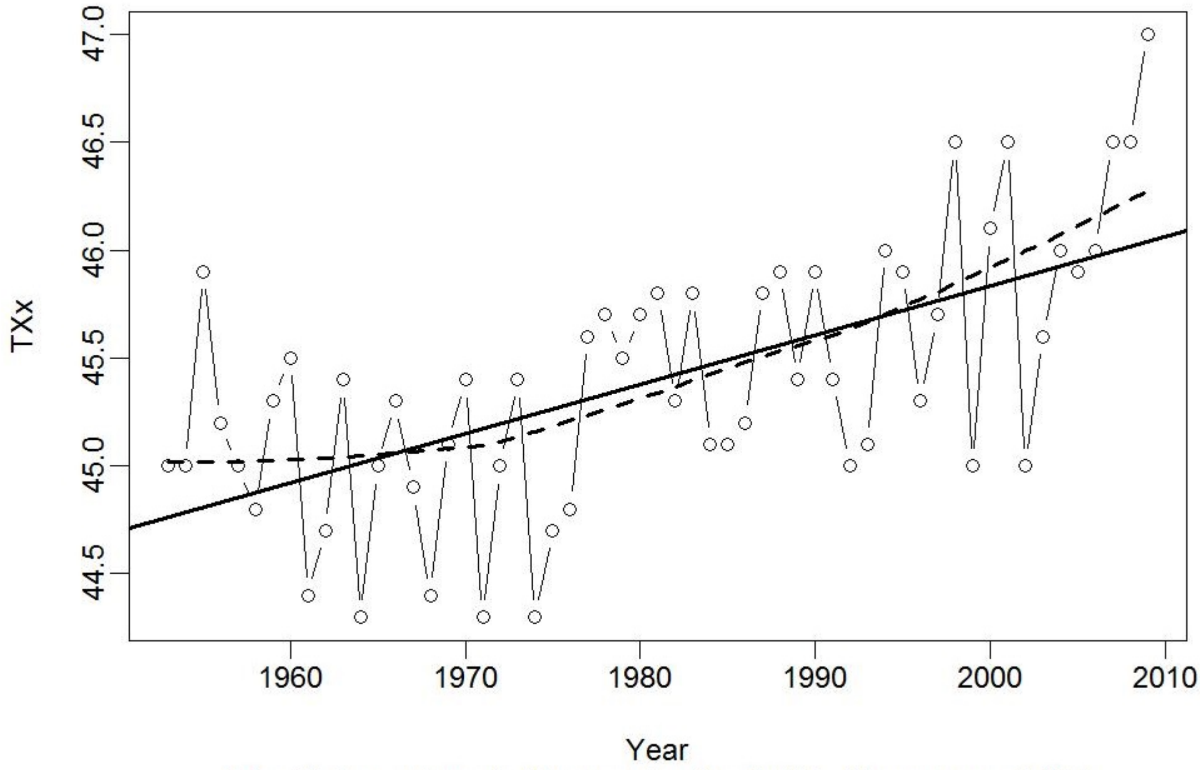

R2= 39.6 p-value= 0 Slope estimate= 0.023 Slope error= 0.004

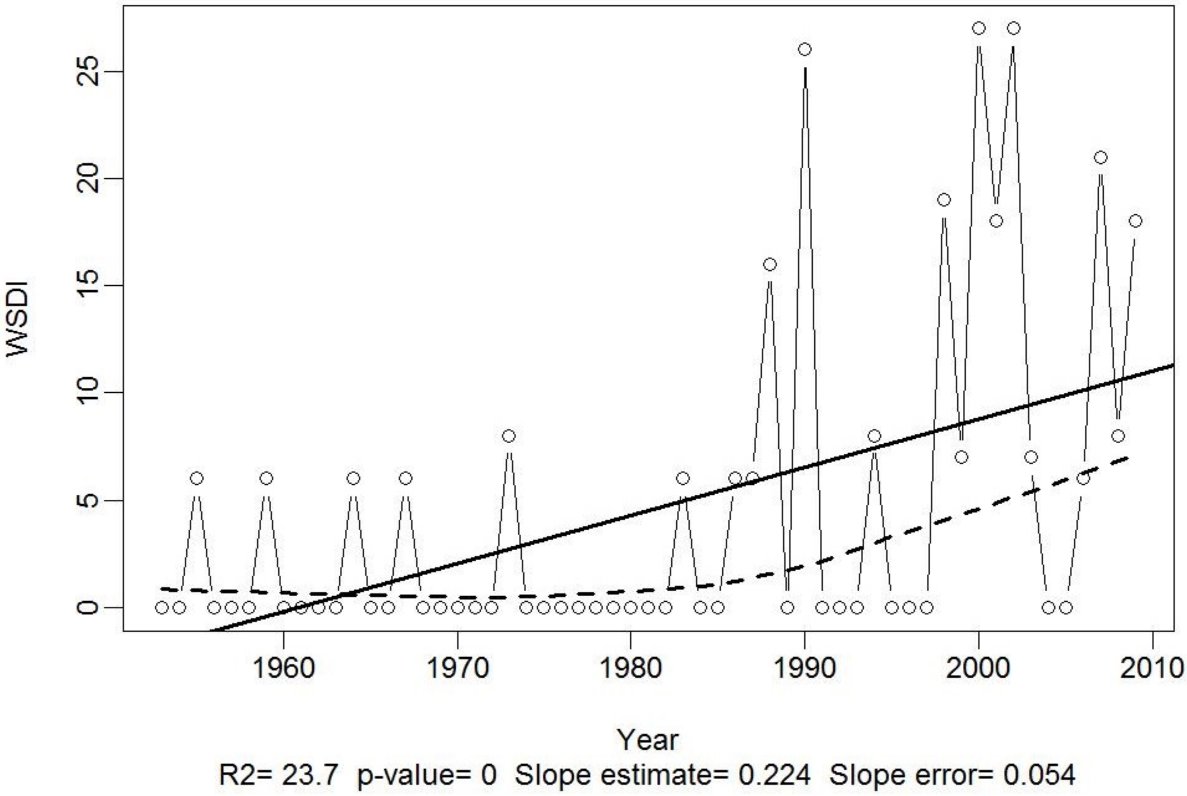

i. **Forecast of Annual Precipitation and Temperature**
ii. **Principal Component Analysis of precipitation and temperature index**
iii. **Spatial Assessment of Precipitation over Djibouti (1980-2017)**
iv. **Anomaly Section**
v. **Standardized section**

- ANNEXE -

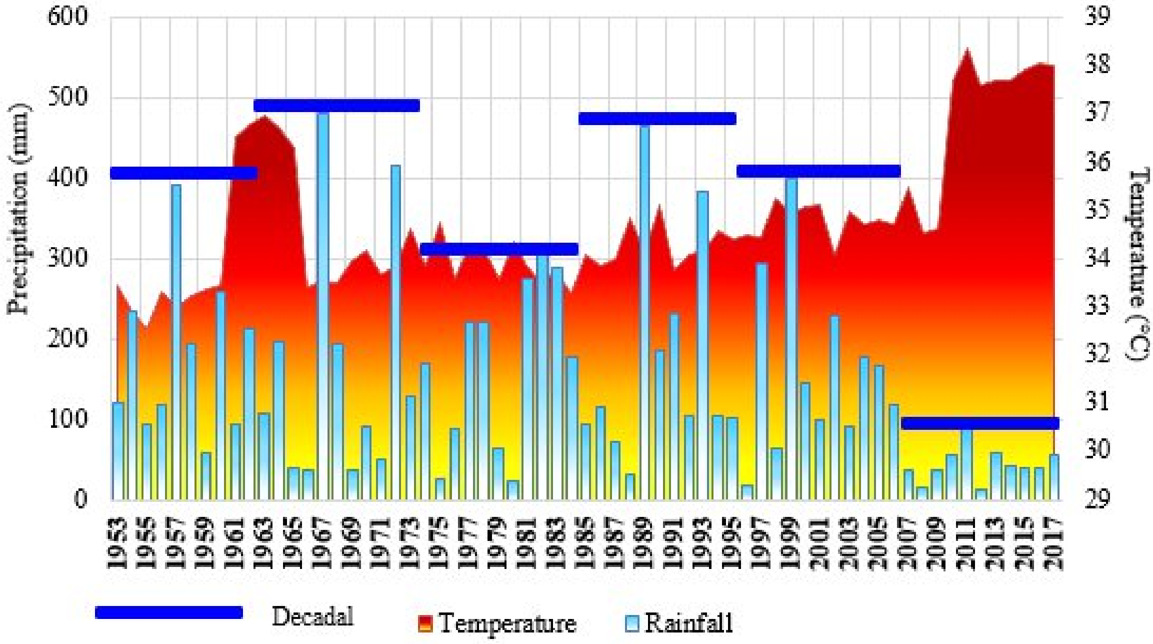

Figure Total precipitation (mm) and max temperature average variation for Djibouti over the period (1953-2017)

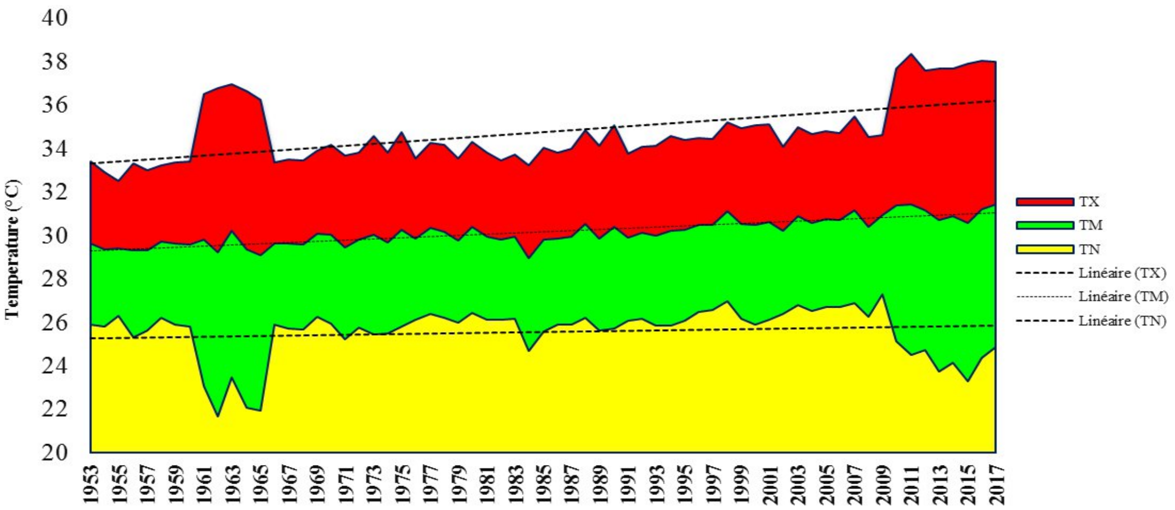

Figure max, min and mean air temperature average variation for Djibouti over the period (1953-2017)

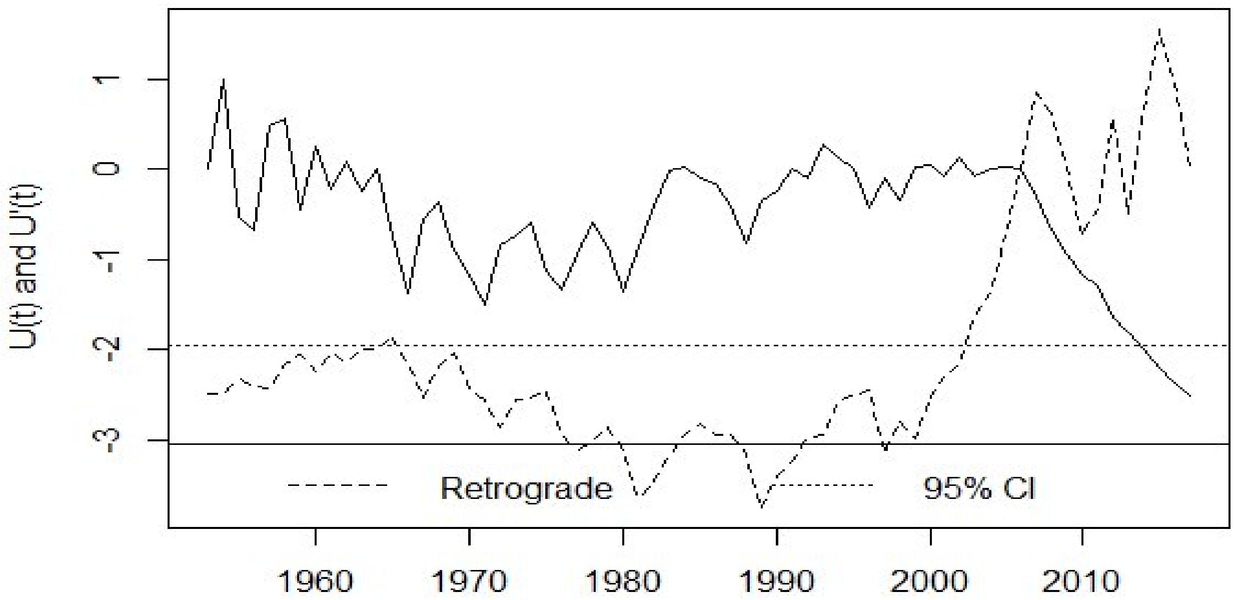

Figure Graphical representation of sequential values of the statistics forward series u(t) (solid line) and backward series u'(t) (dashed line) obtained by SQ-MK test for annual precipitation series observed at Djibouti station (2007).

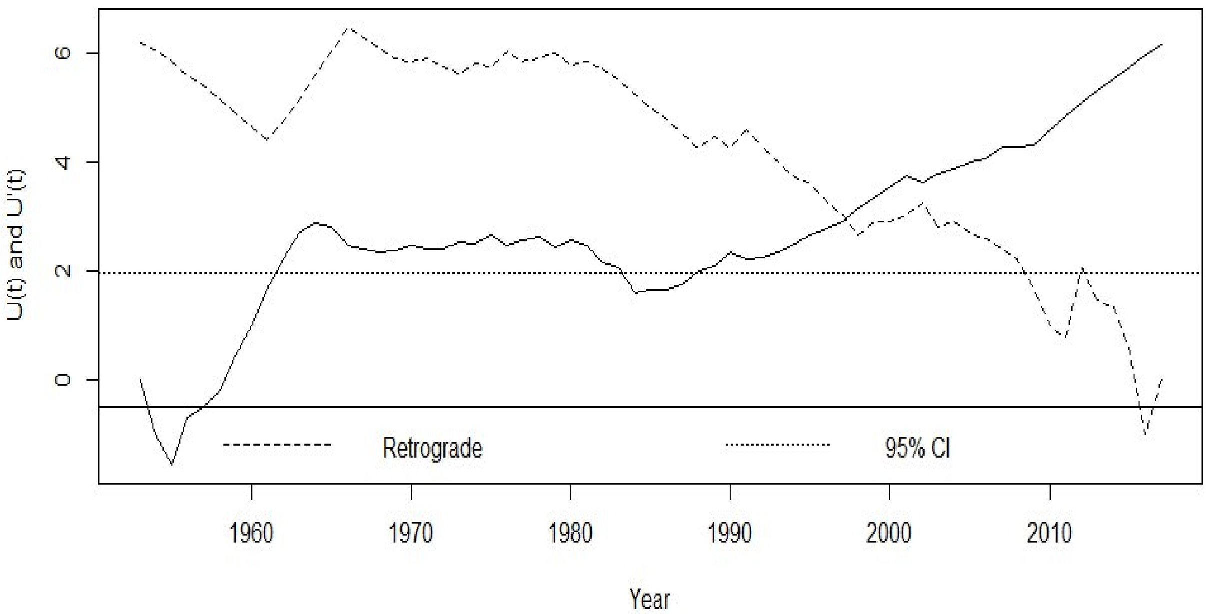

Figure Graphical representation of sequential values of the statistics forward series u(t) (solid line) and backward series u'(t) (dashed line) obtained by SQ-MK test for annual temperature series observed at Djibouti station (1998).

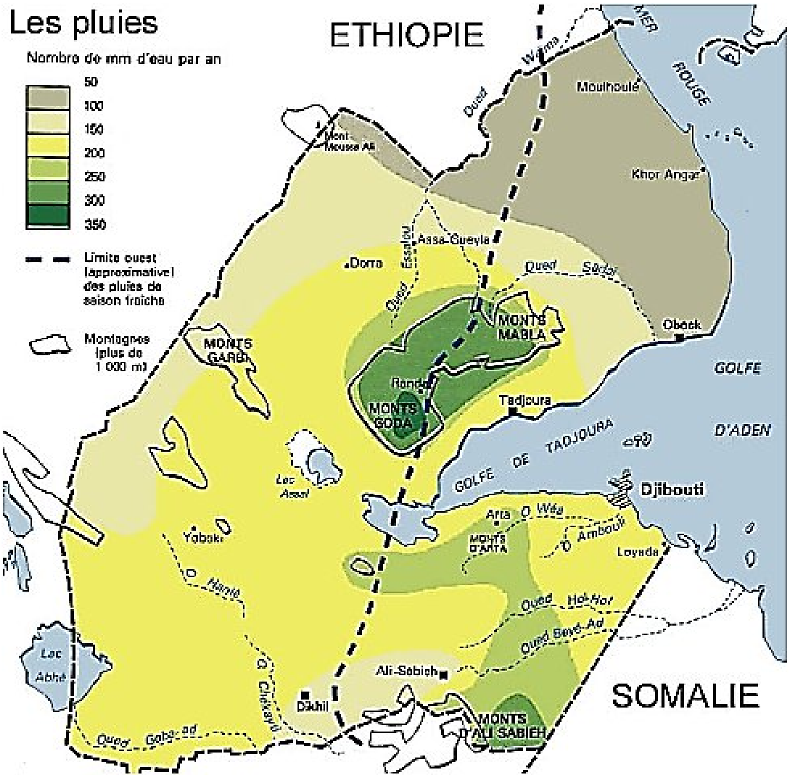

Source : *© 2001- 2002 Benoît Billiet*

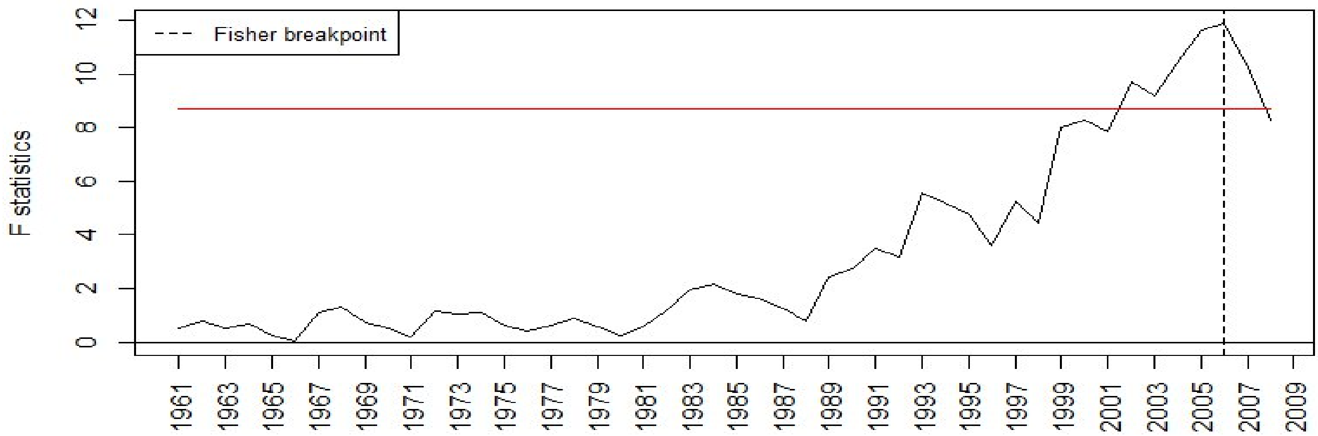

Figure. Fisher break point of total precipitation annual in South west of Djibouti-City

(a)

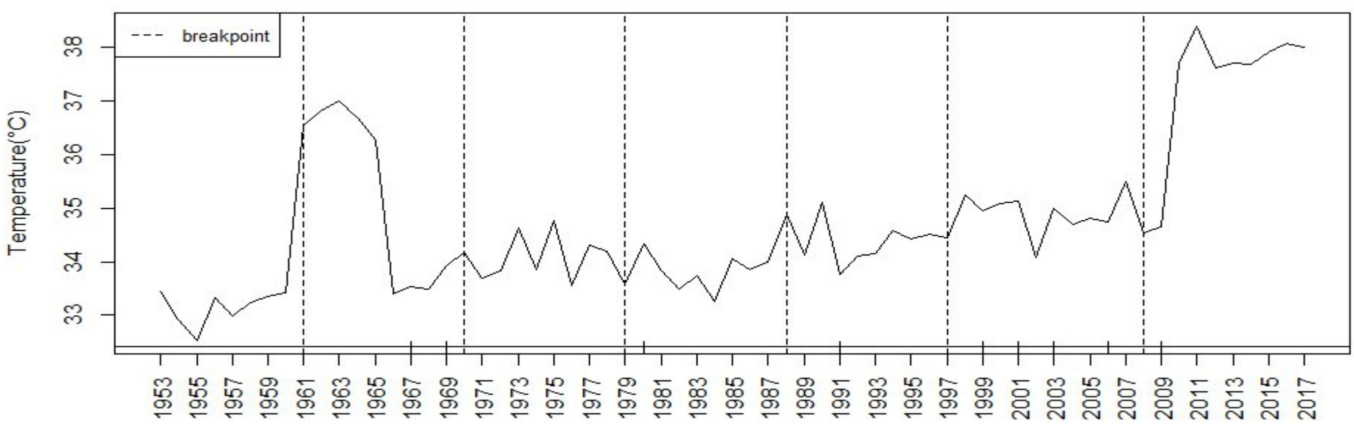

(b)

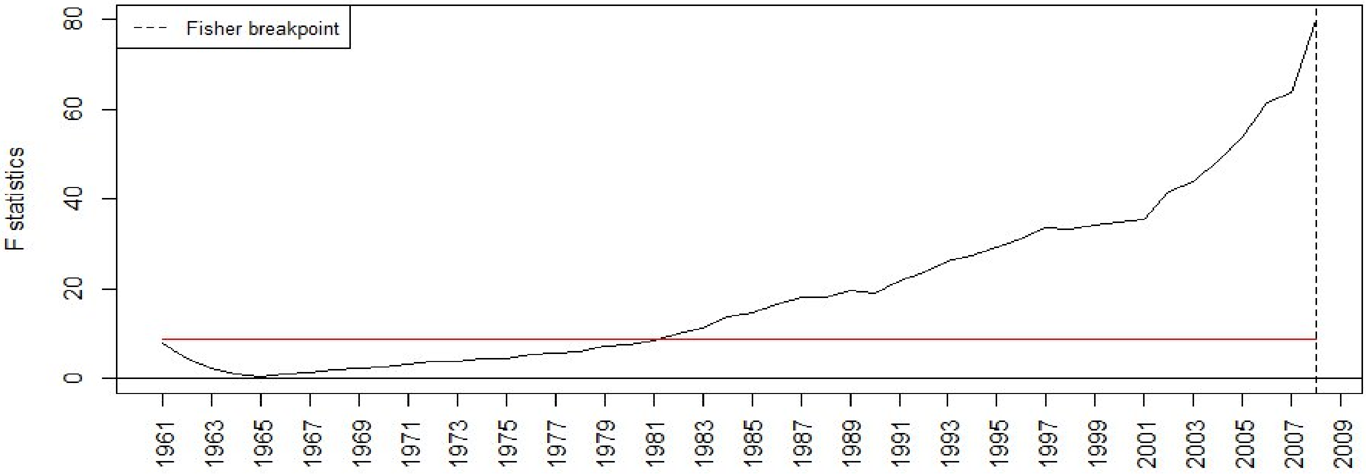

Figure. Fisher break point of Temperature annual in South west of Djibouti-City

Reference

Ghement Statistical Consulting Company Ltd (GSCC). 2014."Performing the Mann-Kendall Test for Trend in R", p5.

William S. Cleveland et Susan J. Devlin, « Locally-Weighted Regression: An Approach to Regression Analysis by Local Fitting », Journal of the American Statistical Association, vol. 83, no 403, 1988, p. 596–610 (DOI 10.2307/2289282, JSTOR 2289282)

Haynes K, Fearnhead P, Eckley IA (2017). “A computationally efficient nonparametric approach for changepoint detection.” *Statistics and Computing*, **27**(5), 1293–1305. ISSN 1573-1375, doi: 10.1007/s11222-016-9687-5, https://doi.org/10.1007/s11222-016-9687-5.

Haynes K, A. Eckley I, Fearnhead P (2015). “Computationally Efficient Changepoint Detection for a Range of Penalties.” *Journal of Computational and Graphical Statistics*, **26**, 1-28. doi: 10.1080/10618600.2015.1116445.

Killick R, Fearnhead P, Eckley I (2012). “Optimal Detection of Changepoints With a Linear Computational Cost.” *Journal of the American Statistical Association*, **107**, 1590-1598. doi: 10.1080/01621459.2012.737745.

Average Monthly air Temperature(°C) and precipitation(mm)

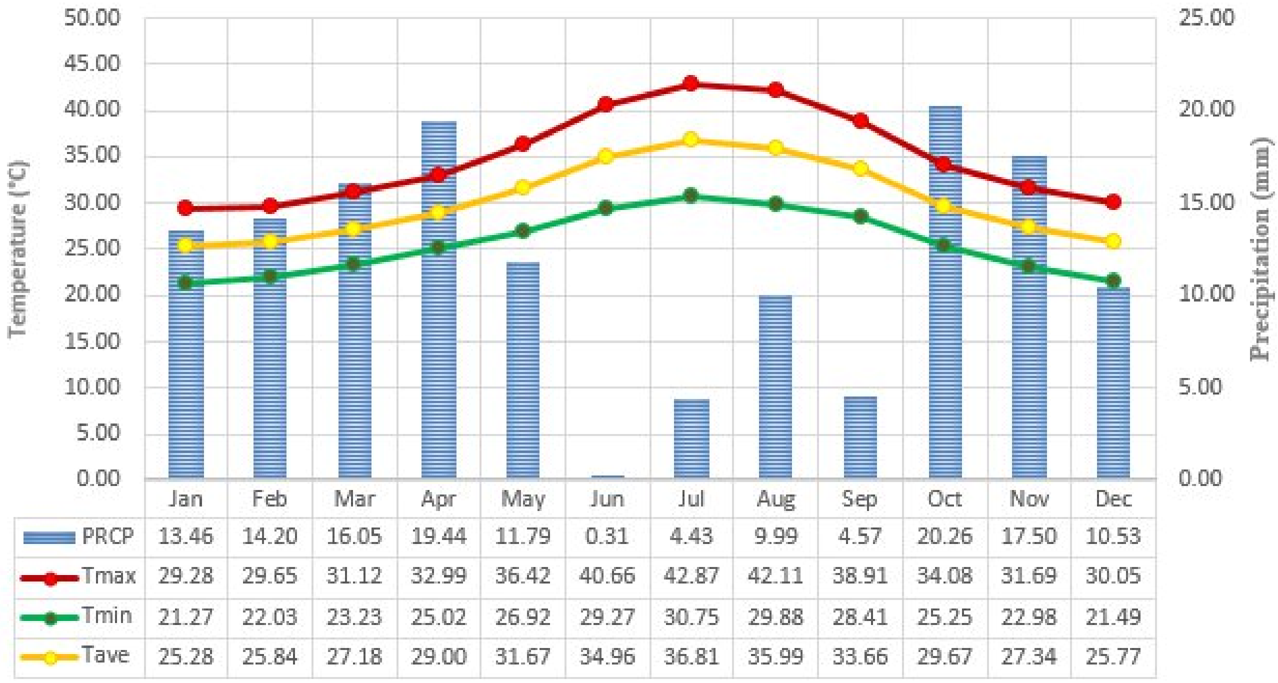

	Jan	Feb	Mar	Apr	May	Jun	Jul	Aug	Sep	Oct	Nov	Dec
PRCP	13.46	14.20	16.05	19.44	11.79	0.31	4.43	9.99	4.57	20.26	17.50	10.53
Tmax	29.28	29.65	31.12	32.99	36.42	40.66	42.87	42.11	38.91	34.08	31.69	30.05
Tmin	21.27	22.03	23.23	25.02	26.92	29.27	30.75	29.88	28.41	25.25	22.98	21.49
Tave	25.28	25.84	27.18	29.00	31.67	34.96	36.81	35.99	33.66	29.67	27.34	25.77

Figure1. Average monthly air temperature (°C) and precipitation (mm) for Djibouti for the study period (**1961-2017**)

Seasonal precipitation(mm). Proposition à faire pour saisonnalité pluviométrie Djibouti

- ✓ **OND = Autumn / AUTUMN**
- ✓ **JFM = Hiver / Winter**
- ✓ **AM = Printemps / SPRING**
- ✓ **JJAS = ETE / SUMMER**

Missing Value Description

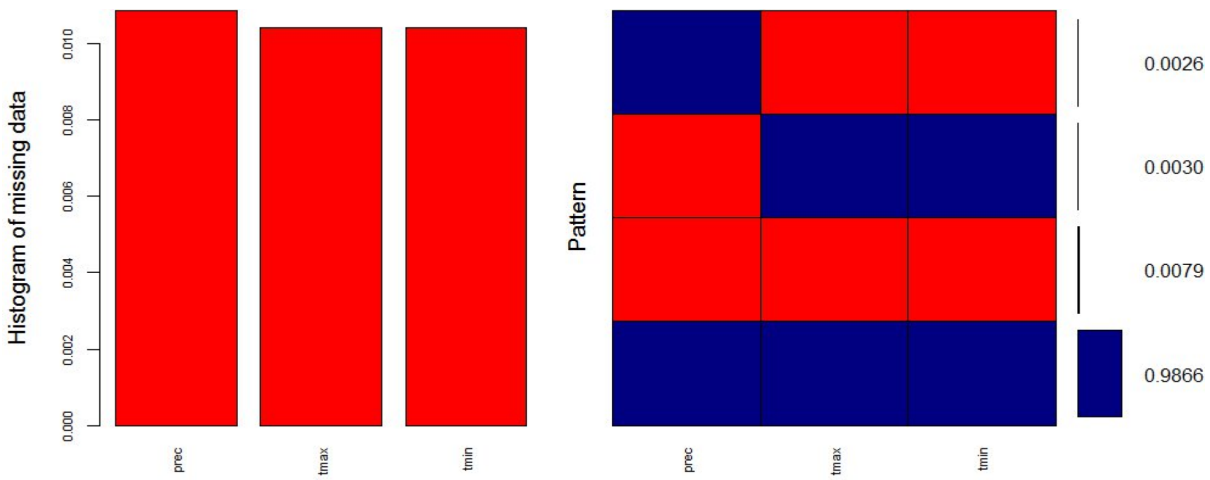

Table 1. Proprotion of Missing value in different site

Rainfall Station (Republic of Djibouti)	Probortion Missing Value in Annual Data	Probortion Missing Value in Deseasonnal Data
Balho	0,54	0,65
Loyada	0,50	0,62
Randa	0,38	0,55
Hol.Hol	0,31	0,51
Tadjoura	0,29	0,49
Obock	0,29	0,49
Ali.Sabieh	0,28	0,49
Dorra	0,25	0,47
Arta	0,18	0,42
Djibouti.Aero	0,16	0,10
Yoboki	0,10	0,38
Dikhil	0,10	0,37
As.Eyla	0,10	0,37
Djibouti.Serpent	0,00	0,28
All Data	**0.25**	**0.44**

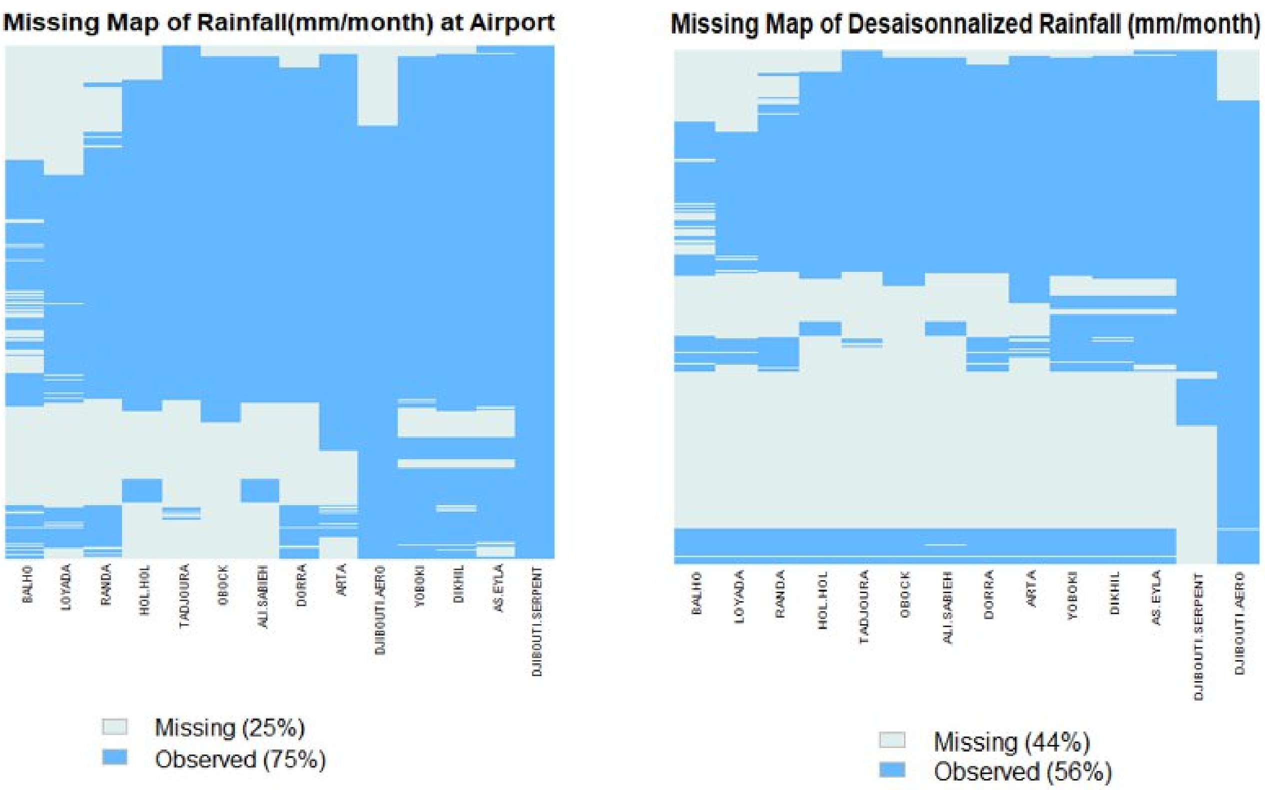

Figure 1. Missing Map of availibility of percentage Data for Analysis

Summary of trends units per decade and annual averages of the precipitation indices at Djibouti Airport

›uti-City		With NA (1980-2011)			Mean Imputation 1 (1980-2011)		
Index	**Units**	'rend	p-value	**nual average**	**rend**	›-value	**nnual average**
PRCPTOT	mm	ʔ.923	0.26	158.99	ʒ.552	0.151	154.17
R99P	mm	⌊.105	0.359	21.32	⌊.131	0.316	20.63
R95P	mm	ʒ.016	0.124	59.71	ʒ.094	0.092	57.79
CWD	day	.009	0.748	2.77	).003	0.914	2.71
CDD	day	.426	0.023	138.03	.943	0.006	142
R20	mm	).042	0.383	2.07	0.05	0.266	2
R10	mm	).027	0.666	3.87	).048	0.423	3.74
SDII	ım/day	).055	0.702	10.77	).101	0.465	10.50
RX5DAY	mm	ʔ.342	0.096	76.26	ʔ.556	0.055	73.94
RX1DAY	mm	⌊.477	0.158	56.02	⌊.659	0.094	54.31

Notes: A trend significant at the 5% (*), 1% (**), less than 1% (***)

TABLE 2: Rainfall trends analysis from 1980 to 2011.

ID	Unit	Average 1981–2010	Trend units/decade	Significance (P level)	Trend %/decade
PTOT	mm	164	−38.0	0.10	−17.4
Rd	days	14.1	−2.3	0.07	−13.5
SDII	mm/day	11.1	−0.5	0.70	−4.2
Rx1d	mm	56.4	−15.6	0.09	−19.5
R10 mm	days	3.9	−0.5	0.38	−10.7
R20 mm	days	2.1	−0.5	0.27	−16.7
R95p	days	0.70	−0.39	0.03	−30.2
R99p	days	0.13	−0.07	0.26	−29.7
R95pSUM	mm	59.7	−31.4	0.07	−29.1
R99pSUM	mm	21.3	−11.5	0.28	−29.5
R95pTOT	%	23.4	−14.2	<0.01	−31.3
R99pTOT	%	5.8	−3.7	0.20	−32.1

Djibouti-City		With NA (1980-2011)			ıN Imputation 2 (1980-2011)		
Index	**Units**	Trend	p-value	**Annual average**	**Trend**	**p-value**	**nual average**
PRCPTOT	mm	-2.923	0.26	158.99	-3.941	0.092	150.25
R99P	mm	-1.105	0.359	21.32	-1.145	0.279	19.99
R95P	mm	-3.016	0.124	59.71	-3.141	0.069	55.98
CWD	day	0.009	0.748	2.77	-0.012	0.626	2.66
CDD	day	2.426	0.023	138.03	3.158	0.002	144.66
R20	mm	-0.042	0.383	2.07	-0.052	0.226	1.97
R10	mm	-0.027	0.666	3.87	-0.059	0.295	3.66
SDII	mm/day	-0.055	0.702	10.77	-0.069	0.596	10.63
RX5DAY	mm	-2.342	0.096	76.26	-2.614	0.037	72.35

RX1DAY	mm	-1.477	0.158	56.02	-1.687	0.07	53.325

outi-City		**With NA (1980-2011)**			**MICE Imputation (1980-2011)**		
Index	**Units**	rend	›-value	**nual average**	**Trend**	**p-value**	**nual average**
PRCPTOT	mm	ː.923	0.26	158.99	-3.34	0.145	153.65
R99P	mm	.105	0.359	21.32	-1.145	0.279	19.99
R95P	mm	ː.016	0.124	59.71	-2.715	0.1	56.27
CWD	day	.009	0.748	2.77	-0.012	0.626	2.66
CDD	day	.426	0.023	138.03	2.227	0.018	139.343
R20	mm	).042	0.383	2.07	-0.041	0.336	2.03
R10	mm	).027	0.666	3.87	-0.048	0.386	3.72
SDII	mm/day	).055	0.702	10.77	-0.001	0.991	11.02
RX5DAY	mm	ː.342	0.096	76.26	-2.215	0.074	74.65
RX1DAY	mm	.477	0.158	56.02	-1.279	0.164	55.68

Table1. List of 11 ETCCDMI core Climate Indices for precipitation

Indicator	**Name**	**Définitions**
RX1day (mm)	Max 1-day precipitation amount	Monthly maximum 1-day precipitation
Rx5day (mm)	Max 5-day precipitation amount	Monthly maximum consecutive 5-day precipitation
SDII (mm/day)	Simple daily intensity index	Annual total precipitation divided by the number of wet days (defined as PRCP>=1.0mm) in the year
R10 (day)	umber of heavy precipitation days	Annual count of days when PRCP>=10mm
R20 (day)	ıber of very heavy precipitation days	Annual count of days when PRCP>=20mm
Rnn (day)	Number of days above nn mm	Annual count of days when PRCP>=nn mm, nn is user defined threshold
CDD (day)	Consecutive dry days	Maximum number of consecutive days with RR<1mm
CWD (day)	Consecutive wet days	Maximum number of consecutive days with RR>=1mm
R95p (mm)	Very wet days	Annual total PRCP when RR>95th percentile
R99p (mm)	Extremely wet days	ınnual total PRCP when RR>99th percentile
ʼRCPTOT (mm)	ʌnnual total wet-day precipitation	ınnual total PRCP in wet days (RR>=1mm)

Method 1 : PPCA

Figure 1 : Correlation Graph and Screet plot

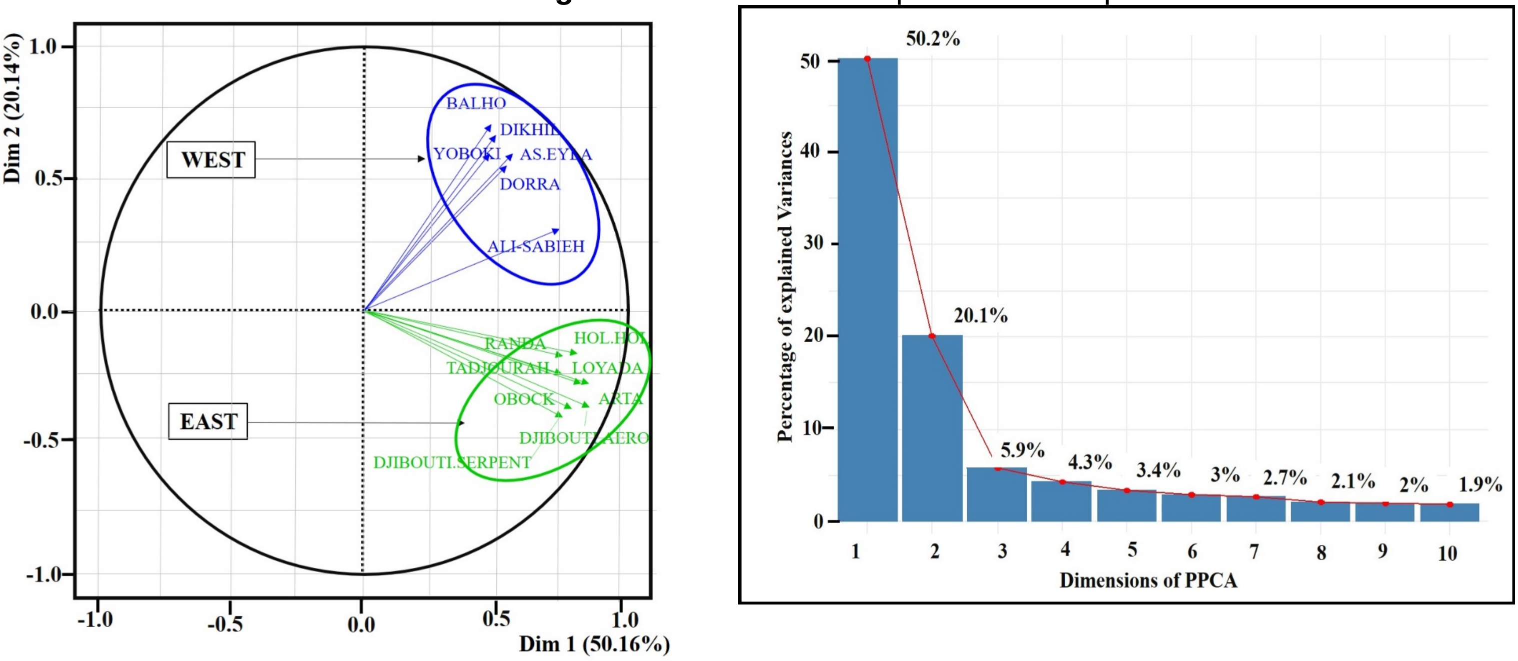

Method 2 & 3 : AMELIA II / MICE

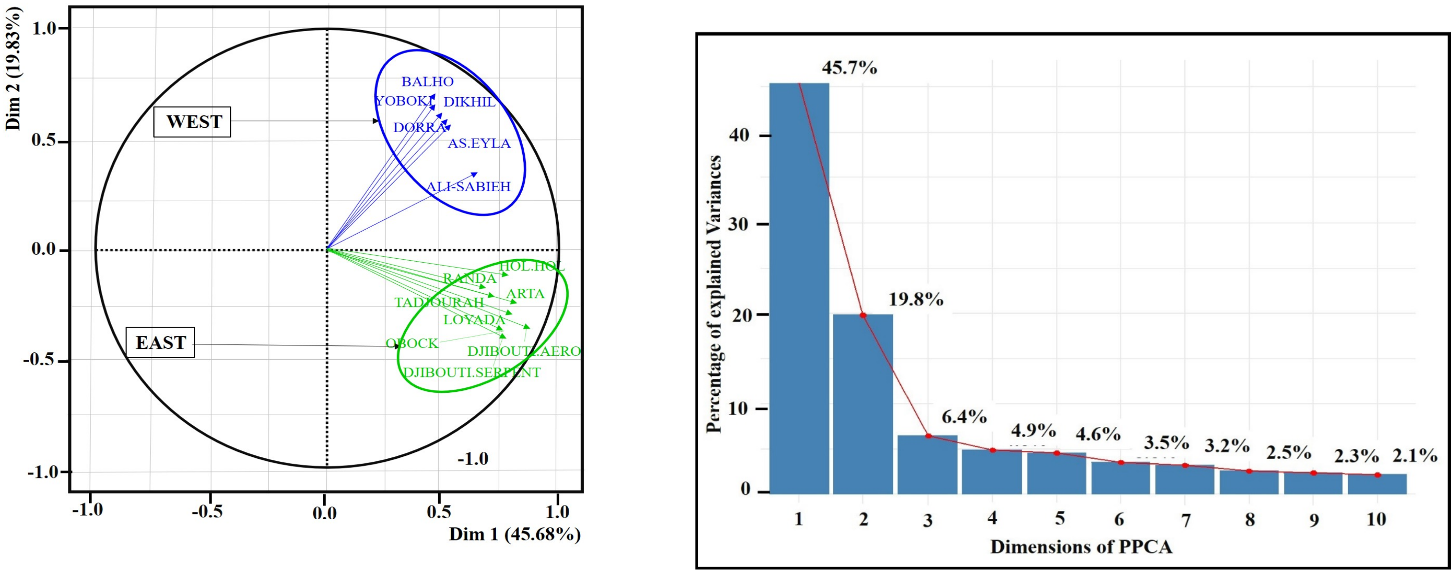

Figure 2 : Correlation Graph and Screet plot

Method 4 : missMDA

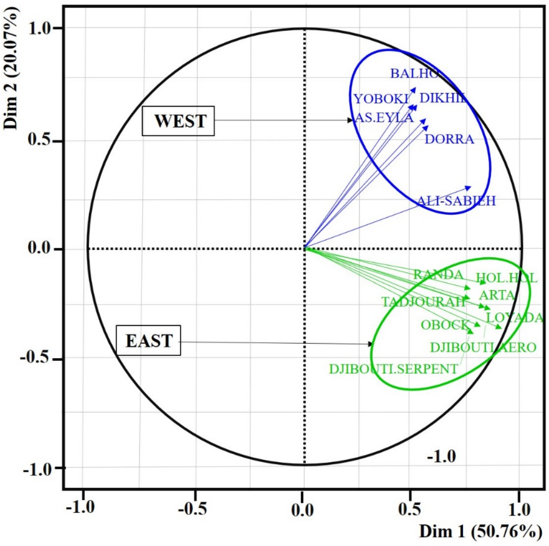

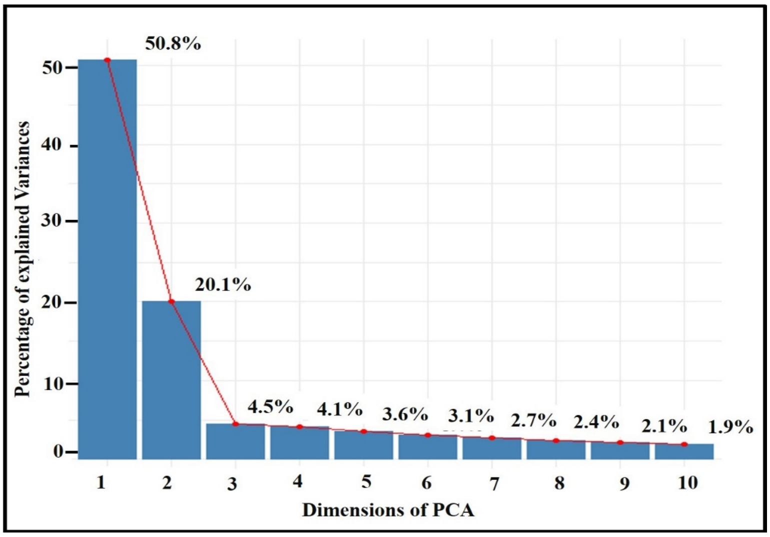

Data Rainfall (mm/month)

Principal Component	Var. explained (%)	Var. Total	Var. Cycle Annuel	(%)	Var. Inter Annuel	(%)
Comp.1	50.157	3784.860	298.821	7.895	3486.039	92.105
Comp.2	20.143	1520.005	619.399	40.750	900.606	59.250
Comp.3	5.857	441.956	35.325	7.993	406.631	92.007
Comp.4	4.251	320.819	13.352	4.162	307.467	95.838
Comp.5	3.353	253.020	15.929	6.296	237.091	93.704
Comp.6	2.958	223.221	9.356	4.191	213.865	95.809
Comp.7	2.669	201.379	13.288	6.599	188.090	93.401
Comp.8	2.110	159.172	4.213	2.647	154.959	97.353
Comp.9	1.978	149.274	2.373	1.590	146.901	98.410
Comp.10	1.916	144.568	3.595	2.487	140.973	97.513
Comp.11	1.728	130.405	6.330	4.854	124.075	95.146
Comp.12	1.415	106.752	2.222	2.082	104.530	97.918
Comp.13	1.103	83.243	2.504	3.008	80.739	96.992
Comp.14	0.361	27.258	0.880	3.230	26.378	96.770

Desaisonnalized Data Rainfall (mm/month)

Principal Component	Var. explained (%)	Var. Total	Var. Cycle Annuel	(%)	Var. Inter Annuel	(%)
Comp.1	55.182	6674.861	6.537	0.098	6668.324	99.902
Comp.2	10.216	1235.759	1.248	0.101	1234.511	99.899
Comp.3	6.616	800.291	1.189	0.149	799.102	99.851
Comp.4	3.836	463.980	0.271	0.058	463.709	99.942
Comp.5	3.734	451.681	1.665	0.369	450.017	99.631
Comp.6	3.115	376.845	0.436	0.116	376.410	99.884
Comp.7	2.996	362.454	0.236	0.065	362.219	99.935
Comp.8	2.862	346.161	1.324	0.382	344.838	99.618
Comp.9	2.536	306.784	1.092	0.356	305.692	99.644
Comp.10	2.412	291.754	1.004	0.344	290.750	99.656
Comp.11	2.236	270.436	0.472	0.174	269.965	99.826
Comp.12	1.715	207.429	0.357	0.172	207.072	99.828
Comp.13	1.539	186.172	0.654	0.351	185.518	99.649
Comp.14	1.004	121.393	0.765	0.630	120.628	99.370

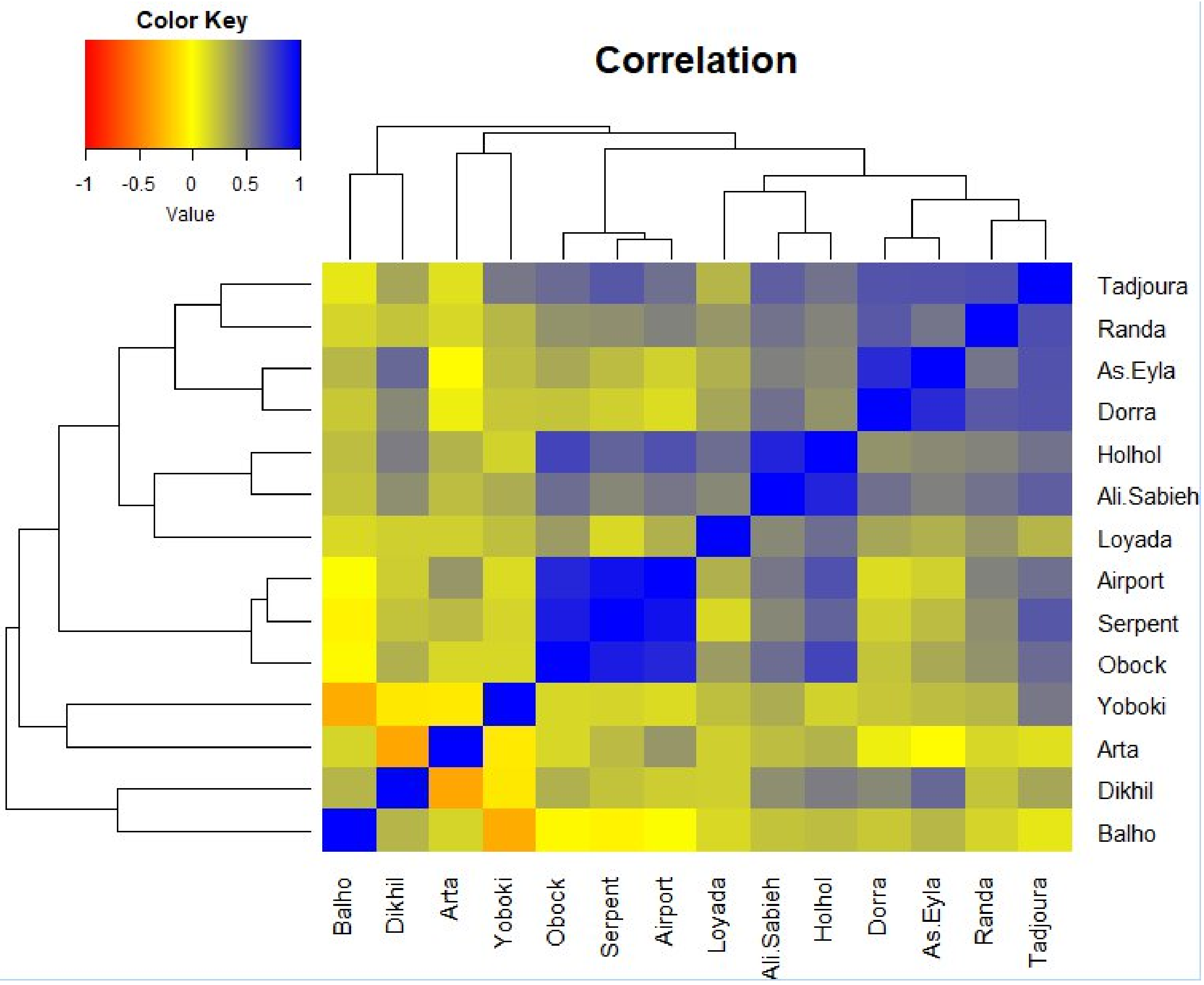

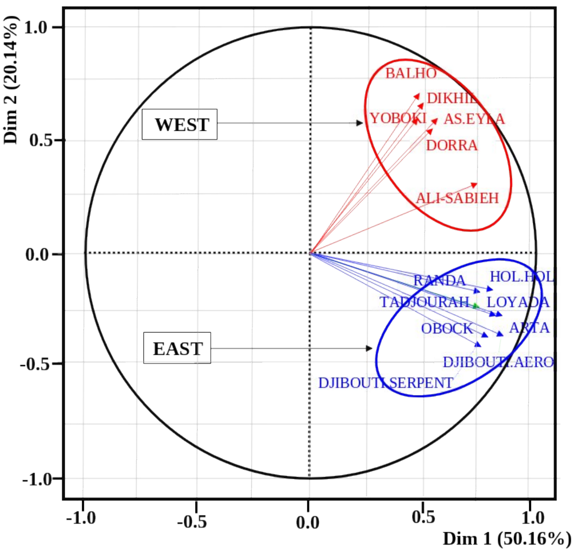

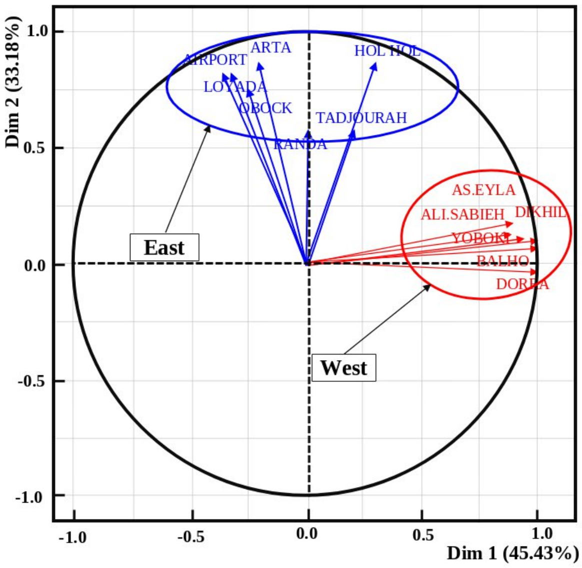

This section presents the regionalization of rainfall patterns in Djibouti. The objective is to assess the organization of the spatial variability of precipitation across the country. Figure 2 shows the PCA applied to the raw monthly time series of rainfall data from the 14 stations. The PCA of seasonally adjusted precipitation data and monthly mean precipitation data are shown in Supplementary Figure 1.

The projection on the factorial plane (1 × 2) (representing 70.30% of the total inertia, with 50.16% and 20.14% respectively for the first and the second main component selected) shows the existence of two group of rainfall stations in the Republic of Djibouti.

In terms of annual variation, the contribution of the annual cycle is much greater in PC2 (40.75%) than in PC1 (7.89%), while for the interannual, PC1 and PC2 represent respectively 92.11% and 59.25%.

All stations are positively projected along the first axis. The second CP puts in opposition the groups of station the east and the west, remarkable in the three PCAs. The first group (represented positively along the first dimension) is made up of the stations located on the coast (EST). While the second group represents the stations located further to the center and to the west on the coast (WEST).

This spatial distribution of precipitation clearly shows that Djibouti's rainfall regime is partly linked to altitude and oceanic influence, which tends to decrease towards the west. The eastern part of Djibouti is predominantly a flat region, where the variability of rainfall is governed more by its proximity to the Red Sea and the Gulf of Aden. The opposition of the two groups shown in figure 2 (a) along the second axis is explained by the annual variability marked more in PC 2 than in PC1.

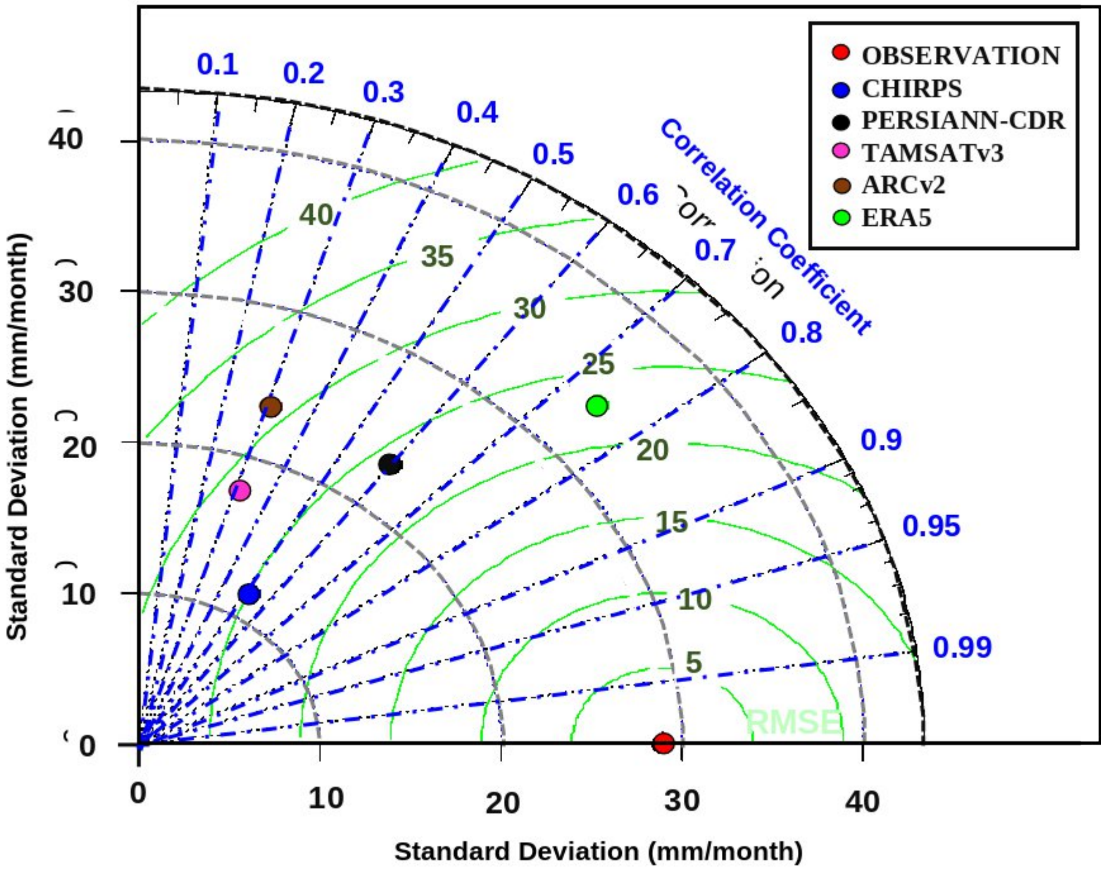

Fig1. Monthly rainfall of Djibouti-Airport station from 1983-2017 with five satellites products (CH : CHIRPS ; PE : Persiann-CDR ; TA : Tamsat ; ER : ERA5 ; AR : ARCV2)

Stations	**STDE**	**RMSE**	**RSQUARED**	**COR**	**BIAIS**
CHIRPS	11.68	24.90	0.27	0.52	-0.22
PERSIANCDR	23.11	24.56	0.35	0.59	-5.39
TAMSATV3	17.43	28.67	0.09	0.31	-0.00
ARCV2	23.49	31.06	0.09	0.31	0.321
ERA5	33.95	24.92	0.56	0.75	-10.00

Table 1. Monthly statistical parameters obtained from the evaluation of in Airport Station against SPEs in Djibouti during 1983–2017

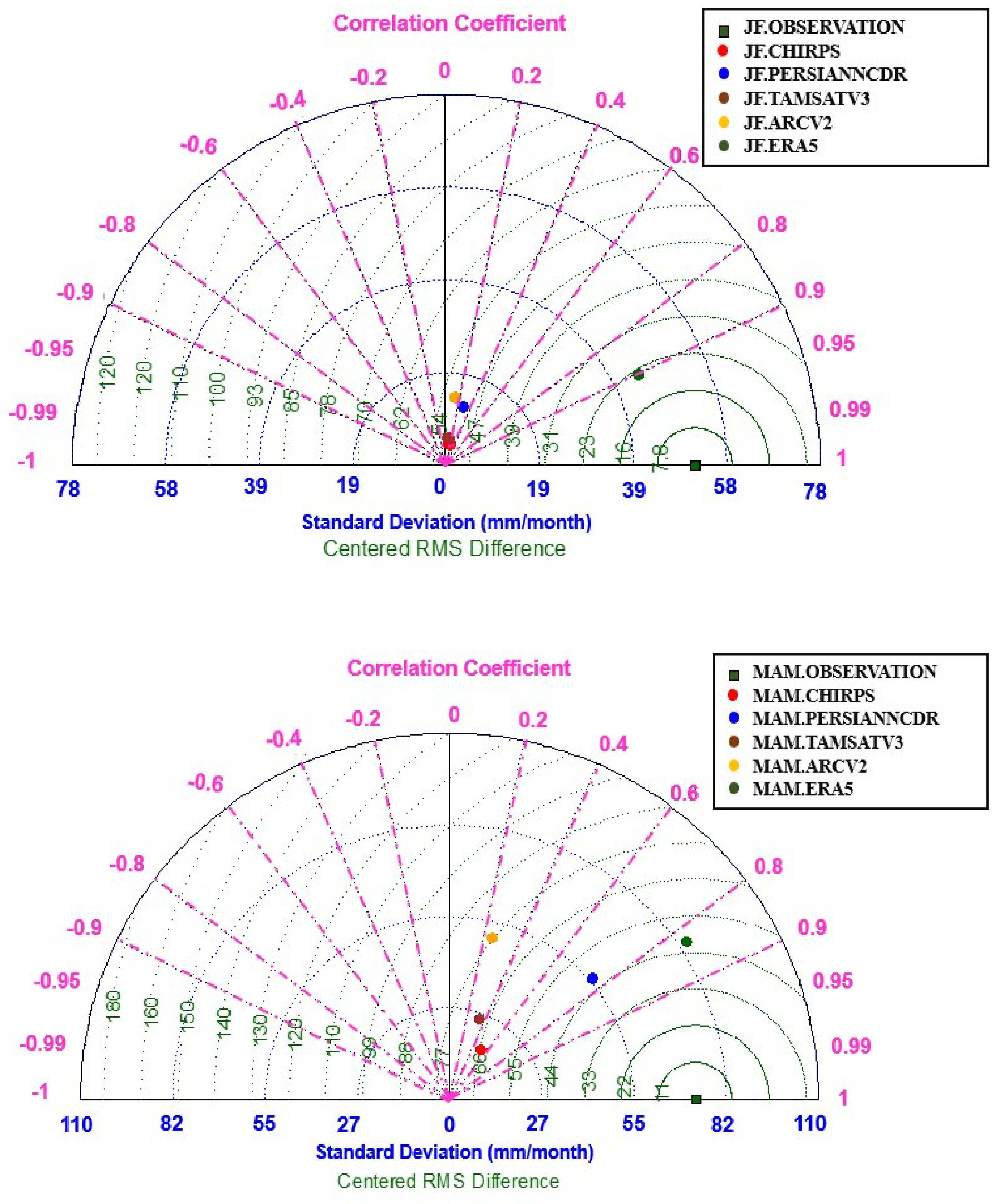

Fig. 2. Taylor diagram showing comparison of seasonal rainfall variation for Djibouti-Airport Station (a; JF, b; MAM, c; JJAS, and d; OND).

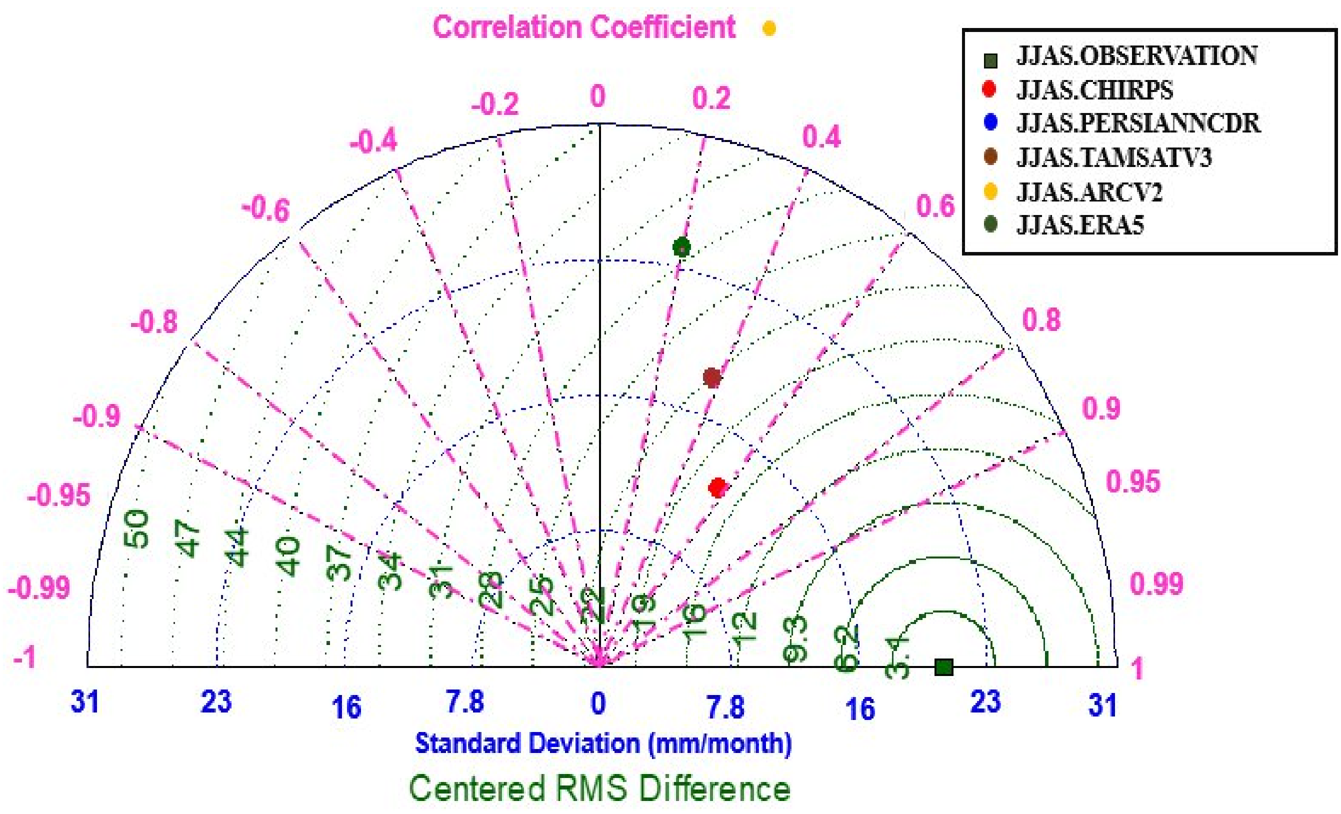
Correlation Coefficient
JJAS.OBSERVATION
JJAS.CHIRPS
JJAS.PERSIANNCDR
JJAS.TAMSATV3
JJAS.ARCV2
JJAS.ERA5
Standard Deviation (mm/month)
Centered RMS Difference

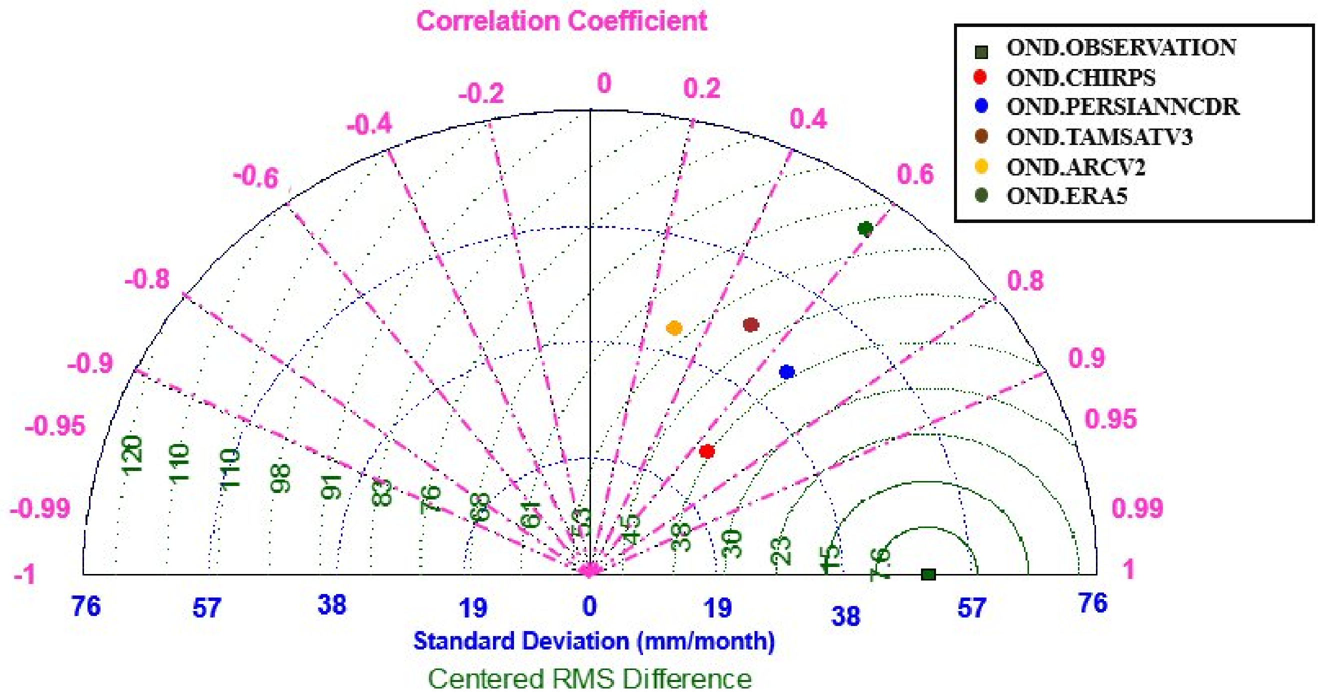
Correlation Coefficient
OND.OBSERVATION
OND.CHIRPS
OND.PERSIANNCDR
OND.TAMSATV3
OND.ARCV2
OND.ERA5
Standard Deviation (mm/month)
Centered RMS Difference

Seasons	Station Zone	Model Name	RMSE	RSQUARED	COR	STDE	Bias
JF	Station Airport	Chirps	50.558	0.0261	0.172	4.62	8.766
		Peseriann	52.963	0.0769	0.277	13.07	18.026
		Tamsat	57.731	0.0027	0.053	5.90	25.42
		ARC2	55.396	0.014	0.120	14.45	18.934
		ERA 5	29.109	0.8141	0.902	45.01	-18.51
MAM	Station Airport	Chirps	65.555	0.2793	0.529	17.994	2.797
		Peseriann	57.685	0.5755	0.759	56.539	-32.53
		Tamsat	68.745	0.1177	0.343	25.961	-3.00
		ARC2	78.371	0.0608	0.247	50.810	-9.743
		ERA 5	62.887	0.6875	0.829	86.015	-41.24
JJAS	Station Airport	Chirps	17.558	0.3231	0.568	12.638	-4.117
		Peseriann	86.69	0.0344	-0.19	56.539	-59.60
		Tamsat	29.363	0.1358	0.368	18.144	-19.64
		ARC2	42.771	0.0695	0.264	38.321	-19.65
		ERA 5	32.536	0.0394	0.199	24.941	-15.07
OND	Station Airport	Chirps	39.94	0.4308	0.656	27.036	-10.13
		Peseriann	39.248	0.4414	0.664	44.996	-0.003
		Tamsat	48.788	0.2569	0.507	48.157	-2.854
		ARC2	57.047	0.0897	0.300	42.756	14.309
		ERA 5	72.956	0.3472	0.589	70.924	-45.23

Table 2. Seasonal statistical parameters obtained from the evaluation of in situ against SPEs over four locations in Kenya during 1983–2017. Notes : CC, Correlation Coefficient ; RMSE, Root Mean Square Error. DC, Determination Coefficient. (Significant codes : 0 '***' 0.001 '**' 0.01 '*' 0.05 '.' 0.1)

(a)

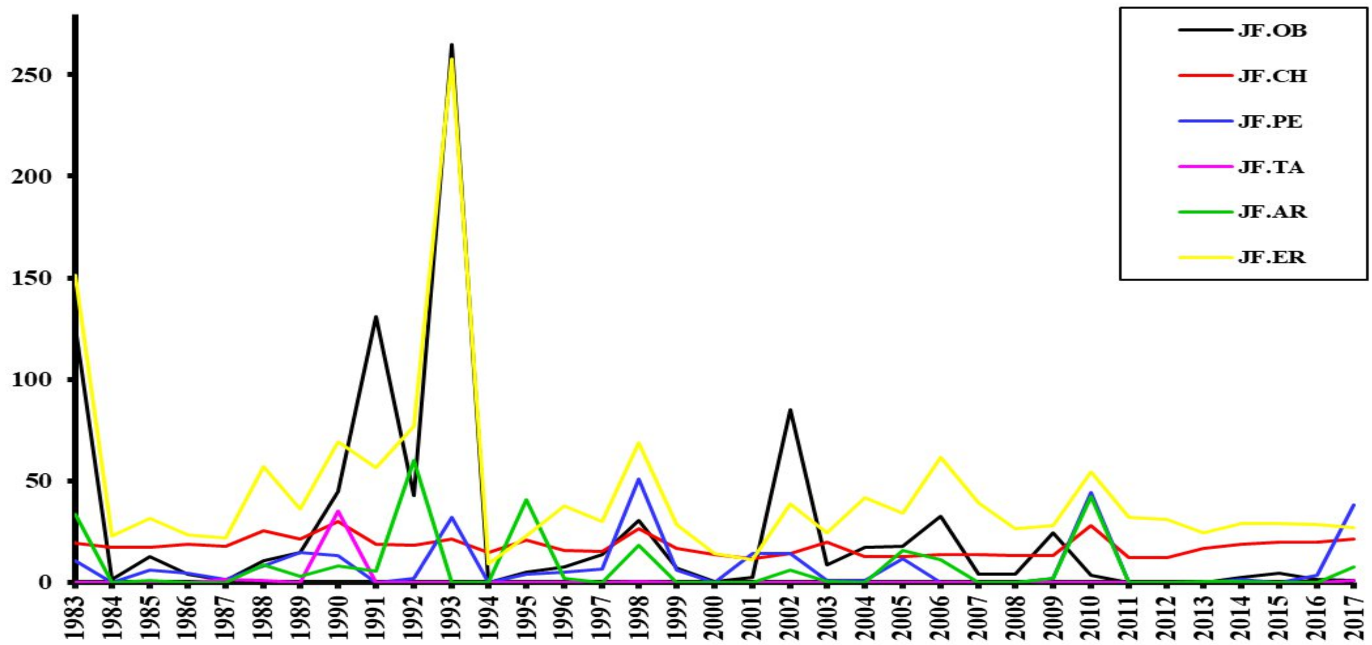

(b)

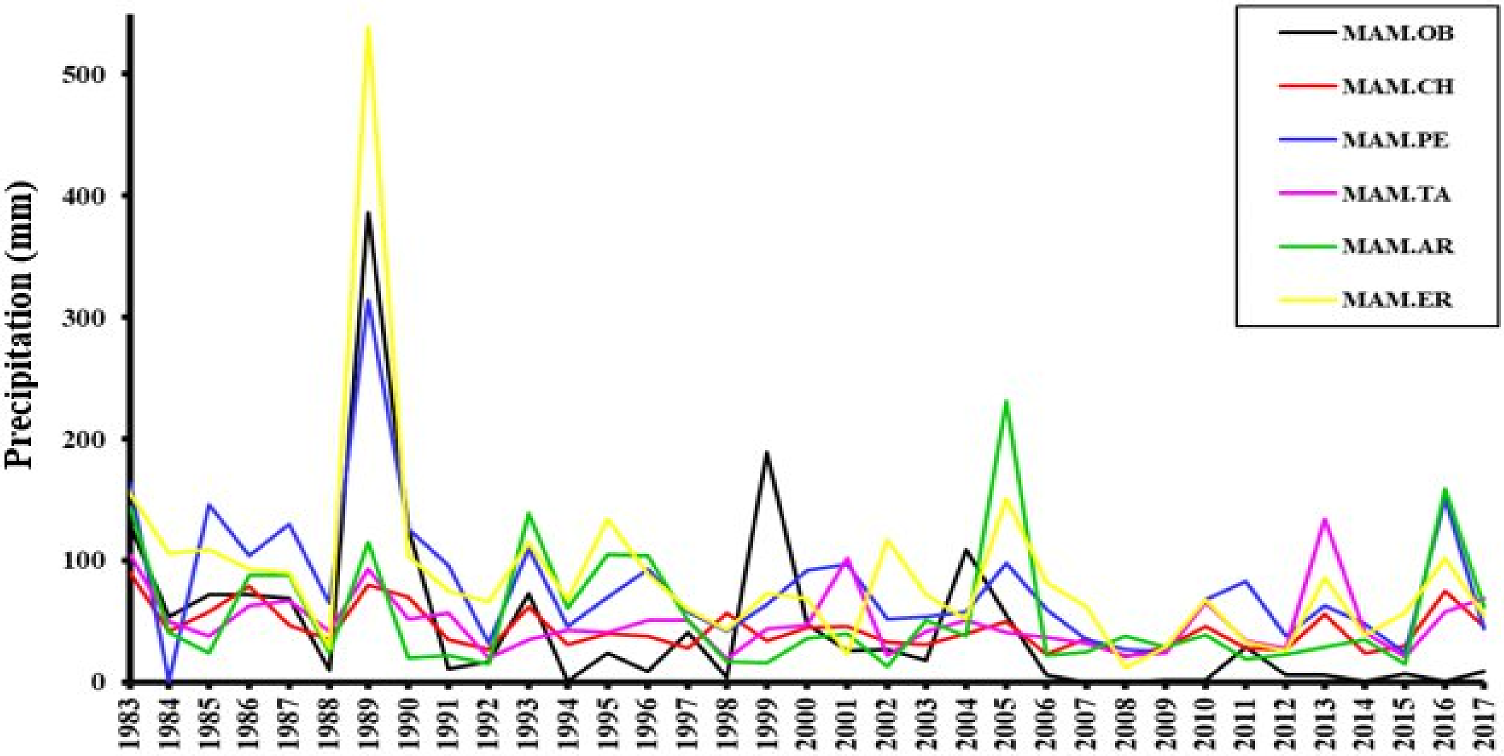
Precipitation (mm)
MAM.OB
MAM.CH
MAM.PE
MAM.TA
MAM.AR
MAM.ER

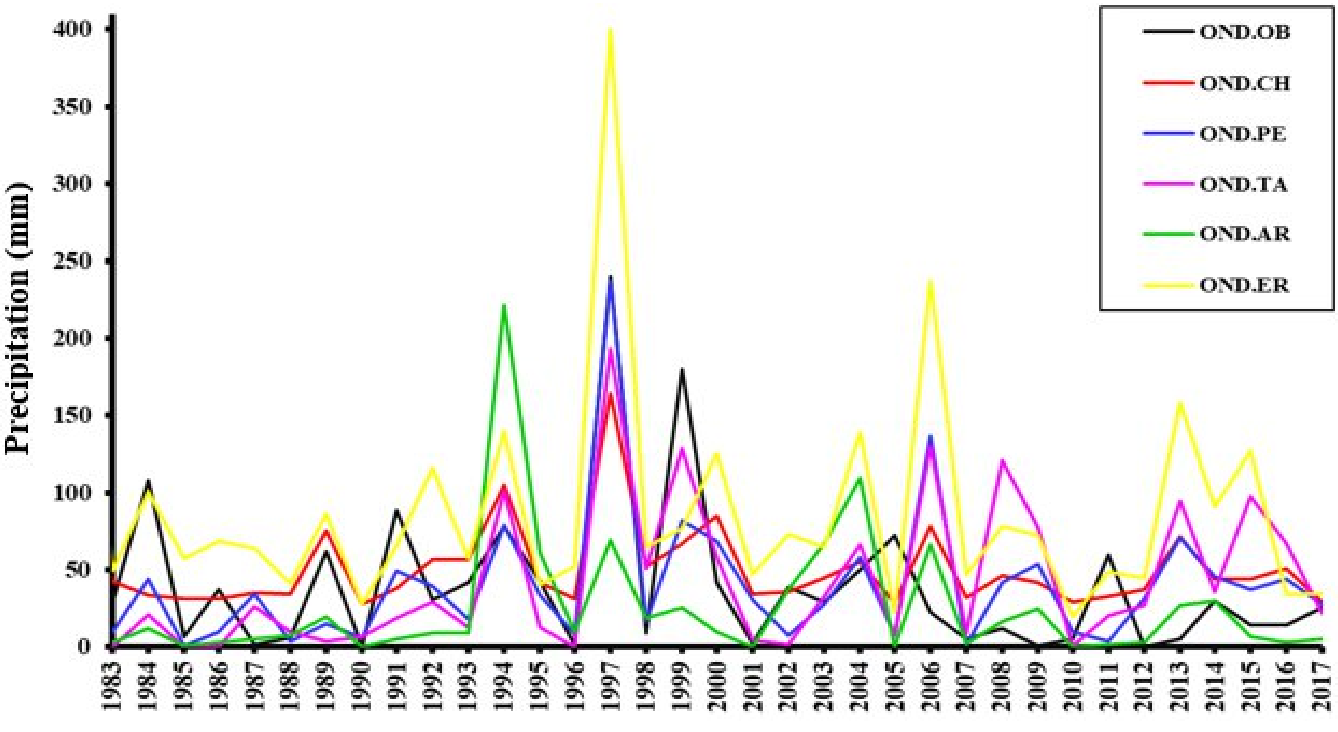
Precipitation (mm)
OND.OB
OND.CH
OND.PE
OND.TA
OND.AR
OND.ER

c)

(d)

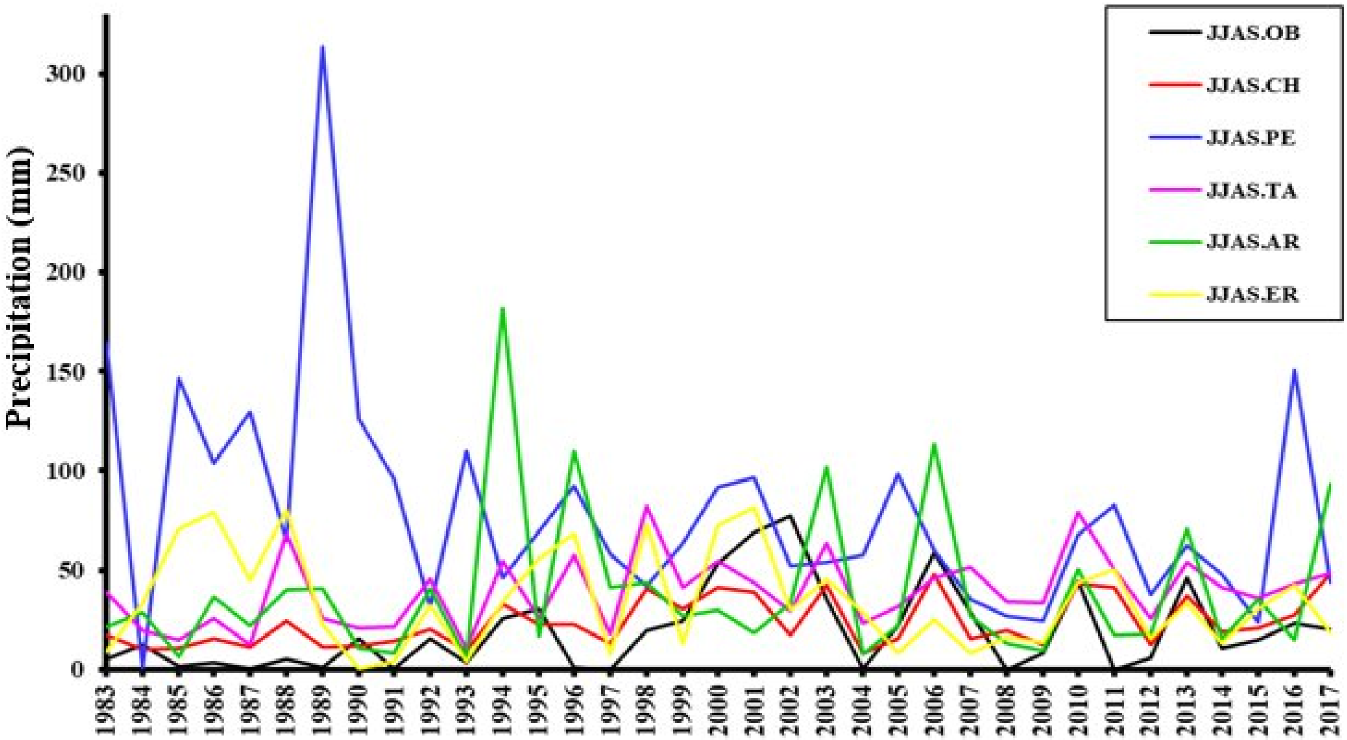

Fig1. Seasonal variability representation of Djibouti-Airport station from 1983-2017 with five satellites products (CH : CHIRPS ; PE : Persiann-CDR ; TA : Tamsat ; ER : ERA5 ; AR : ARCV2)

Stations	Statistic	JF	MAM	JJAS	OND
AIRPORT	**Trend**	-1,590	**-3,150**	0,600	-0,980
	Prob.	0,070	0,009	0,080	0,260
CHIRPS	**Trend**	-0,110	**-0,710**	**0,530**	-0,080
	Prob.	0,153	0,010	0,009	0,850
PERSIANCDR	**Trend**	0,037	**-2,100**	-0,220	0,490
	Prob.	0,870	0,020	0,670	0,530
TAMSATV3	**Trend**	-0,100	-0,330	**0,590**	1,400
	Prob.	0,300	0,460	0,047	0,060
ARCV2	**Trend**	-0,230	-0,680	0,270	-0,070
	Prob.	0,350	0,430	0,680	0,920
ERA5	**Trend**	-1,065	**-2,680**	-0,761	-0,597
	Prob.	0,082	0,025	0,056	0,588

Table 1. Seasonal statistical parameters obtained from the evaluation of in Airport Station against SPEs over four locations in Djibouti during 1983–2017

	JF		MAM		JJAS		OND	
	Trend	P-value	Trend	P-value	Trend	P-value	Trend	P-value
Est -CHIRPS	-0.039	0.54	**-0.470**	0.034	**0.62**	0.008	-0.079	0.83

Est - PERSIANN-CDR	0.231	0.16	-1.054	0.20	0.027	0.95	0.549	0.49
Est -ARC V2	-0.074	0.69	0.282	0.70	0.605	0.22	0.23	0.71
Est -TAMSAT V3	0.006	0.84	0.652	0.09	**0.837**	0.008	1.33	0.07
Est -ERA 5	-1.075	0.08	**-1.70**	0.02	-0.25	0.69	-0.508	0.57
West - CHIRPS	-0.025	0.64	-0.305	0.12	**1.53**	0.00	0.047	0.69
West - PERSIANN-CDR	0.258	0.09	-0.545	0.51	1.189	0.21	0.44	0.32
West -ARC V2	-0.137	0.59	1.125	0.22	1.898	0.055	0.94	0.13
West - TAMSAT V3	0.013	0.91	**0.708**	0.03	**1.78**	0.00	**0.804**	0.03
West -ERA 5	-0.550	0.055	**-1.708**	0.00	-0.08	0.92	-0.193	0.57

(* Values in bold are significant at the 5% level.)

Table 1. Significant Statistics of Trend for Average regional seasonnal precipitation (mm) of five products (Chirps, Persiann-CDR, ARCV2, TAMSATV3, ERA5) over the Republic of Djibouti in he period (1983-2017).

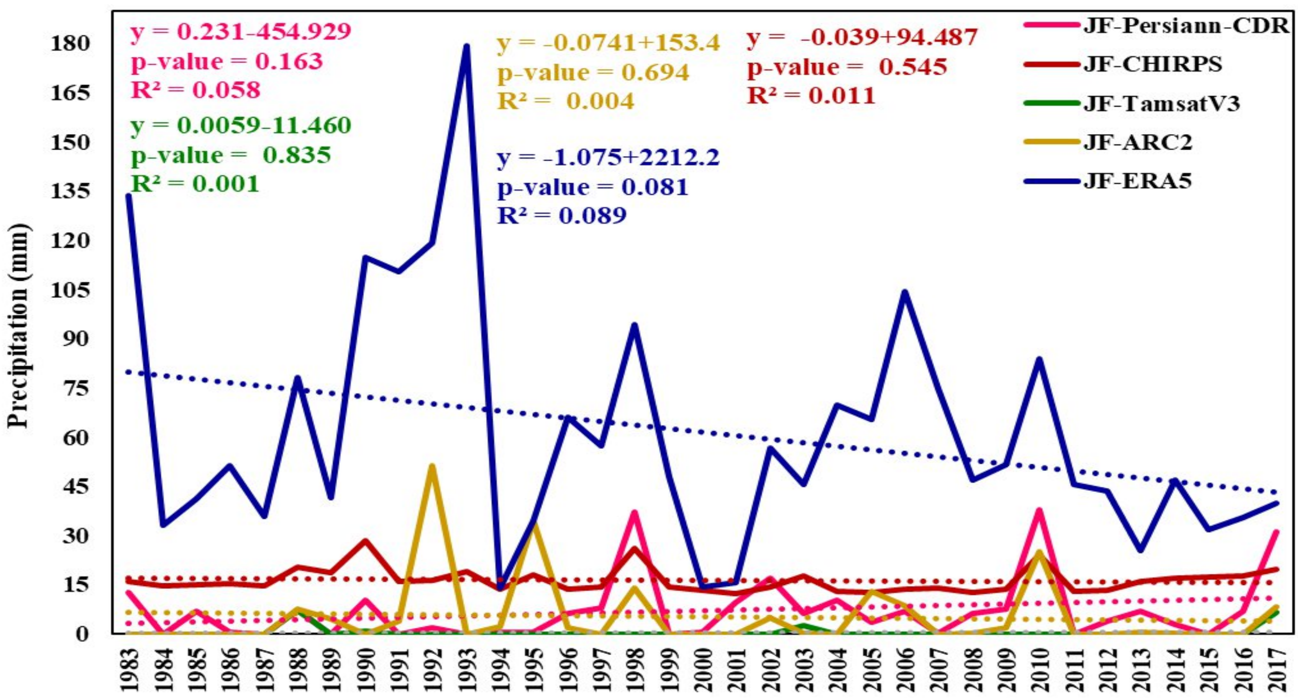

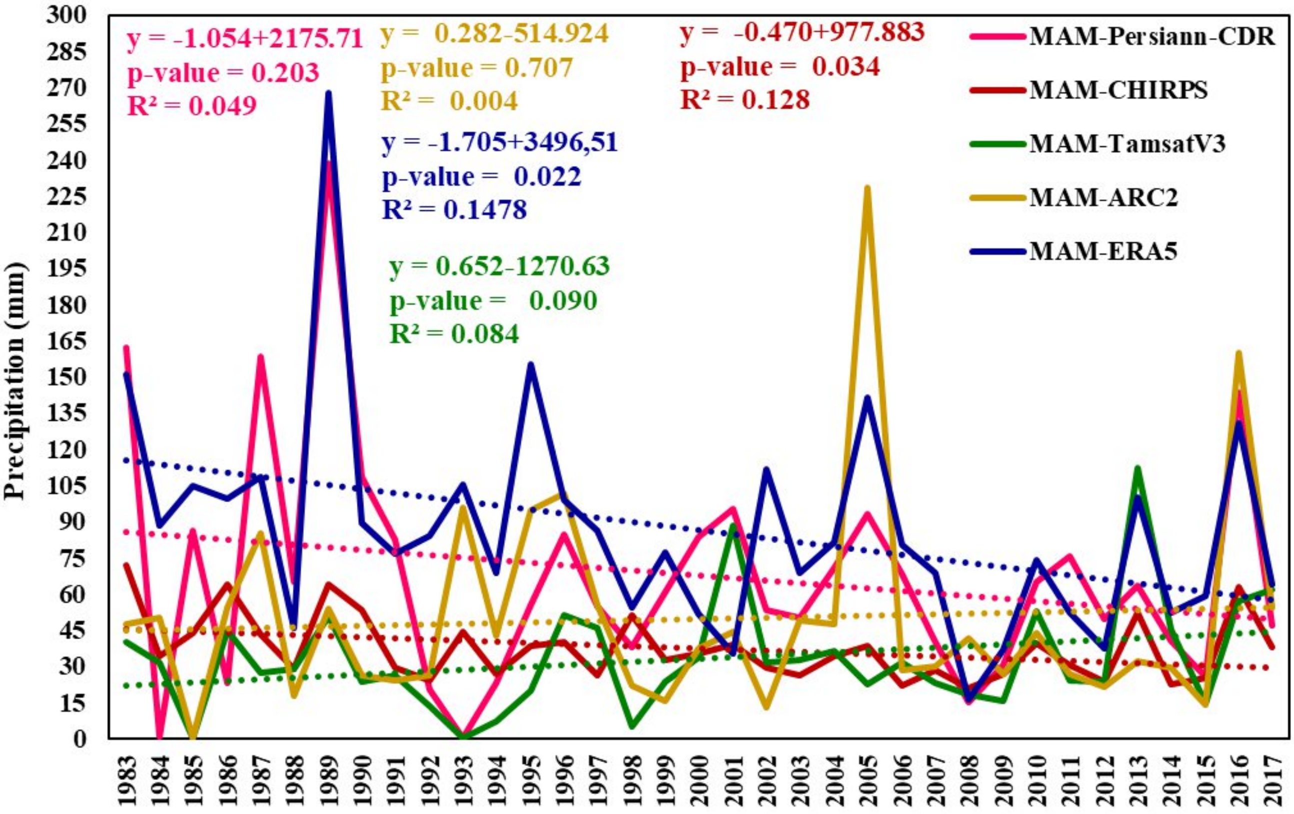
y = -1.054+2175.71
p-value = 0.203
R² = 0.049
y = 0.282-514.924
p-value = 0.707
R² = 0.004
y = -1.705+3496,51
p-value = 0.022
R² = 0.1478
y = 0.652-1270.63
p-value = 0.090
R² = 0.084
y = -0.470+977.883
p-value = 0.034
R² = 0.128
MAM-Persiann-CDR
MAM-CHIRPS
MAM-TamsatV3
MAM-ARC2
MAM-ERA5
Precipitation (mm)

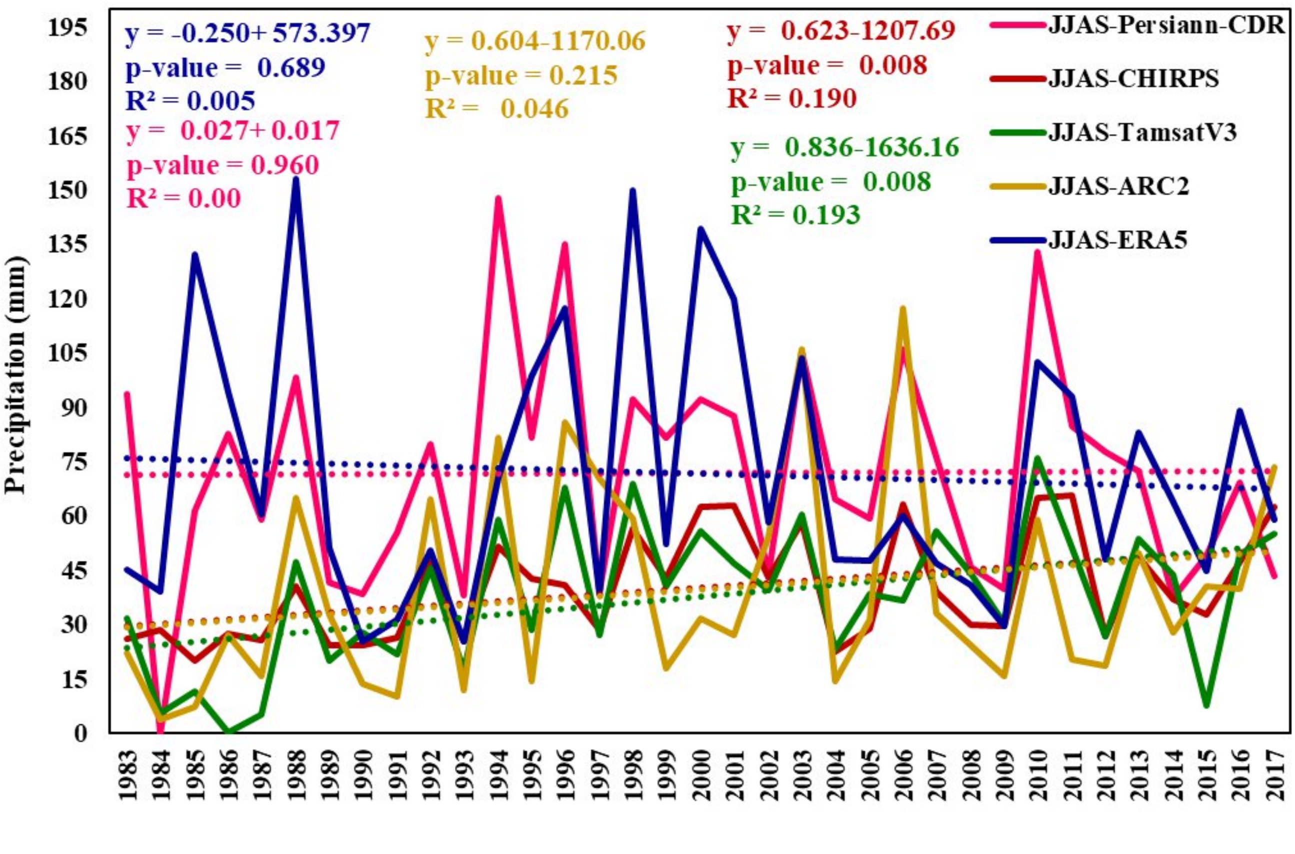
y = -0.250+ 573.397
p-value = 0.689
R² = 0.005
y = 0.027+ 0.017
p-value = 0.960
R² = 0.00
y = 0.604-1170.06
p-value = 0.215
R² = 0.046
y = 0.623-1207.69
p-value = 0.008
R² = 0.190
y = 0.836-1636.16
p-value = 0.008
R² = 0.193
JJAS-Persiann-CDR
JJAS-CHIRPS
JJAS-TamsatV3
JJAS-ARC2
JJAS-ERA5
Precipitation (mm)

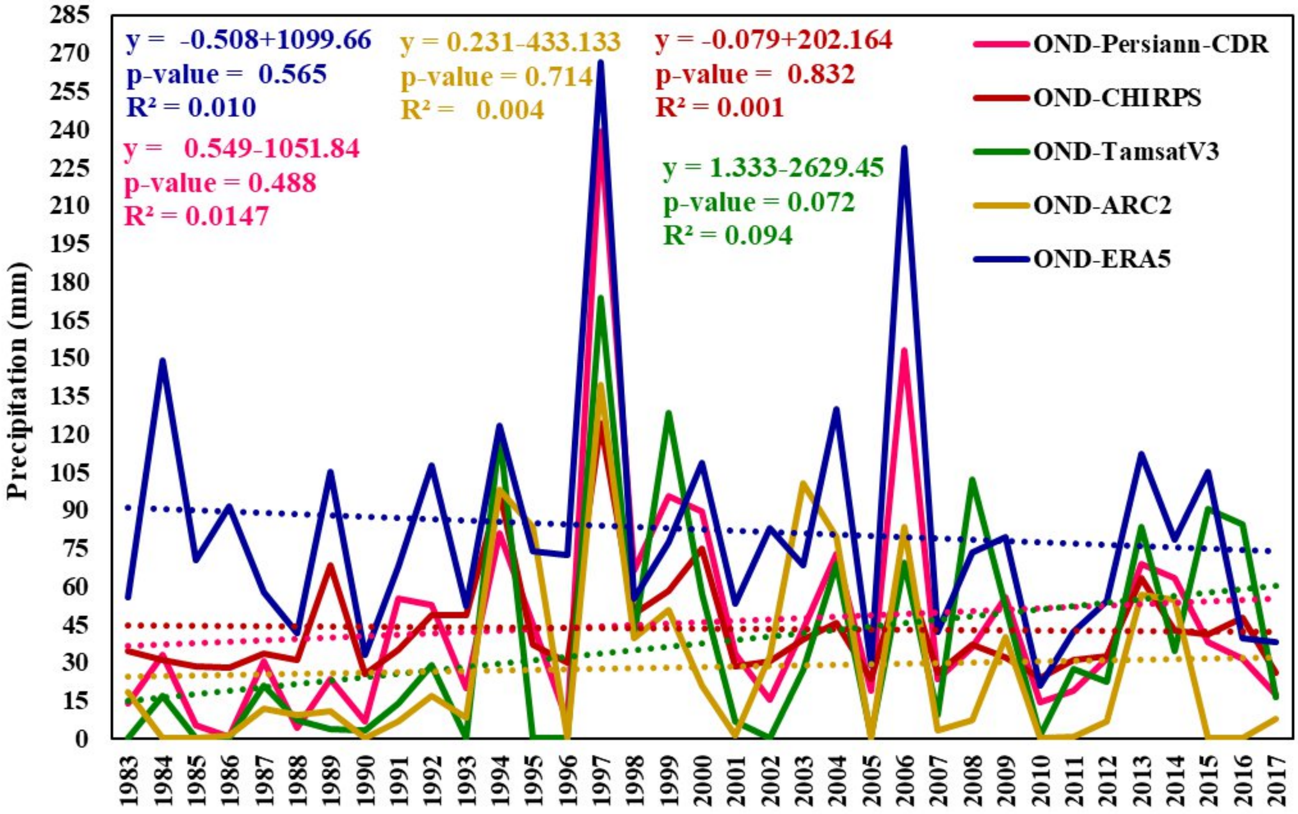

Figure 1. Est Trend of Seasonnal Variability of precipitation (mm) of five products (Chirps, Persiann-CDR, ARCV2, TAMSATV3, ERA5) over the Republic of Djibouti in he period (1983-2017).

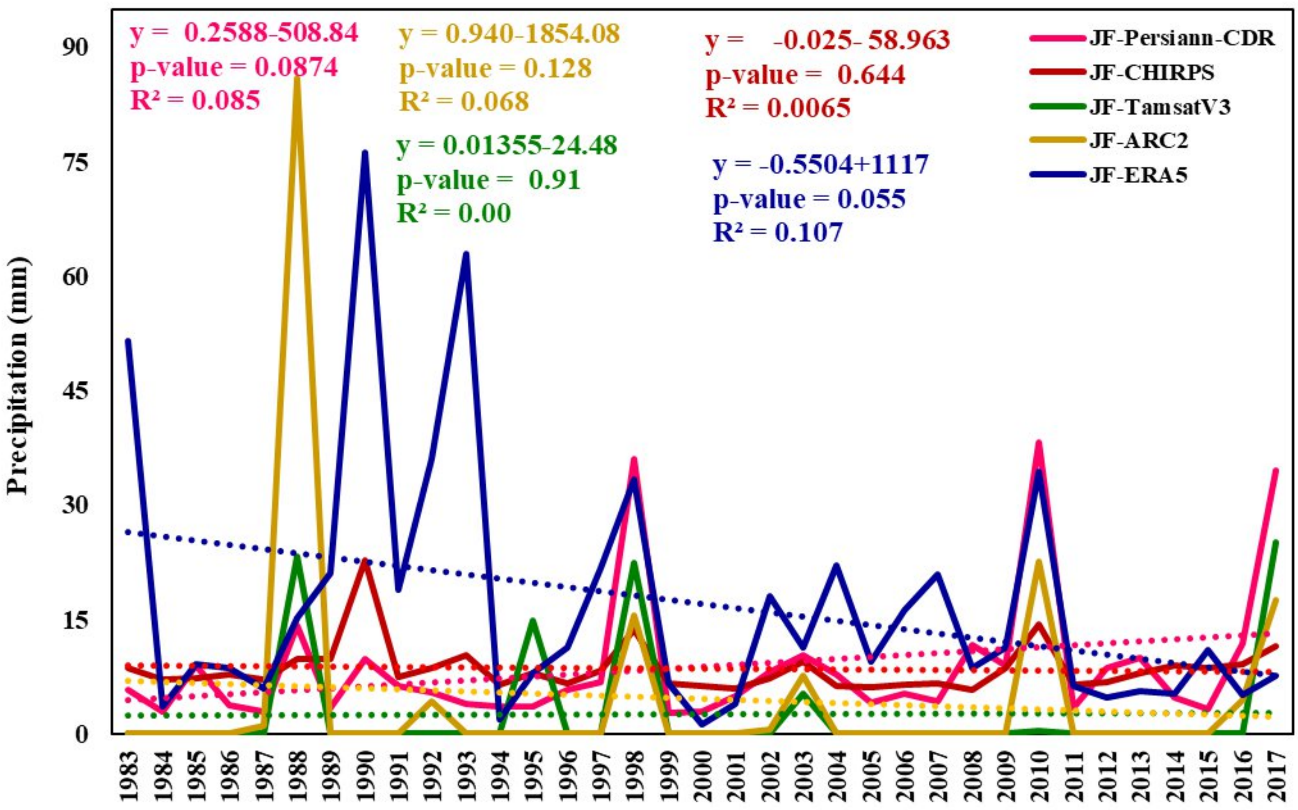

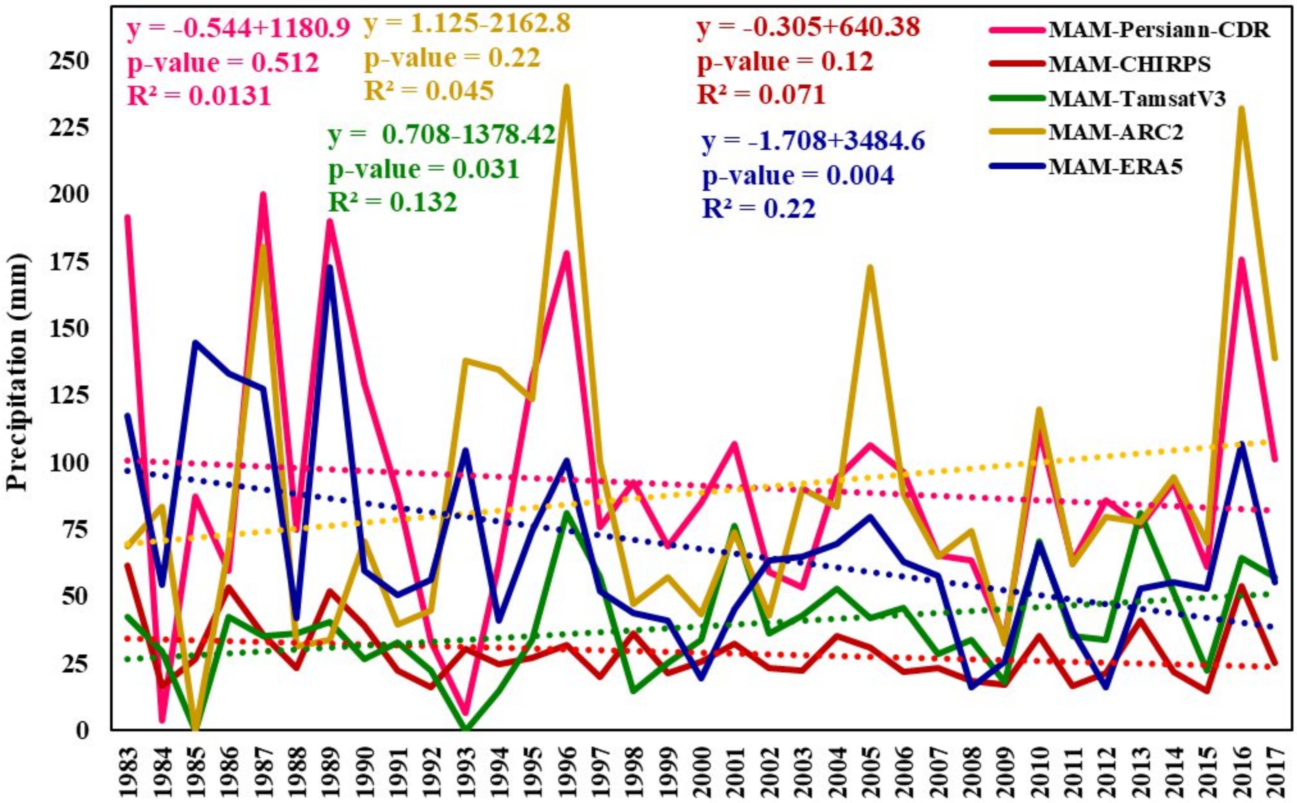
y = -0.544+1180.9
p-value = 0.512
R² = 0.0131
y = 1.125-2162.8
p-value = 0.22
R² = 0.045
y = 0.708-1378.42
p-value = 0.031
R² = 0.132
y = -0.305+640.38
p-value = 0.12
R² = 0.071
y = -1.708+3484.6
p-value = 0.004
R² = 0.22
MAM-Persiann-CDR
MAM-CHIRPS
MAM-TamsatV3
MAM-ARC2
MAM-ERA5
Precipitation (mm)

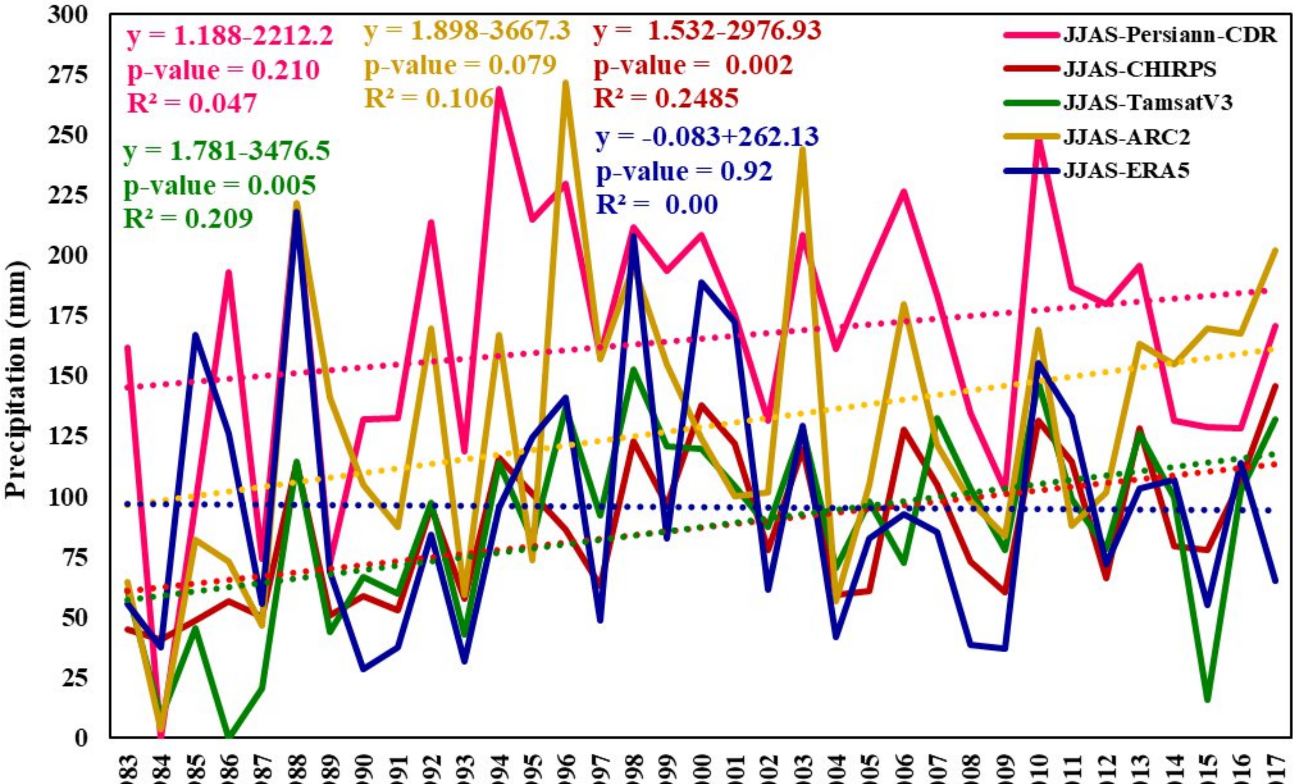
y = 1.188-2212.2
p-value = 0.210
R² = 0.047
y = 1.898-3667.3
p-value = 0.079
R² = 0.106
y = 1.532-2976.93
p-value = 0.002
R² = 0.2485
y = 1.781-3476.5
p-value = 0.005
R² = 0.209
y = -0.083+262.13
p-value = 0.92
R² = 0.00
JJAS-Persiann-CDR
JJAS-CHIRPS
JJAS-TamsatV3
JJAS-ARC2
JJAS-ERA5
Precipitation (mm)

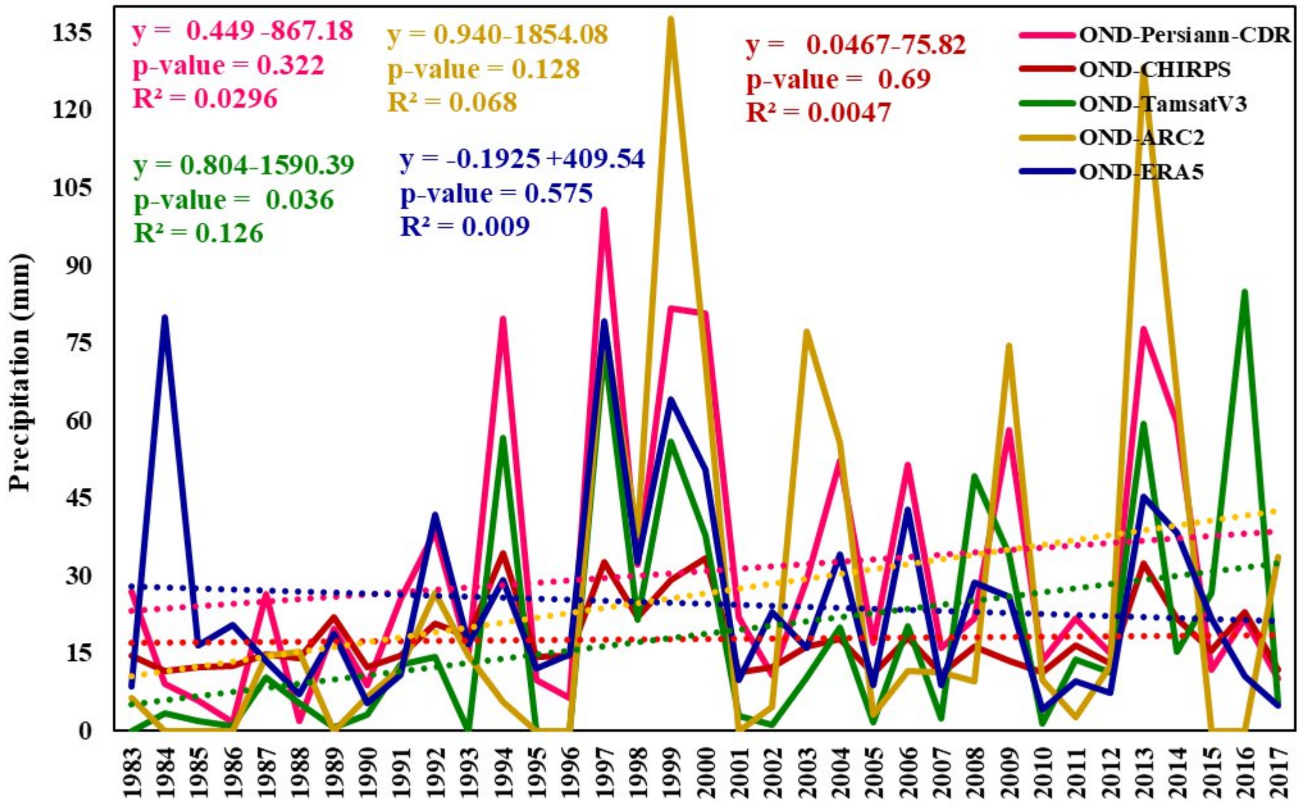

Figure 2. West Trend of Seasonnal Variability of precipitation (mm) of five products (Chirps, Persiann-CDR, ARCV2, TAMSATV3, ERA5) over the Republic of Djibouti in he period (1983-2017).

SATELLITE DATA PRECIPITATION NAME:

1. **PERSIANN** (Precipitation Estimation from Remotely Sensed Information using Artificial Neural Networks): http://chrsdata.eng.uci.edu/
2. **CHIRPS** (Climate Hazards Group InfraRed Precipitation with Station data) : https://iridl.ldeo.columbia.edu/SOURCES/.UCSB/.CHIRPS/.v2p0/
3. **IMERG** (The Integrated Multi-satellitE Retrievals for GPM): https://disc.gsfc.nasa.gov/datasets/GPM_3IMERGDF_06/summary
4. **ERA5** : https://cds.climate.copernicus.eu/cdsapp#!/dataset/reanalysis-era5-single-levels-monthly-means?tab=form
5. **CRU TS :** https://crudata.uea.ac.uk/cru/data/hrg/cru_ts_4.05/ge/
6. **CMORPH CDR :** https://www.ncei.noaa.gov/products/climate-data-records
7. **ALADIN**
8. **SAFRAN**
9. **MESCAN**
10. **AROME**
11. **HRAC**
12. **GTOPO**
13. **TMPA3**
14. **GSMap MUK**

15. **Global IR**
16. **ARCV2**
17. **TAMSAT**
18. **MERRA2**
19. **NCEP NOAA**
20. **TRIMM**
21. **NLDAS**
22. **GLDAS**
23. **CFSR**
24. **JRA 55**
25. **Grid MET**
26. **ANUSPLIN**
27. **ERO4M**
28. **…..ETC**

Abdi-Basid Ibrahim Adan – abdi-basid@outlook.com - 2018-2019